Quantum Sensing of Quantum Materials

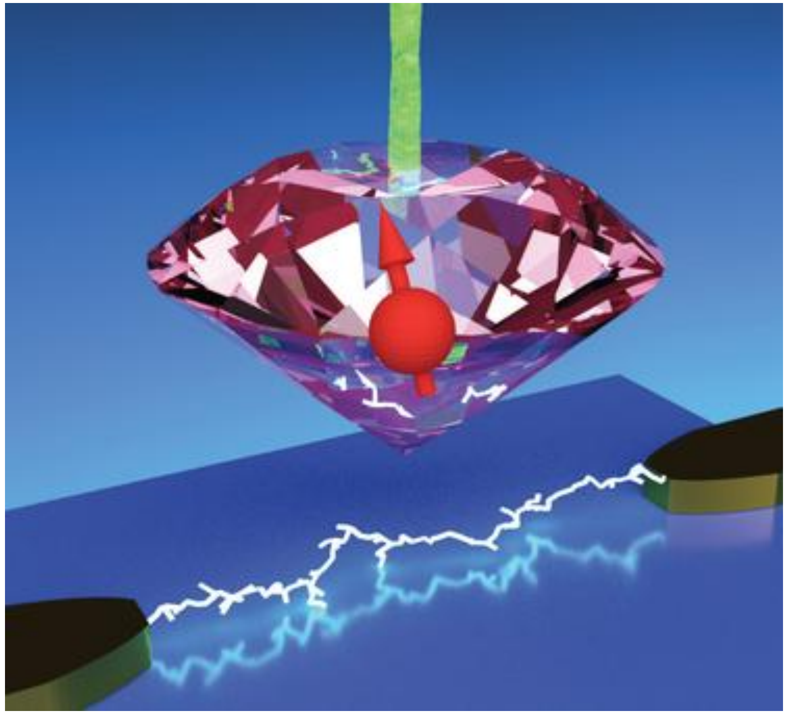

2026 Principles and Applications of Symmetry in Magnetism Summer School, Colorado State University

Chunhui (Rita) Du

Georgia Institute of Technology

Outline

- ***Part 1: Quantum sensing mechanism and its application to static magnetic field sensing***

  - ❑ (Anti)ferromagnet
  - ❑ Moiré magnetism
  - ❑ Altermagnetism
  - ❑ Current in metal and superconductor

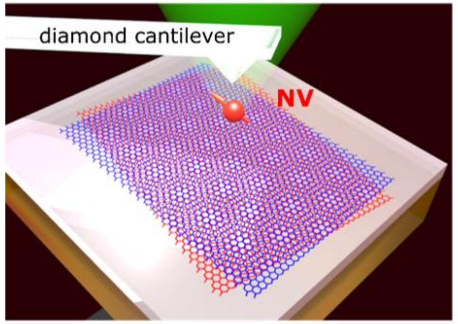

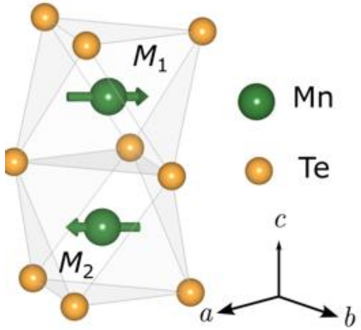

L. Zhou et al., arXiv:2605.25241 (2026)

S. Li et al., *Nature Communications* **15**, 5712 (2024)

M. Huang et al., *Nature Communications* **14**, 5259 (2023)

- ***Part 2: Quantum sensing of dynamic electromagnetic field (spin & charge dynamics)***

  - ❑ Spin wave and magnon excitations
  - ❑ Spin transport and magnetic phase transition
  - ❑ Magnetic noise from charges in metal and superconductor

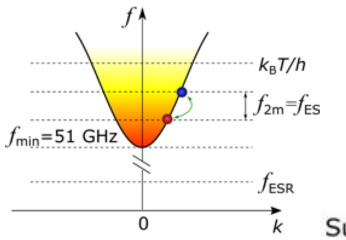

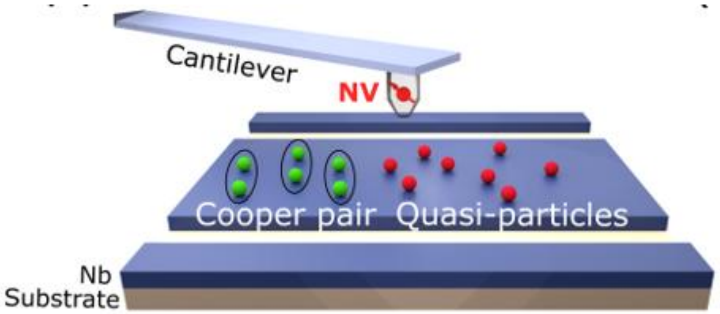

S. Li et al., *Phys. Rev. Lett.* **136**, 076004 (2026)

N. McLaughlin et al., *Nano Letters* **22**, 5810 (2022)

- ***Part 3: Emerging quantum sensing platforms and hybrid quantum devices***

X. Zhang et al., Nature Communications (2026)
arXiv:2502.04561

M. Huang et al., *Nature Communications* **13**, 5369 (2022)

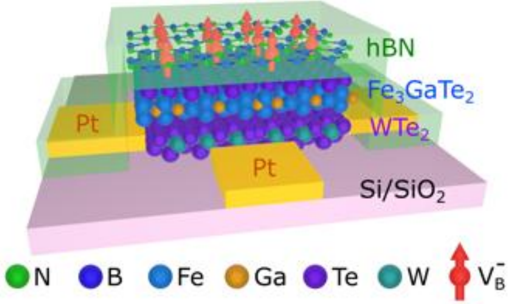

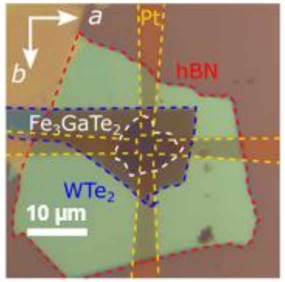

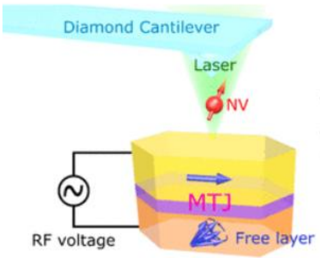

G. Q. Yan et al., *Nano Letters* **24**, 14273-14278 (2024)

Color centers with accessible spin

Various color centers in diamond

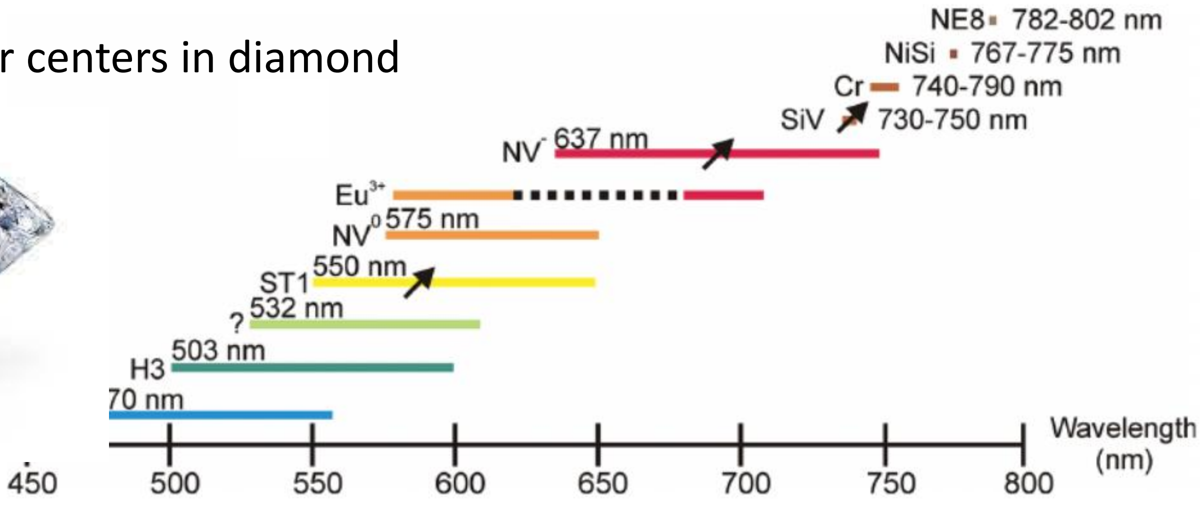

Adv. Opt. Mater. **2**, 911 (2014)

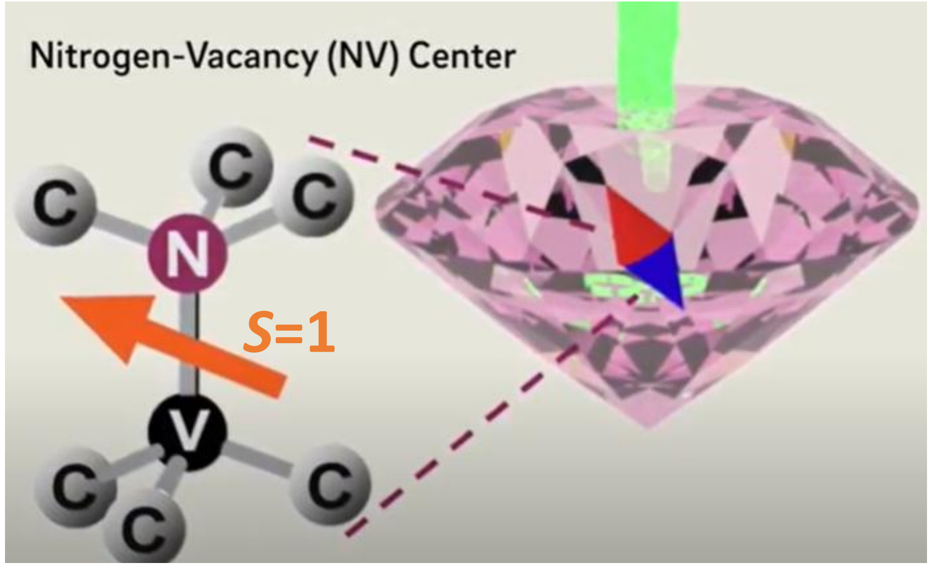

Other color centers with accessible spin

Spin defects in hBN

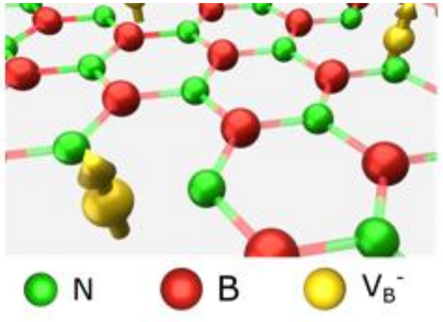

Silicon vacancy

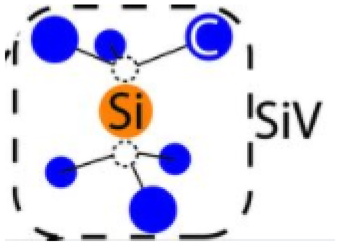

Nat. Commun. **12**, 4480 (2021)

Science **354**, 847 (2016)

Color centers with accessible spin

NV center in diamond

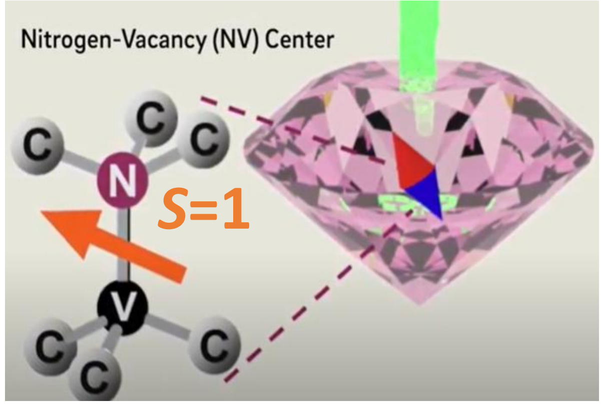

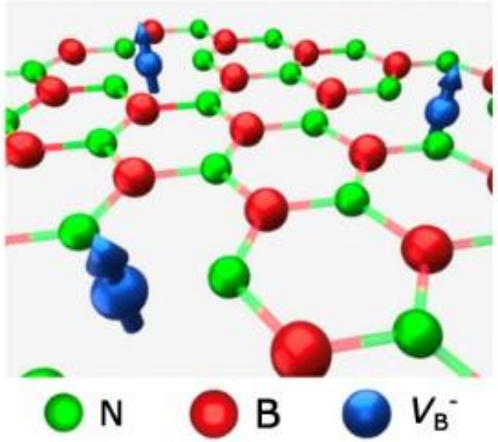

Color centers in 2D materials

Quantum sensing/imaging

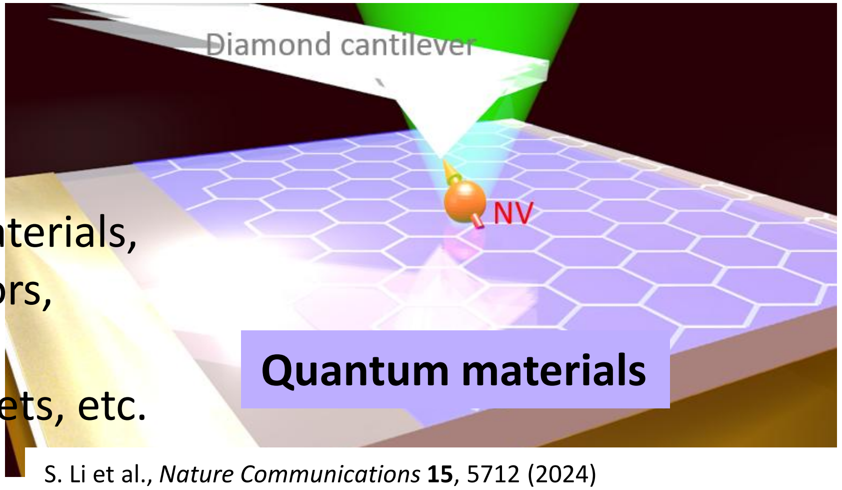

Topological materials,
superconductors,
2D materials,
antiferromagnets, etc.

S. Li et al., *Nature Communications* **15**, 5712 (2024)
J. Zhou et al., *Science Advances* **10**, eadk8495 (2024)
G. Q. Yan et al., *Advanced Materials* **34**, 2200327 (2022)
H. L. Wang et al., *Science Advances* **8**, eabg8562 (2022)
M. Huang et al., *Nature Communications* **14**, 5259 (2023)
M. Huang et al., *Nature Communications* **13**, 5369 (2022)
S. Li et al., *Nano Letters* **23**, 5326 (2023)
N. McLaughlin et al., *Nano Letters* **22**, 5810 (2022)

Hybrid quantum devices for QIS

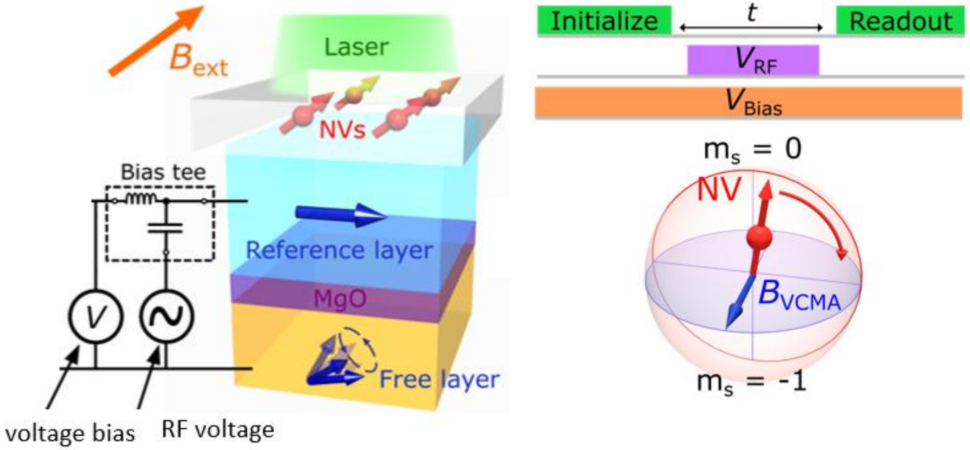

X. Wang et al., *npj Quantum Inf.* **6**, 78 (2020)
G. Q. Yan et al., *Phys. Rev. Appl.* **18**, 064031 (2022)
N. McLaughlin et al., *ACS Nano* **17**, 25689 (2023)
G. Q. Yan et al., *Nano Letters* **24**, 14273-14278 (2024)
S. Li et al., arXiv:2412.18896 (2024)
IEEE Transactions on Quantum Engineering, **2**, 1, (2021)

Quantum sensing using NV centers

Nitrogen vacancy (NV) center

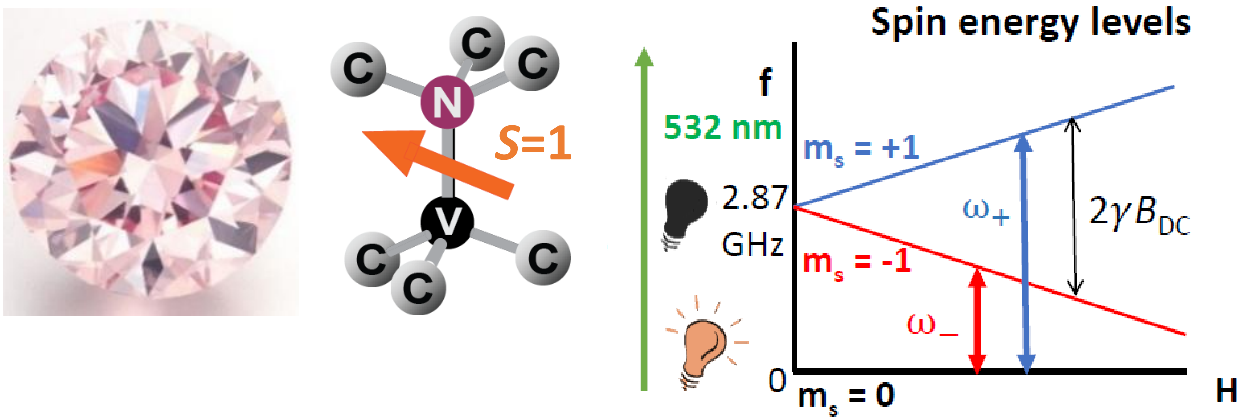

- **Sensitive to magnetic field, temperature, pressure, electrical field, etc.**
- **Broad range of working temperature and conditions (mK to 600 K)**
- **Magnetic field sensitivity ~10 nT**
- **Nanometer spatial resolution**

Static field

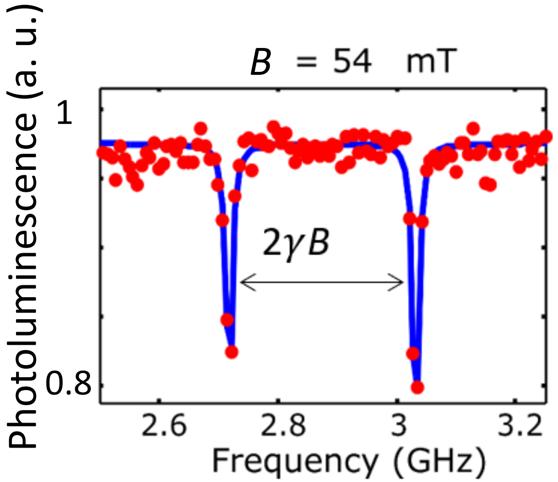

- Spin textures (stray field)
- Static currents (Oersted field)
- ~10 nT sensitivity

Temperature

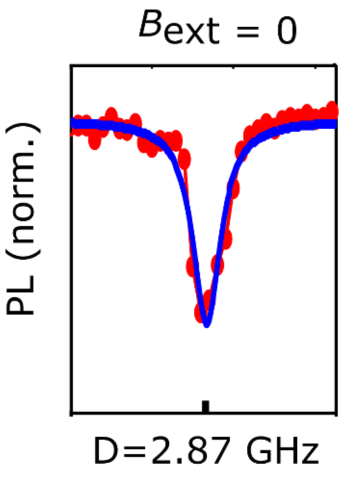

- D= 2.87+ AΔT
  A~ -75 kHz/K

  V. M. Acosta et al., *Phys. Rev. Lett.* **104**, 070801 (2010)
- Thermally-driven phenomena
- ~mK sensitivity

AC magnetic field sensing

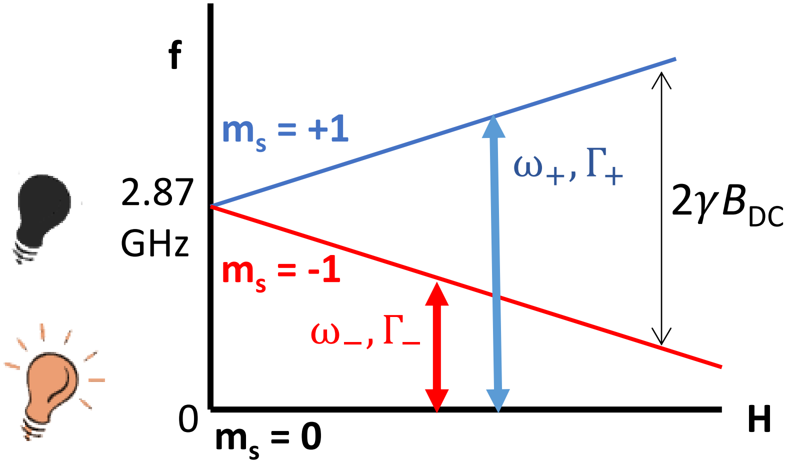

Measure AC fields (coherent)

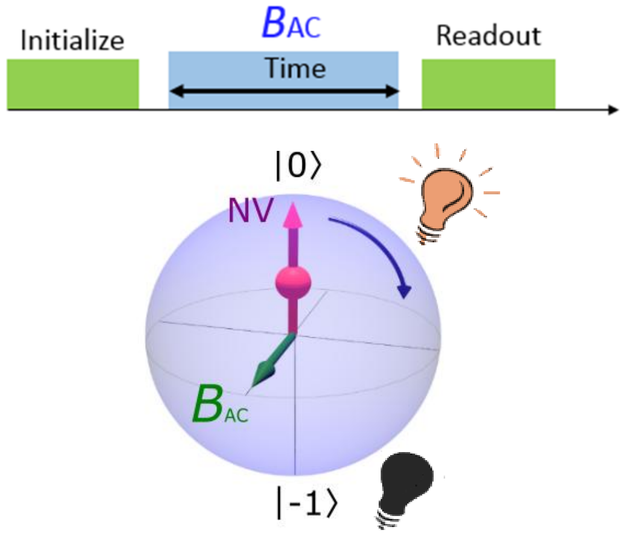

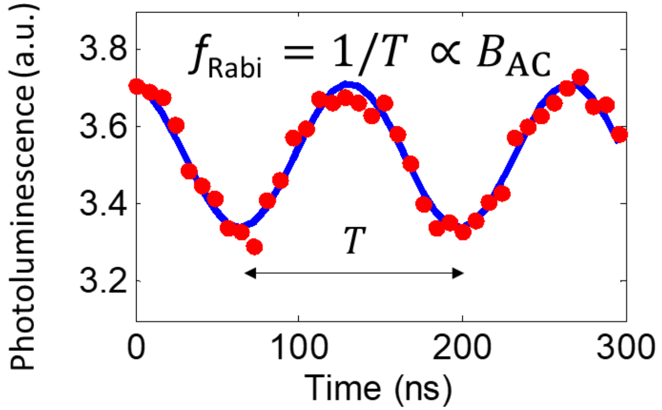

- MW amplitude and phase
- Magnetic resonance

Measure field fluctuations (non-coherent)

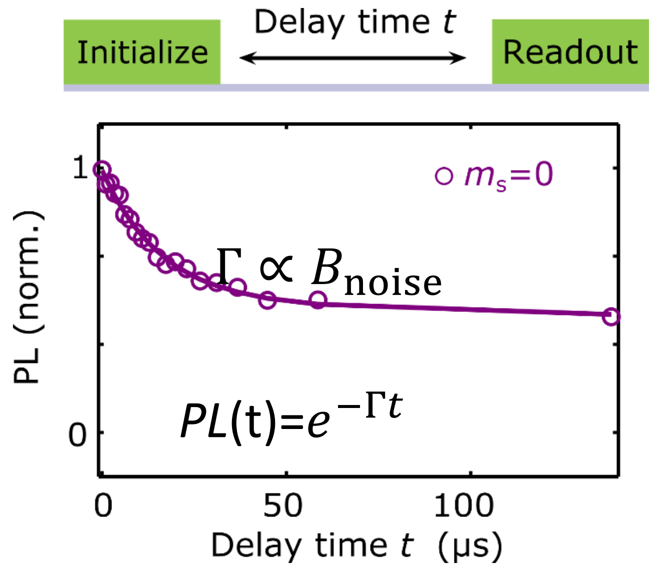

C.H.R.Du et al., *Science* **357**, 195 (2017)

- Spin dynamics (spin excitations)
- Electrical conductivity (Johnson noise)
- Long spin relaxation rate

(ms @RT; s @ cryogenic temperature)

Quantum sensing using NV centers

Nitrogen vacancy (NV) center

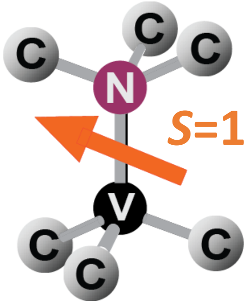

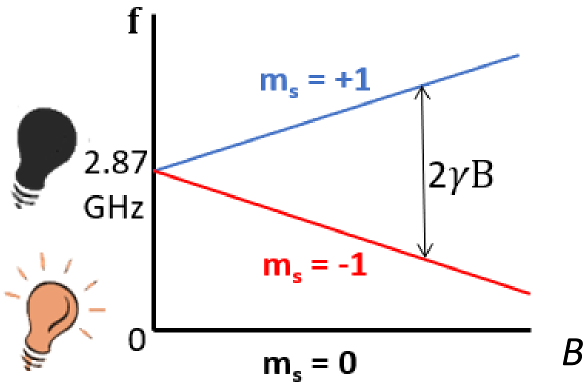

- **Sensitive to magnetic field, temperature, pressure, electrical field, etc.**
- **Broad range of working temperature and conditions (mK to 600 K)**
- **Magnetic field sensitivity ~ 10 nT**
- **Nanometer spatial resolution**
- **Long coherence time (QIS)**

Multi-modal sensing platform:

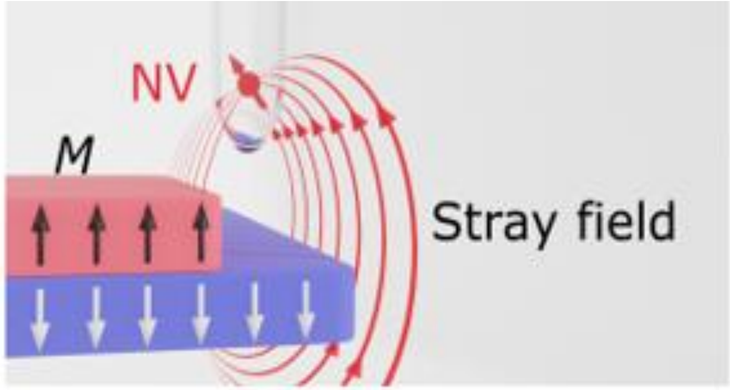

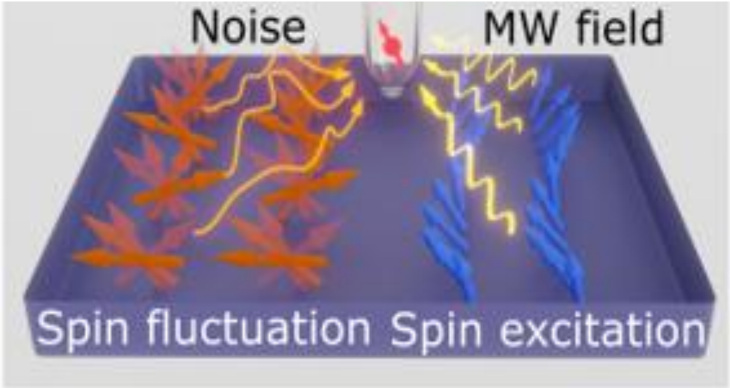

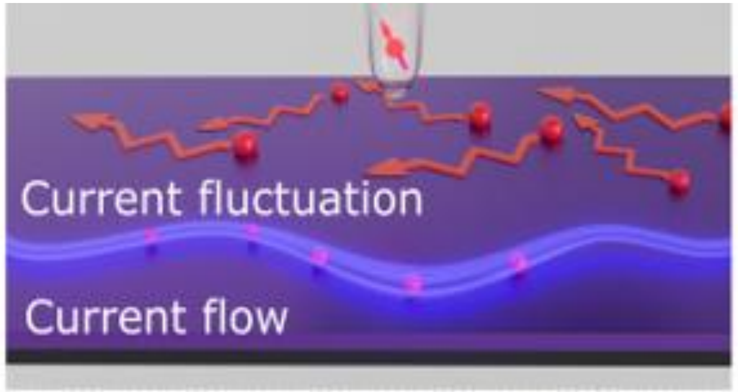

F. Casola, T. van der Sar, A. Yacoby, *Nature Reviews Materials* **3**, 17088 (2018)
J.Rovny, S. Gopalakrishnan, A. C. B. Jayich, P. Maletinsky, E. Demler, N. P. de Leon, *Nature Reviews Physics* **6**, 753–768 (2024)
S. Li, V. Jacques, P. Maletinsky, C. L. Degen, and C. R. Du, *Nature Materials* (2026)

Creation of NV centers

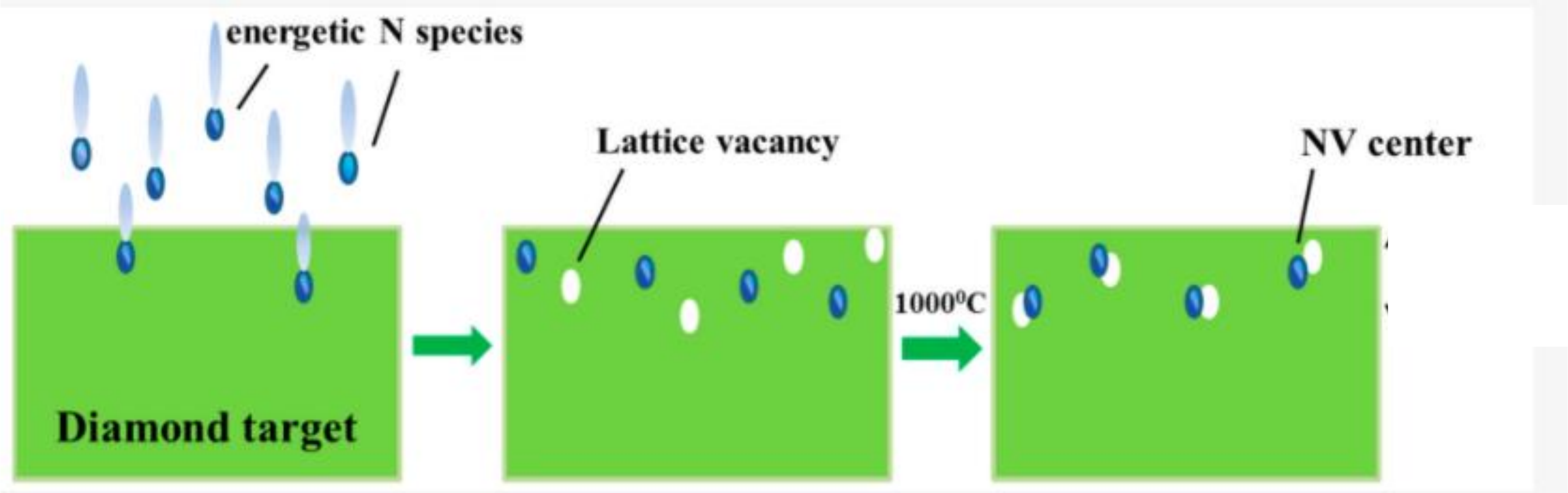

Shallow NV (~ 5 keV, ~10 nm)

A. Haque at al., *J. Manuf. Mater. Process.* **1**, 6, 2017.

State-of-the art quantum sensing platforms

Resolution~
500 nm

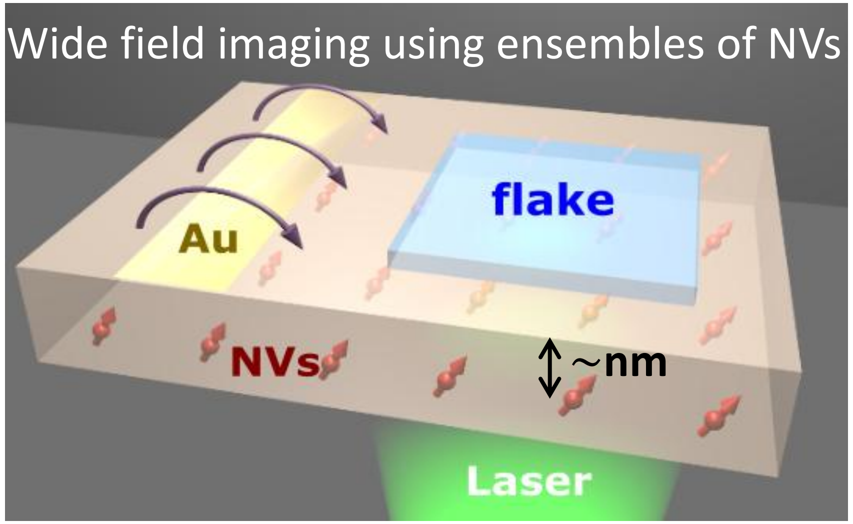

N. McLaughlin,… C. R. Du, *Nano Letters* **21**, 7277 (2021)

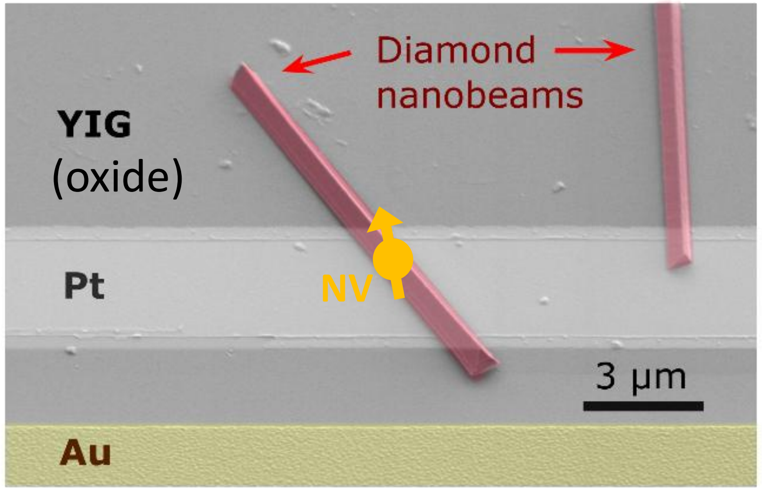

C. R. Du et al., *Science* **357**, 195 (2017)

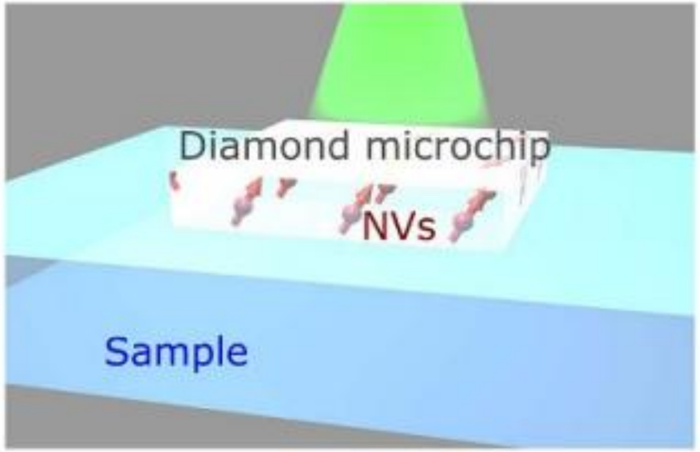

Y. Schlussel et al., *Phys. Rev. Appl.* **10**, 034032 (2018)
A. Kimel, …C. R. Du, …, *J. Phys. D: Appl. Phys.* **55**, 463003 (2022)

P. Maletinsky et al., *Nat. Nanotechnol.* **7**, 320 (2012)

Resolution~
50 nm

Imaging static magnetism

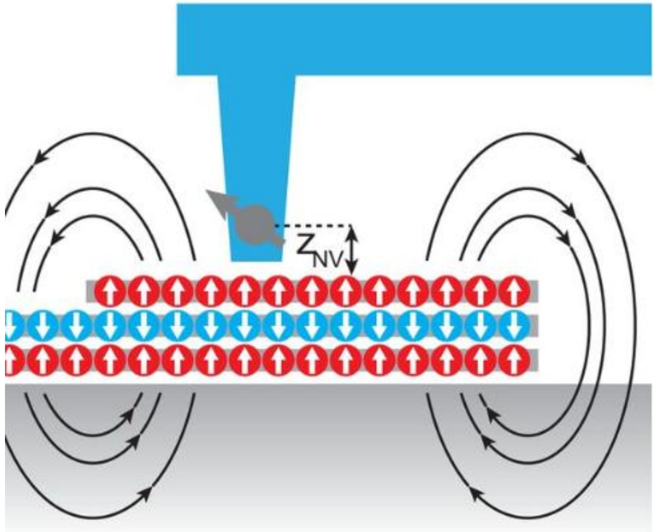

Atomically thin CrI_3

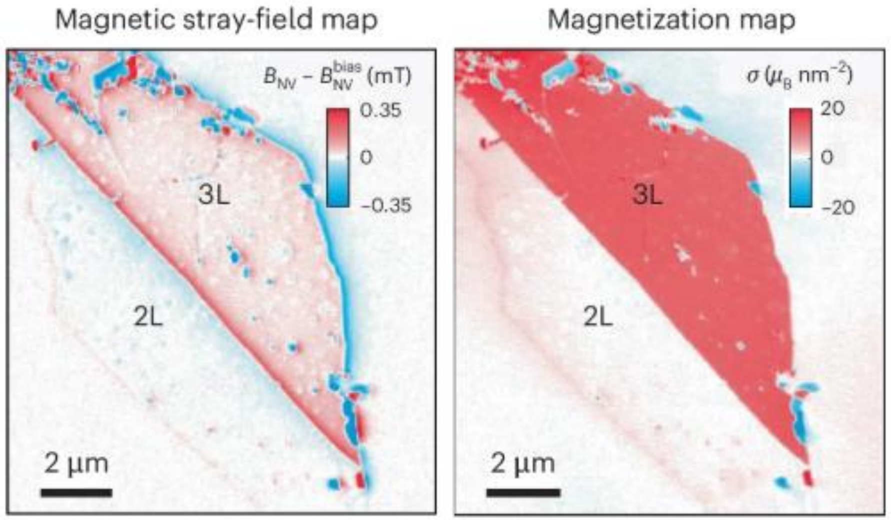

Thiel, L. et al. *Science* **364**, 973–976 (2019)

Antiferromagnetic Cr_2O_3

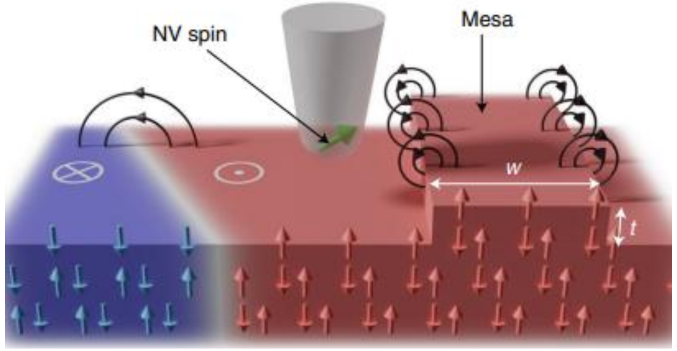

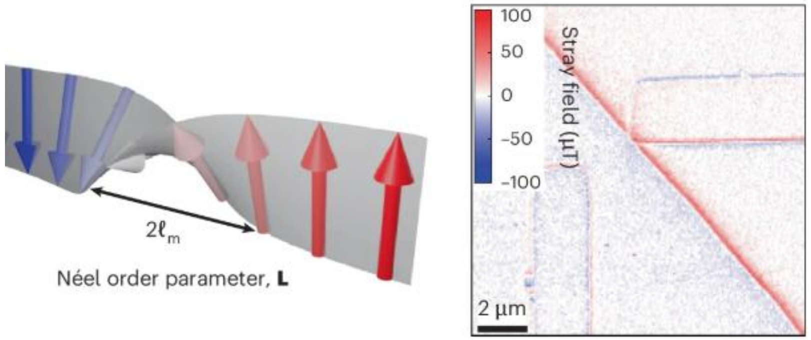

Hedrich, N. et al. *Nat. Phys.* 17, 574–577 (2021)

Noncolinear AF Mn_3Sn film

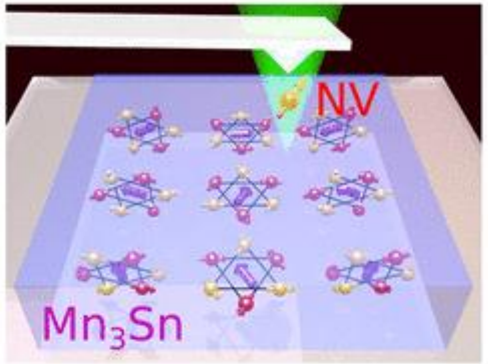

~10^{-3} u_B /Mn

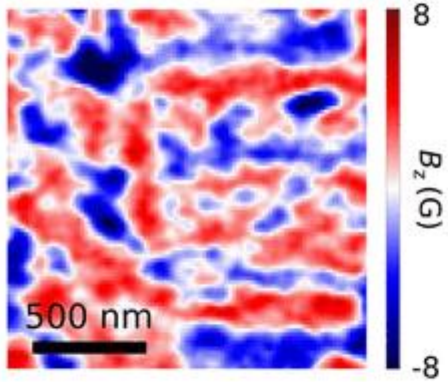

S. Li et al., *Nano Letters* **23**, 5326 (2023)

- Imaging static field from antiferromagnetic domains would typically requires net/uncompensated moment

Magnetization reconstruction

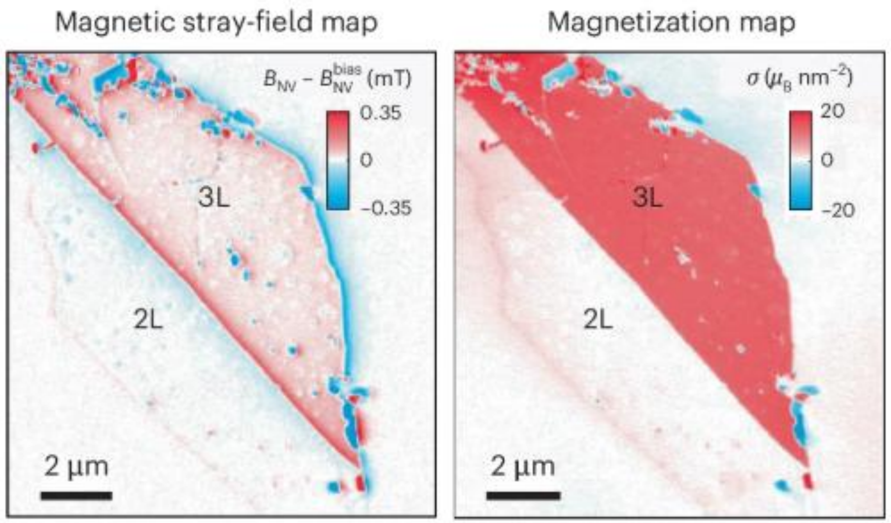

Thiel, L. et al. *Science* **364**, 973–976 (2019)

$$B_F(x, y) = \int m(x,y) D dx dy$$

D is the magnetostatic Green's function tensor, *d* is NV to sample distance

FFT

$$\mathbf{B}_F(\mathbf{k}, d) = D(\mathbf{k}, d)\mathbf{m}(\mathbf{k})$$

$$\begin{cases} D_{\alpha\beta}(\mathbf{k}, d) = -2\pi\left(k_\alpha k_\beta / k\right)e^{-kd}, \\ D_{\alpha z}(\mathbf{k}, d) = -2\pi i k_\alpha e^{-kd}, \\ D_{zz}(\mathbf{k}, d) = 2\pi k e^{-kd}, \end{cases}$$

Due to the spontaneous out-of-plane anisotropy of CrI_3, $\mathbf{m}(\mathbf{k}) = m_z(\mathbf{k})\hat{\mathbf{z}}$

$$B_F(\mathbf{k}, d) = 2\pi e^{-kd}(k\cos\theta - ik_x \sin\theta\cos\phi - ik_y \sin\theta\sin\phi)m_z(\mathbf{k})$$

θ and ϕ are angles characterizing the NV direction

inverse FFT

$$m(x, y)$$

Imaging moiré magnetism

Small angle twisted double trilayer (tDT) CrI_3

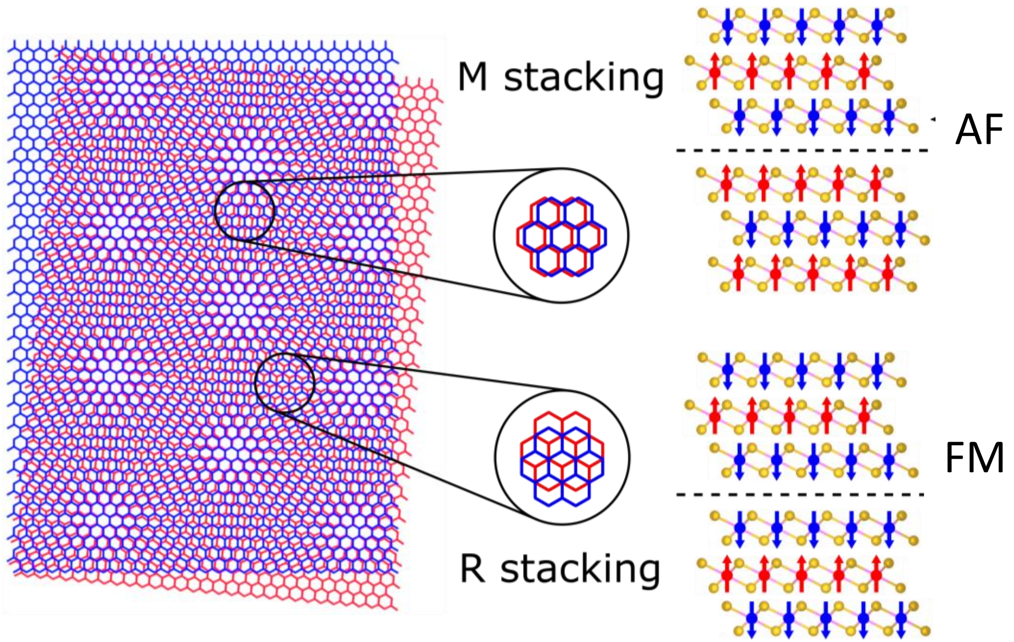

S. Li et al., *Nature Communications* **15**, 5712 (2024)

- Autocorrelation function

$$AC(\delta x, \delta y) = \sum_{x,y} M(x+\delta x, y+\delta y) M(x,y)$$

gives the degree of similarity between the map shifted by (δx, δy) and the original map.

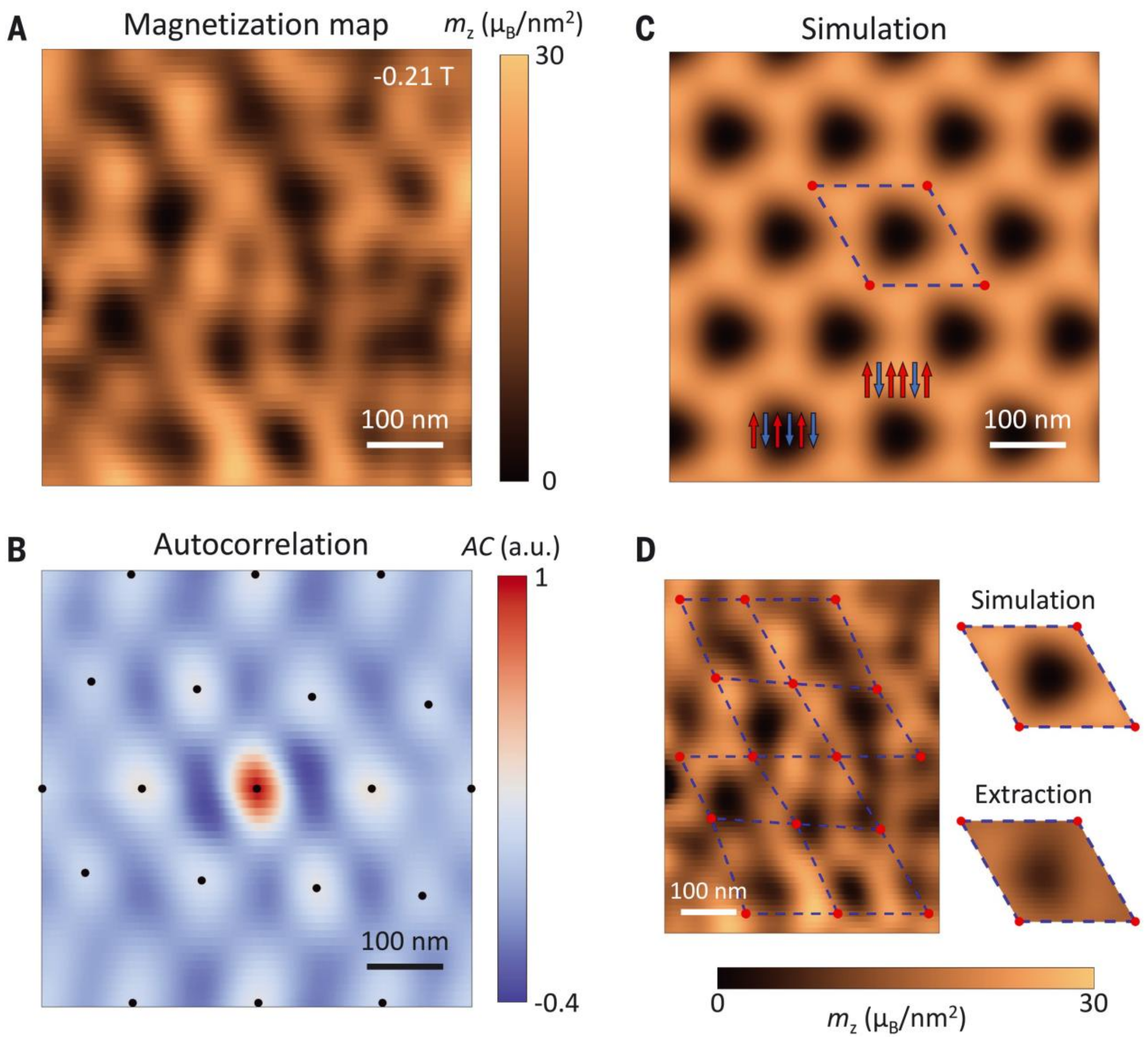

Slightly disordered hexagonal lattice with a lattice constant of ~150 nm (twist angle of ~0.25°)

T. Song et al., *Science* **374**, 1140 (2021)

Wide-field imaging of intrinsic domains of moiré magnetism

Twisted double trilayer (tDT) CrI_3
twist-angle (0.3°), period ~ 130 nm

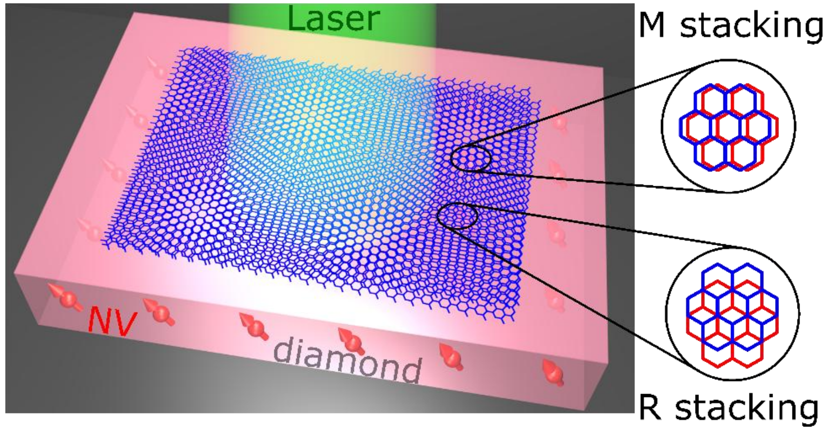

Rhombohedral (FM) Monoclinic (AF)

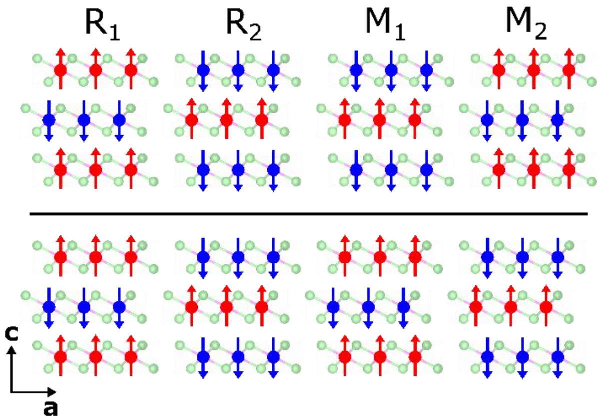

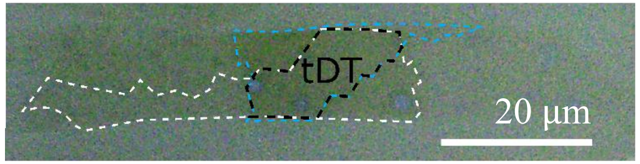

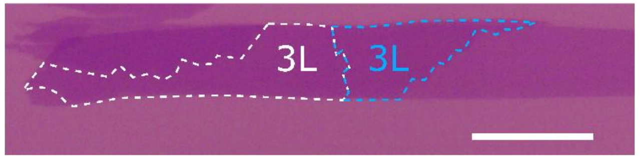

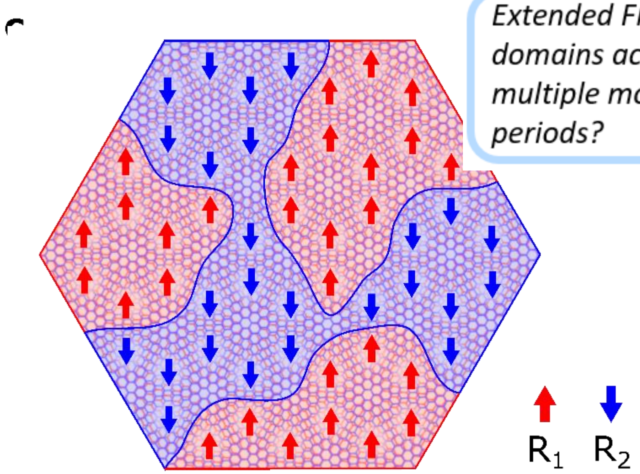

Extended FM domains across multiple moiré periods?

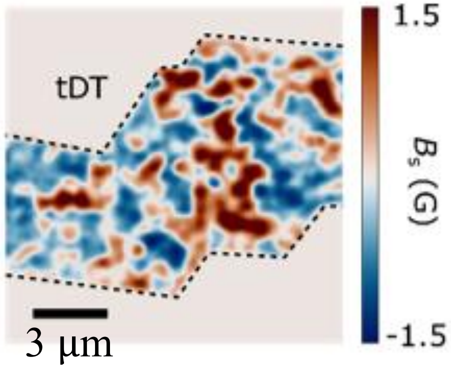

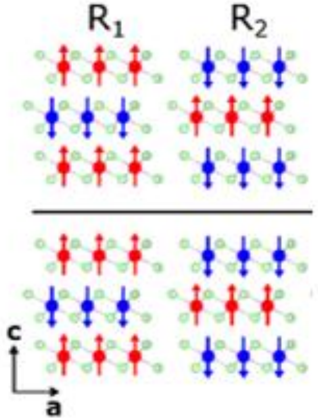

Degenerate FM domains across multiple moiré periods in tDT CrI_3

Liuyan Zhao
(U Michigan)

Zeliang Sun

M. Huang, … C. R. Du, *Nature Communications* **14**, 5259 (2023)

MnTe as an altermagnet candidate

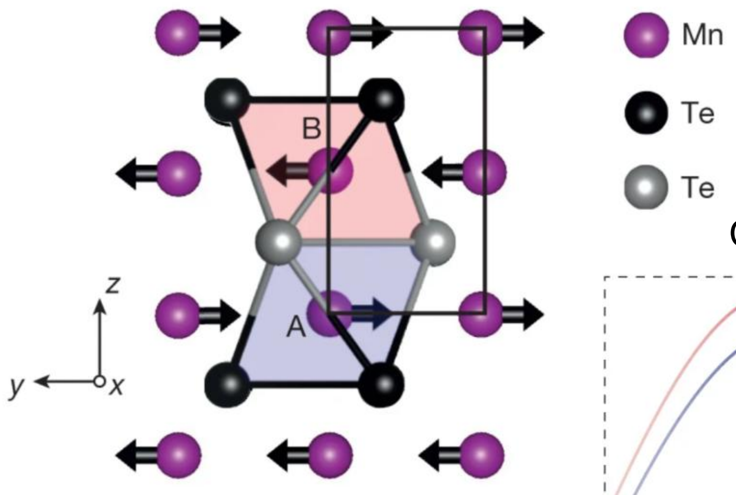

Calculation

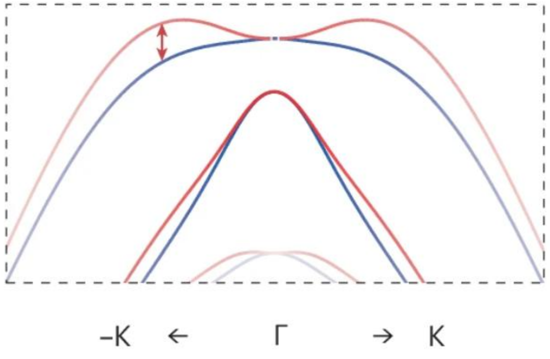

Experiment

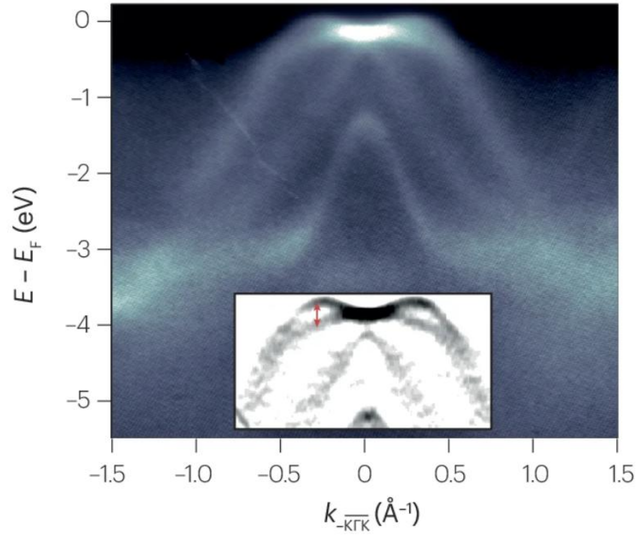

J. Krempasky et al., *Nature* ***626***, 517 (2024)

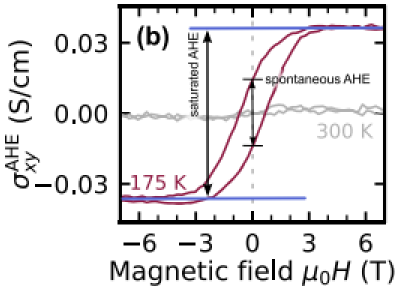

R. D. Gonzalez Betancourt et al., *Phys. Rev. Lett.* **130**, 036702 (2023)

Imaging and control altermagnetic domains in MnTe

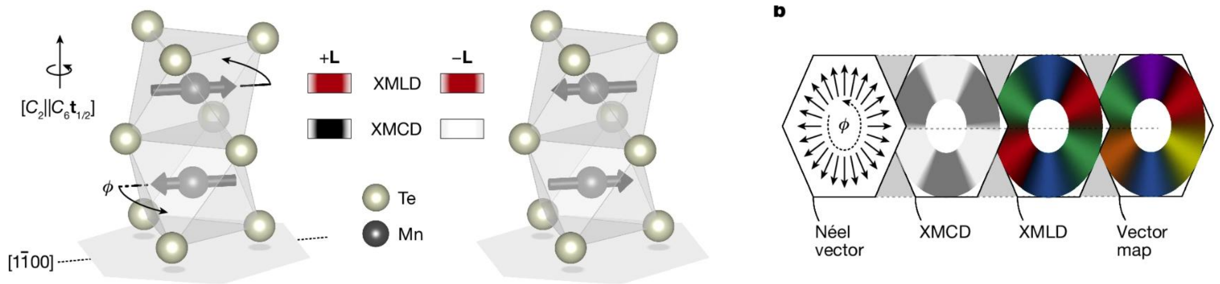

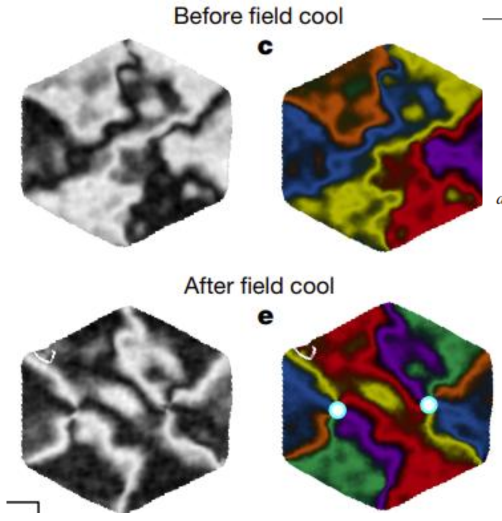

O. J. Amin et al., *Nature* **636**, 348 (2024)

PHYSICAL REVIEW B **110**, 214436 (2024)

Origin of the gossamer ferromagnetism in MnTe

I. I. Mazin
Department of Physics and Astronomy, George Mason University, Fairfax, Virginia 22030, USA and Quantum Science and Engineering Center, George Mason University, Fairfax, Virginia 22030, USA

K. D. Belashchenko
Department of Physics and Astronomy and Nebraska Center for Materials and Nanoscience, University of Nebraska-Lincoln, Lincoln, Nebraska 68588, USA

$$(3L_x^2 - L_y^2)L_yM_z = M_z \sin 3\phi_L$$

Bulk *Mz* ~ 10^{-5} uB/Mn

K. P. Kluczyk et al., *Phys. Rev. B* **110**, 155201 (2024)

Quantum sensing of MnTe films

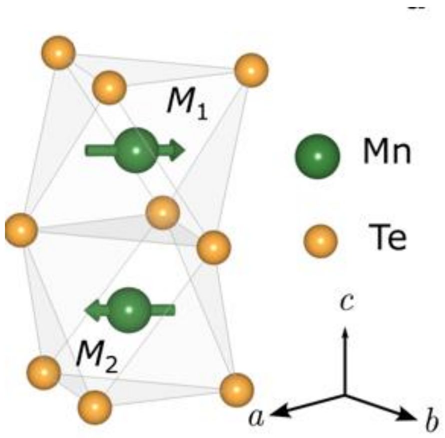

Cui-Zu Chang
(Penn State)

Zijie Yan

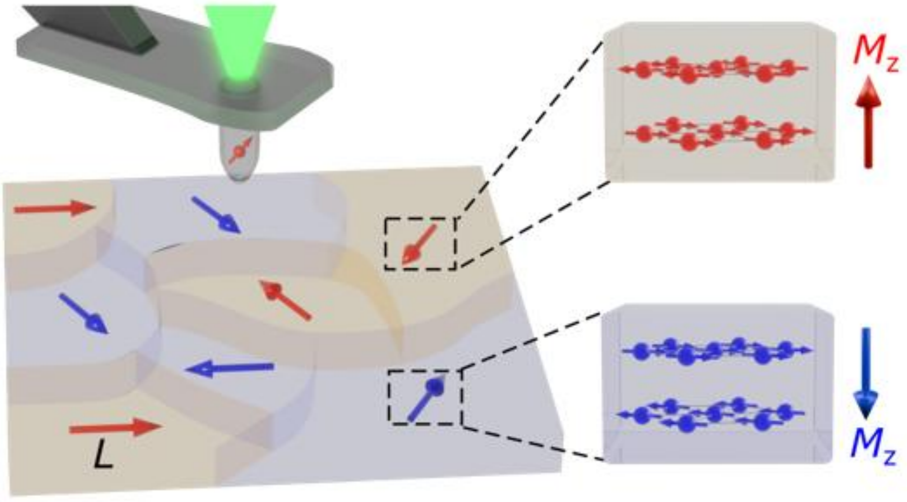

T = 2 K

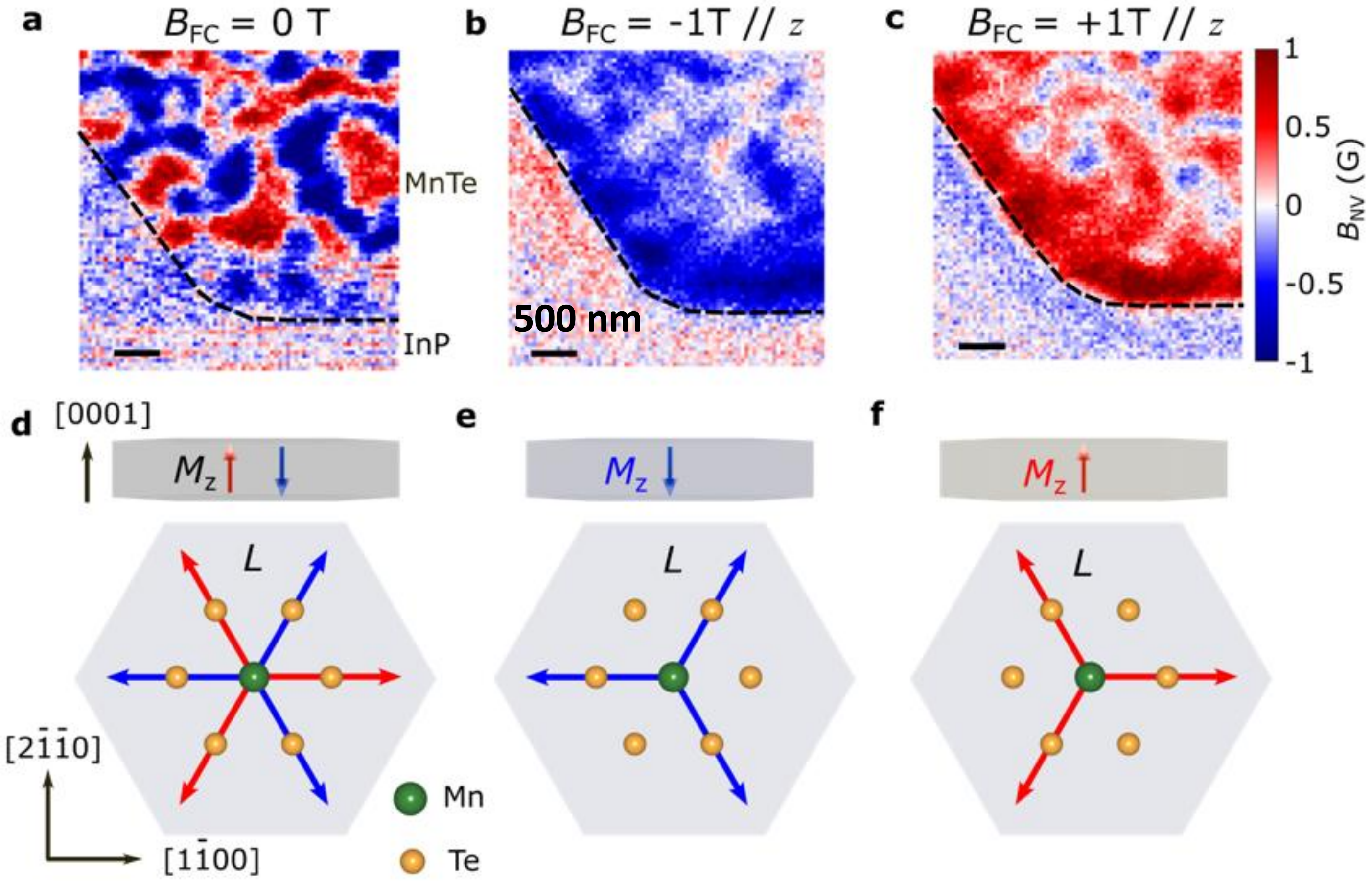

Zhou, et al. arXiv:2605.25241 (2026)

- Field-controllable stray field patterns
- Net magnetization is dominated by M_z

Quantum sensing of surface magnetism in MnTe

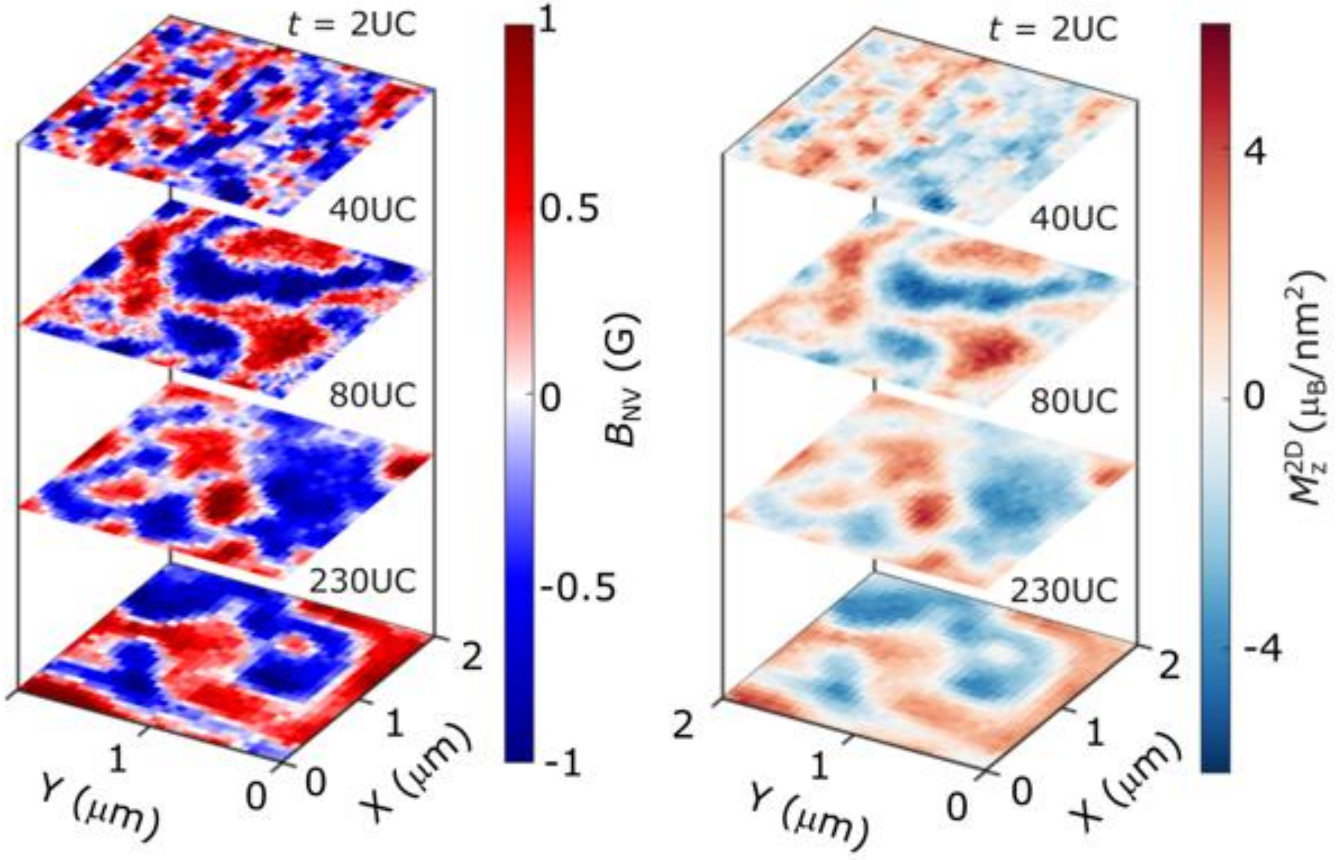

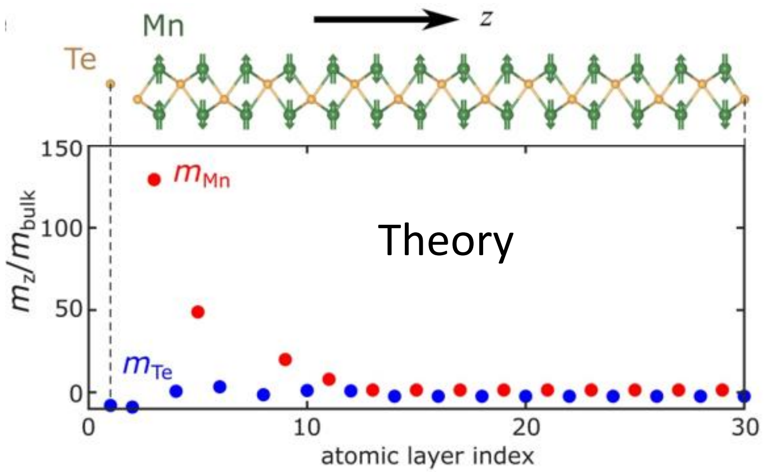

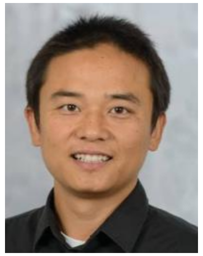

Binghai Yan
(Penn State)

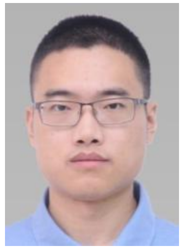

Yufei Zhao

Zhou, et al. arXiv:2605.25241 (2026)

- Stray field is insensitive to film thickness
- Net magnetization is **surface dominated** due to symmetry breaking
- Consistent with first-principles calculations
- T_c ~ 250 K for surface *Mz*, correlated with the onset temperature of AHE

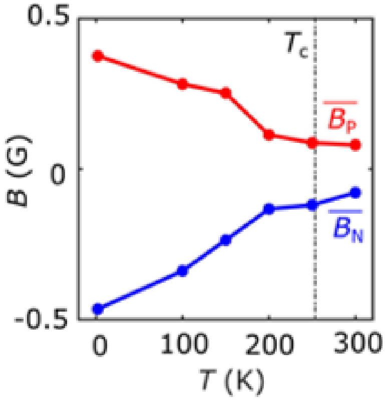

T_c ~ 250 K

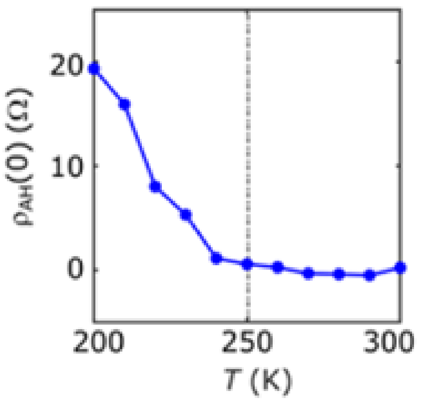

Imaging current

Biot-Savart law

$$\vec{B}(\vec{r}) = \frac{\mu_0}{4\pi}\int \frac{\vec{J}(\vec{r}\,') \times (\vec{r} - \vec{r}\,')}{|\vec{r} - \vec{r}\,'|^3}\, d^3\vec{r}\,'$$

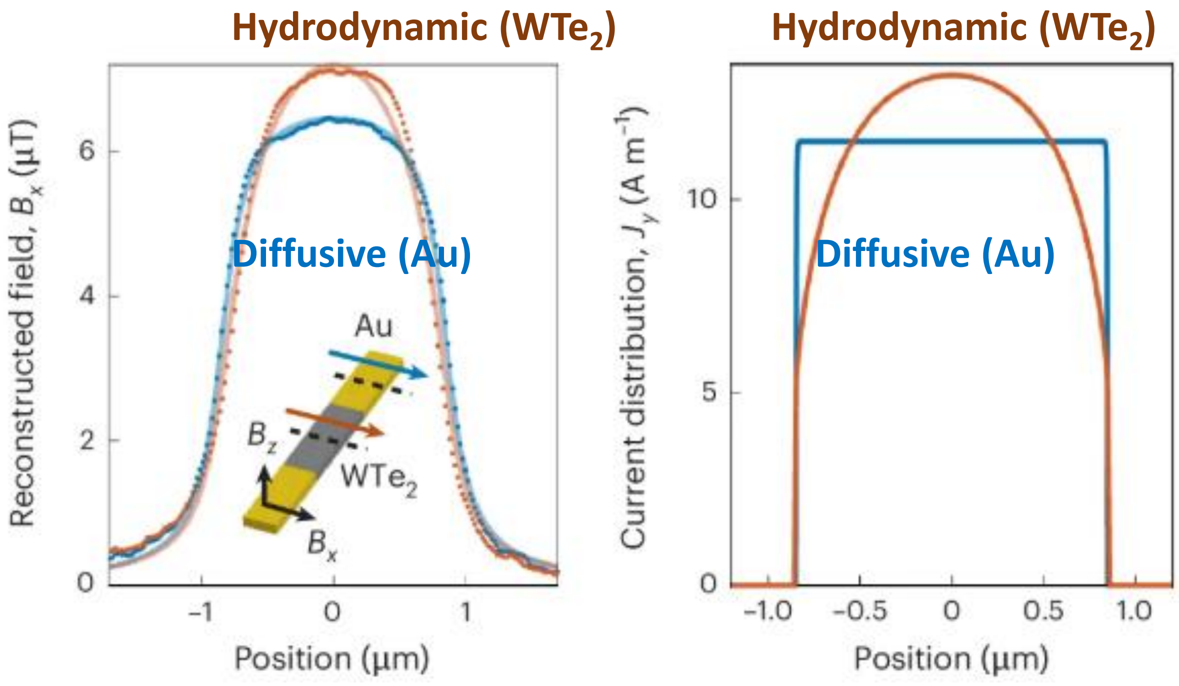

U. Vool et al., *Nat. Phys.* **17**, 1216 (2021)

Current whirlpools in graphene at room temperature

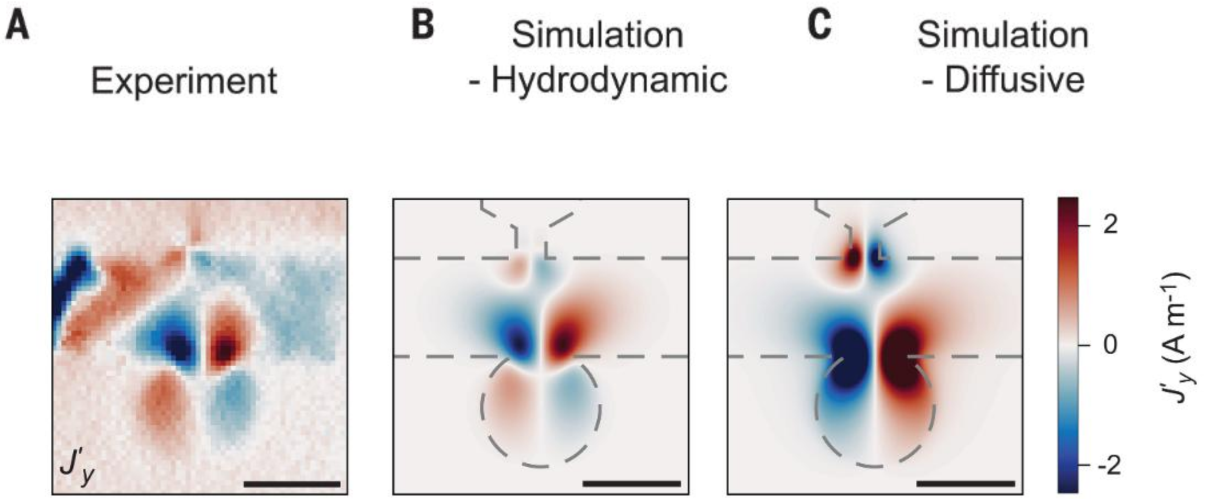

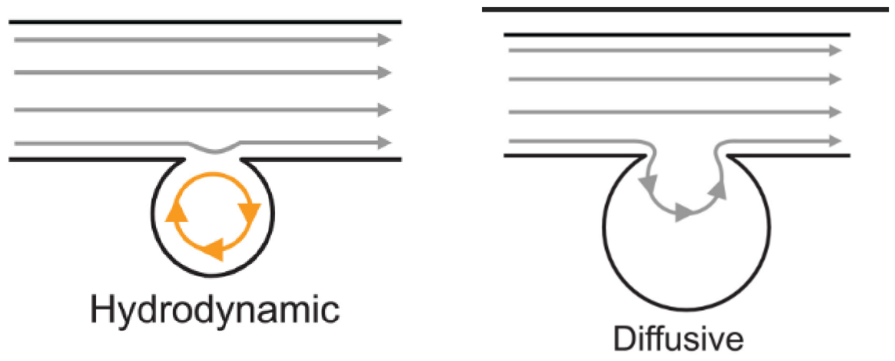

M. L. Palm *et al.*, *Science* **384**, 465 (2024)

Quantum imaging of superconductor

- Superconducting Vortices

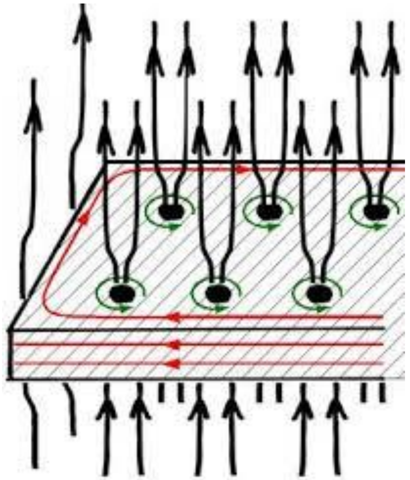

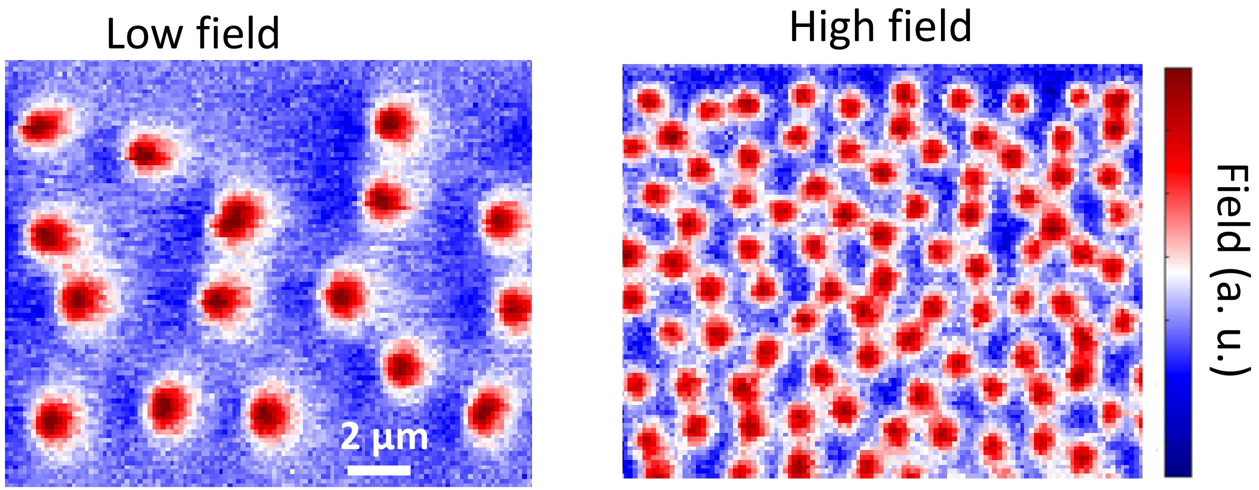

S. Li et al., arxiv 2606.20904 (2026)

- Meissner effect of $FeTe_xSe_{1-x}$

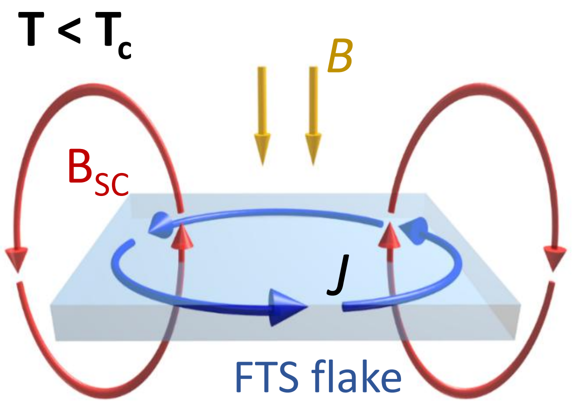

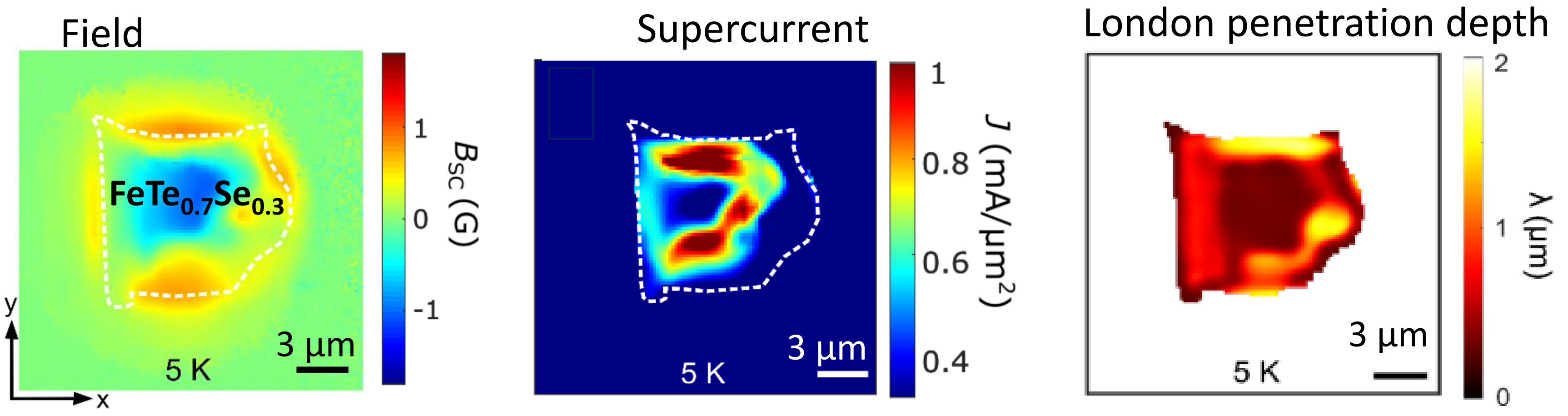

N. McLaughlin et al., *Nano Letters* **21**, 7277 (2021)

Part 2: Quantum sensing of dynamic electromagnetic field (spin & charge dynamics)

- ❑ **Spin wave and magnon excitations**
- ❑ **Spin transport and magnetic phase transition**

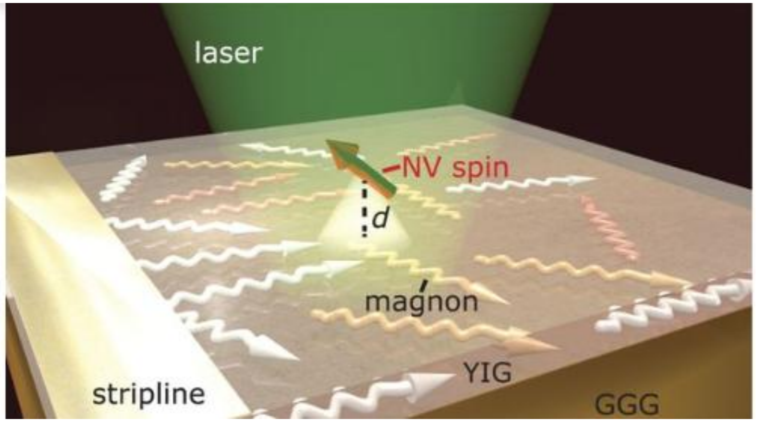

C. Du et al., *Science* **357**, 195 (2017)

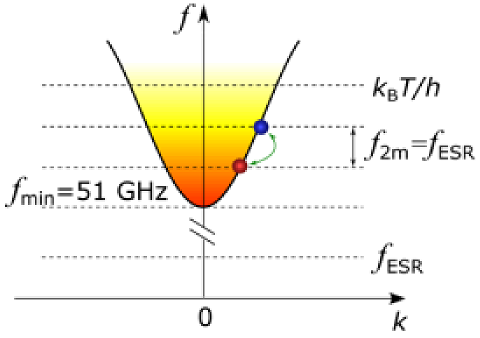

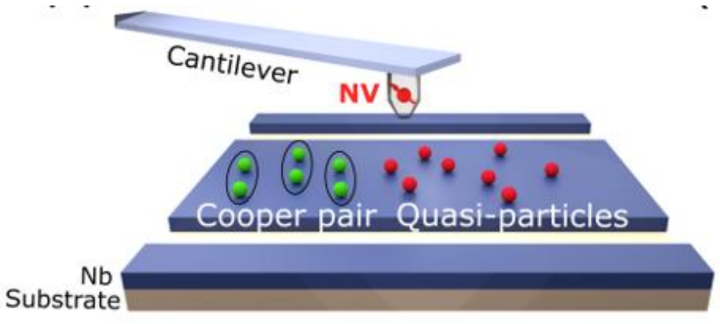

S. Li et al., *Phys. Rev. Lett.* **136**, 076004 (2026)

Spin wave in ferromagnetic materials

Ferromagnetic resonance (k ~ 0)

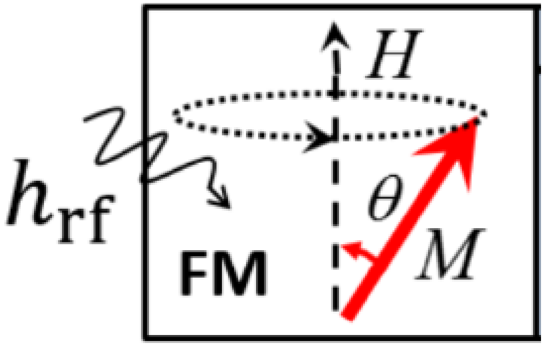

Landau-Lifshitz-Gilbert (LLG) equation:

$$\frac{d\mathbf{M}}{dt} = -\gamma(\mathbf{M} \times \mathbf{H}_{\text{eff}}) + \frac{\alpha}{M_s}\left(\mathbf{M} \times \frac{d\mathbf{M}}{dt}\right)$$

$k > 0$

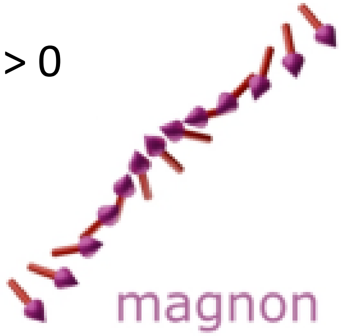

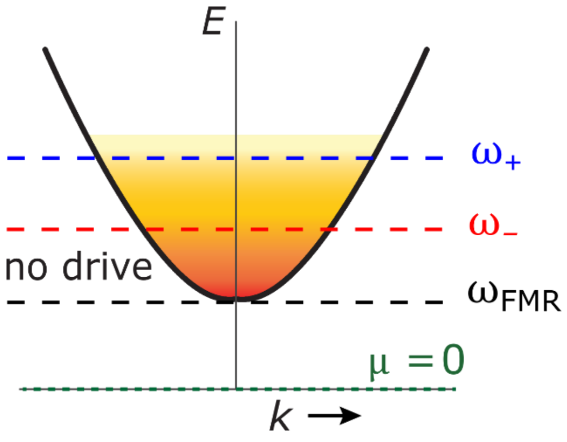

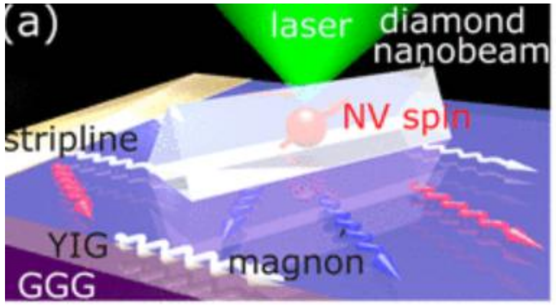

Magnon density is described by Bose-Einstein Distribution Function:

$$n_{\mathrm{B}} = (e^{hf/k_{\mathrm{B}}T} - 1)^{-1}$$

$\frac{K_B T}{f\hbar}$ (high temperature limit)

Rayleigh-Jeans distribution

NV spin relaxation rate $\Gamma_{\pm} \propto \frac{K_B T}{\omega_{\pm}\hbar}$

C. Du et al., *Science* **357**, 195 (2017)
E. Lee-Wong *et al.*, *Nano Lett.* **20**, 3284 (2020)

Sensing thermal magnon using NV relaxation rate measurement

Rate $\Gamma_{\pm} \propto \frac{K_B T}{\omega_{\pm}\hbar}$

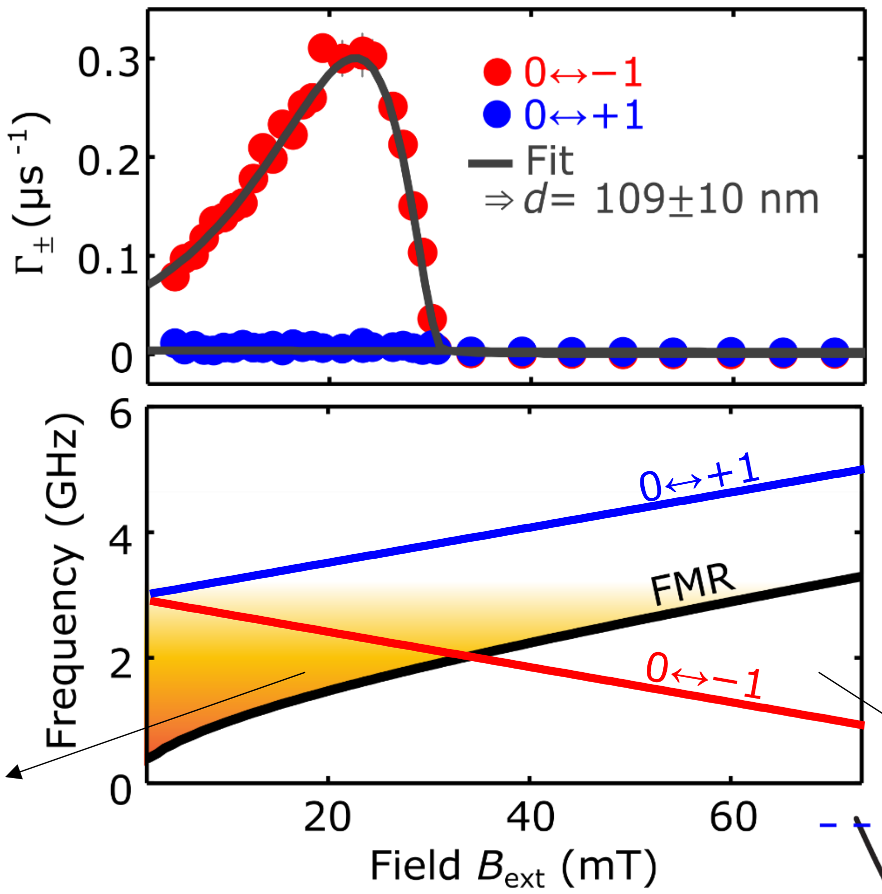

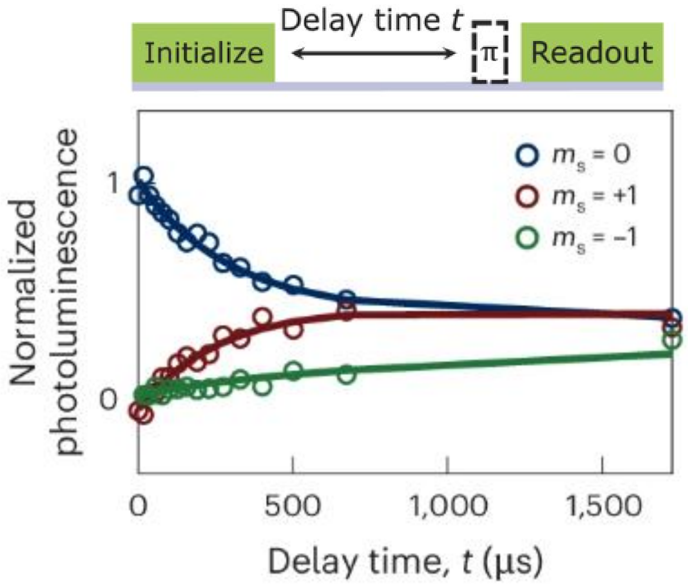

High magnon density

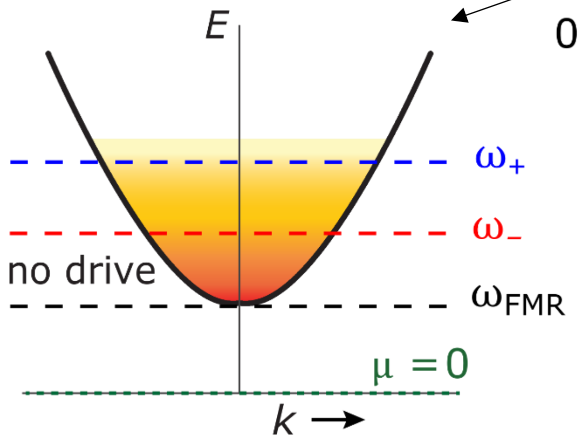

Low magnon density

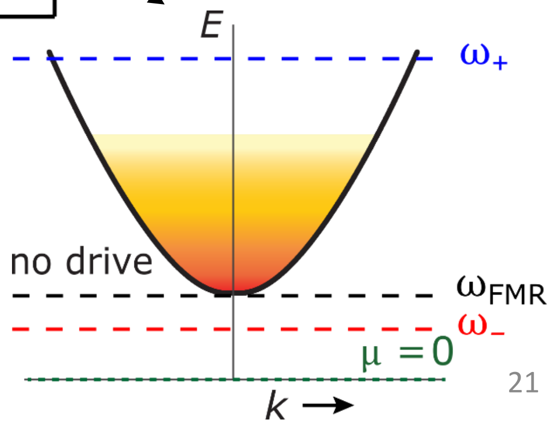

C. Du et al., *Science* **357**, 195 (2017)

Sensing thermal magnon using NV relaxation rate measurement

magnon spectral density

$$\text{Rate } \Gamma_{\pm} \propto \frac{K_B T}{\omega_{\pm}\hbar} \int f(k,d) D(f,K) dk$$

filter function

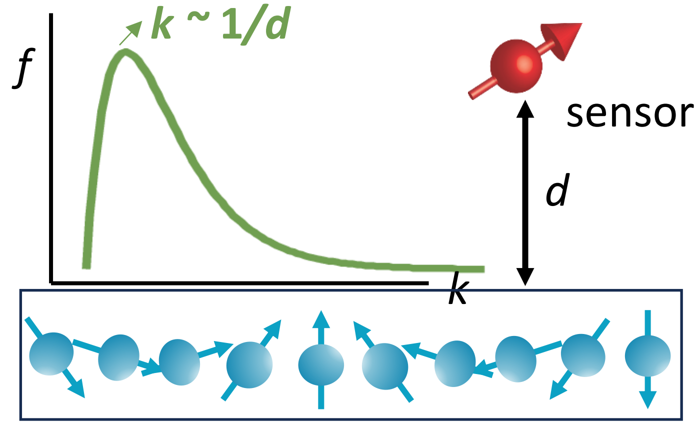

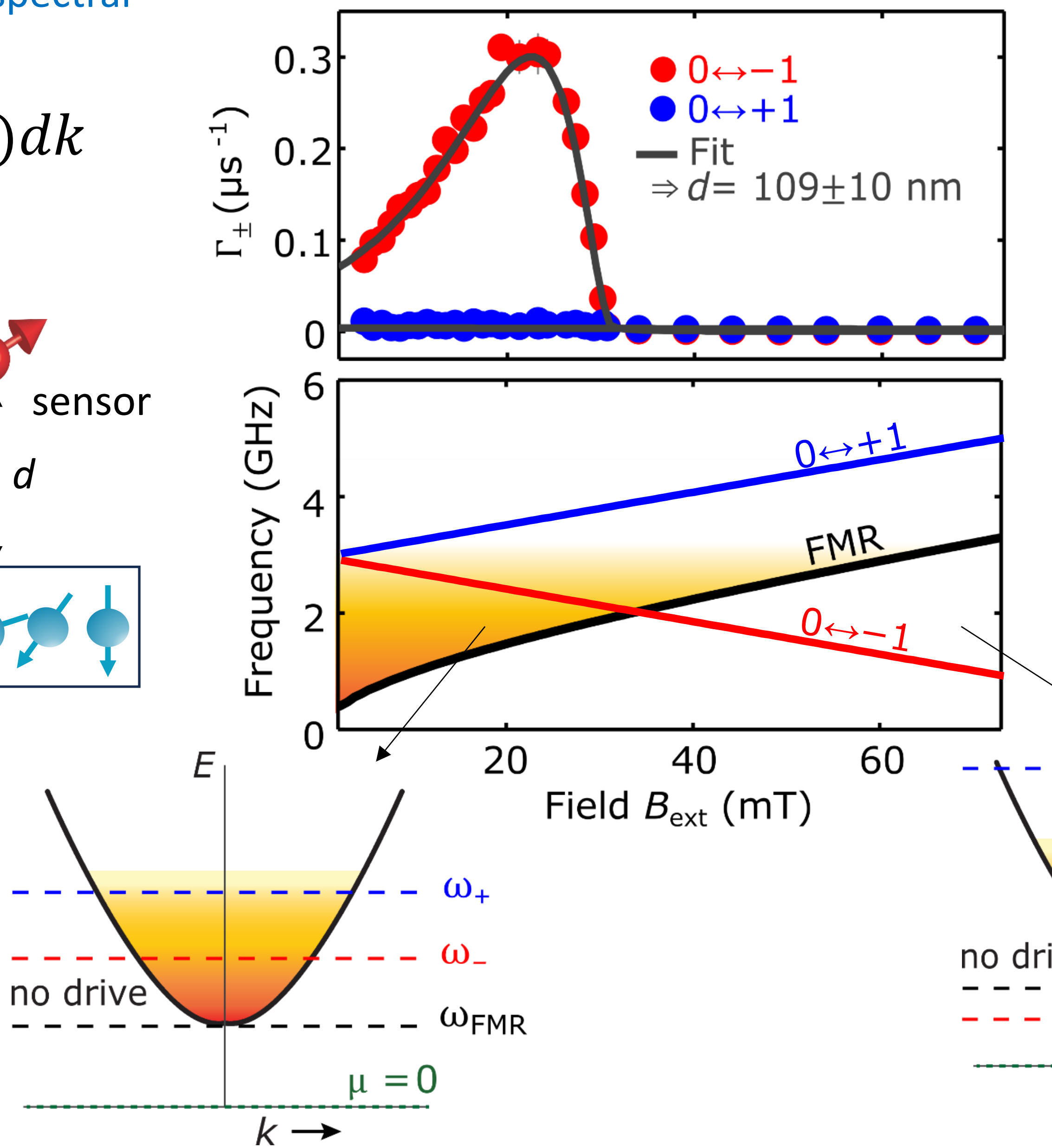

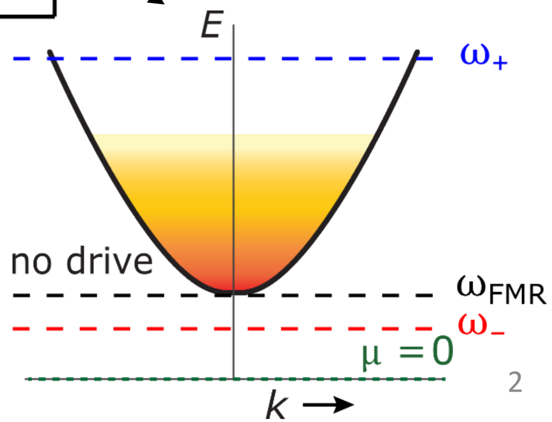

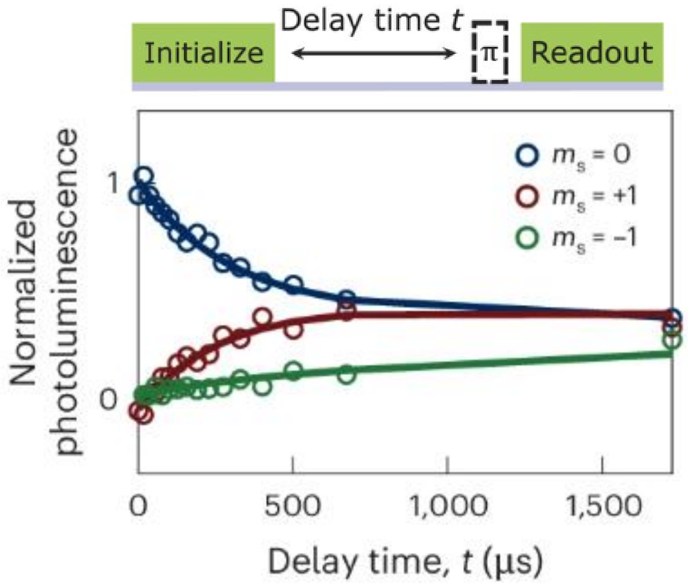

C. Du et al., *Science* **357**, 195 (2017)

NV relaxation rate due to FMR drive

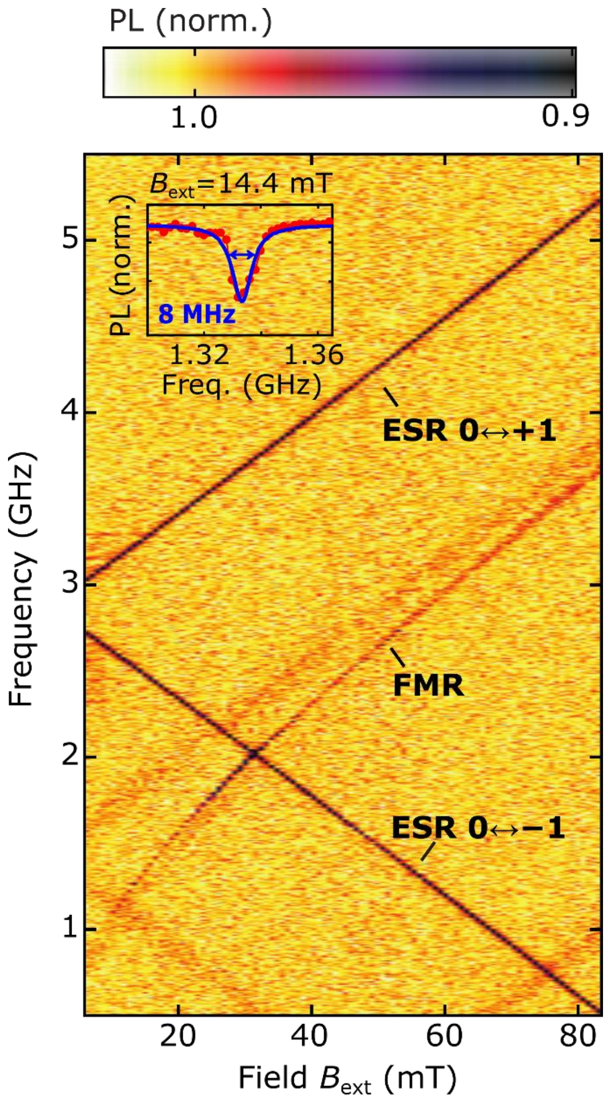

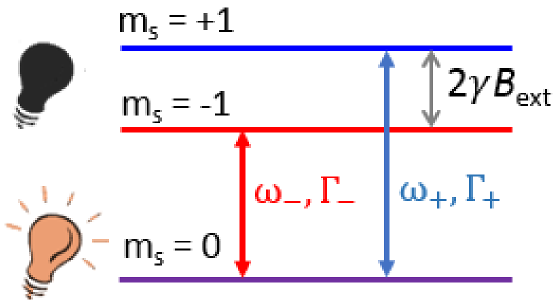

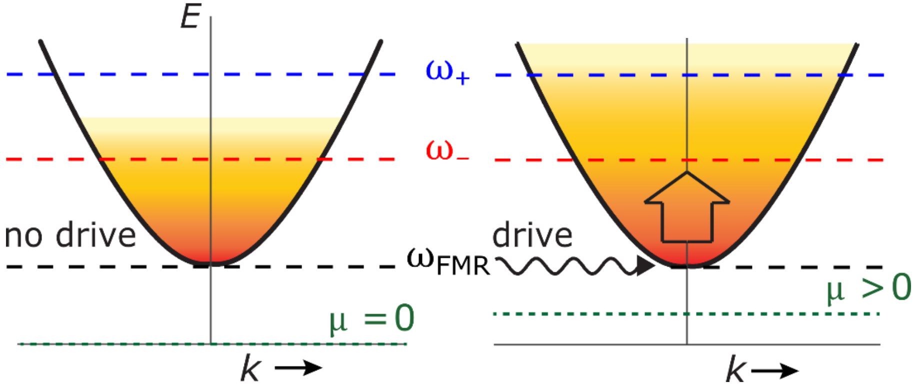

- FMR drive increases magnon density at NV frequency due to four magnon scattering process, increasing NV relaxation rate and decreasing NV PL

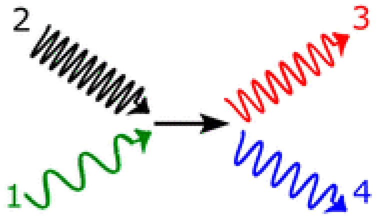

Four-magnon scattering process

C. Du et al., *Science* **357**, 195 (2017)

FMR vs parametric drive

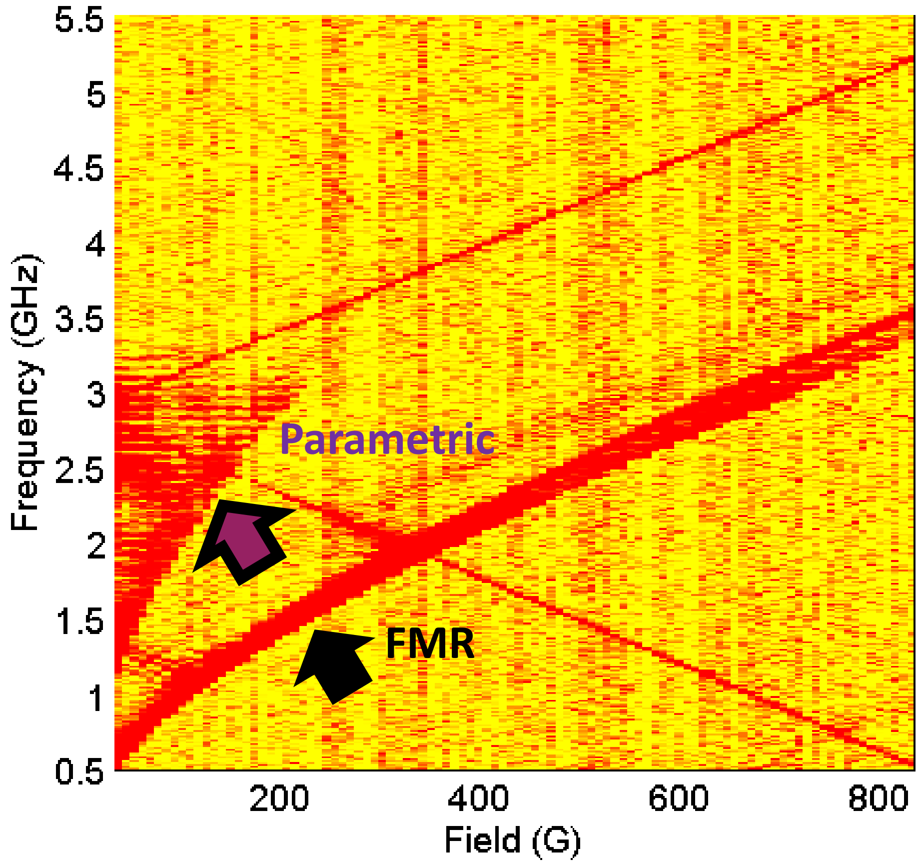

Drive at higher power

Parametric excitations ($k > 0$)

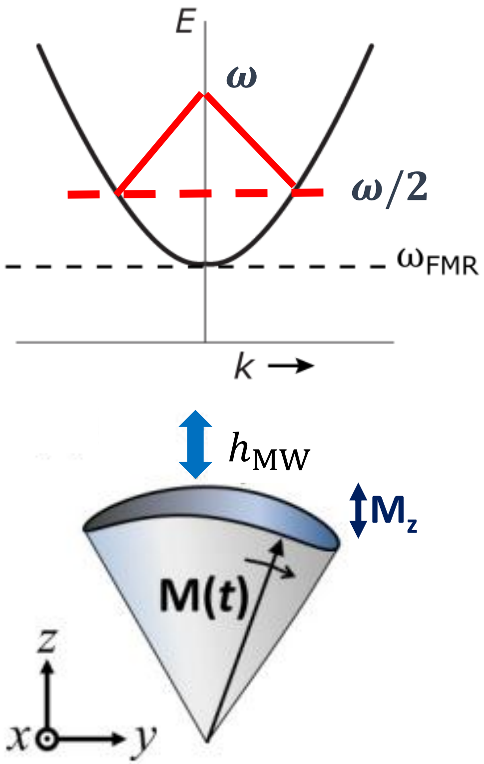

Phys. Rev. B. **89**, 104422 (2014)

E. Lee-Wong *et al.*, *Nano Lett.* **20**, 3284 (2020)

Magnon excitations with variable wavevectors

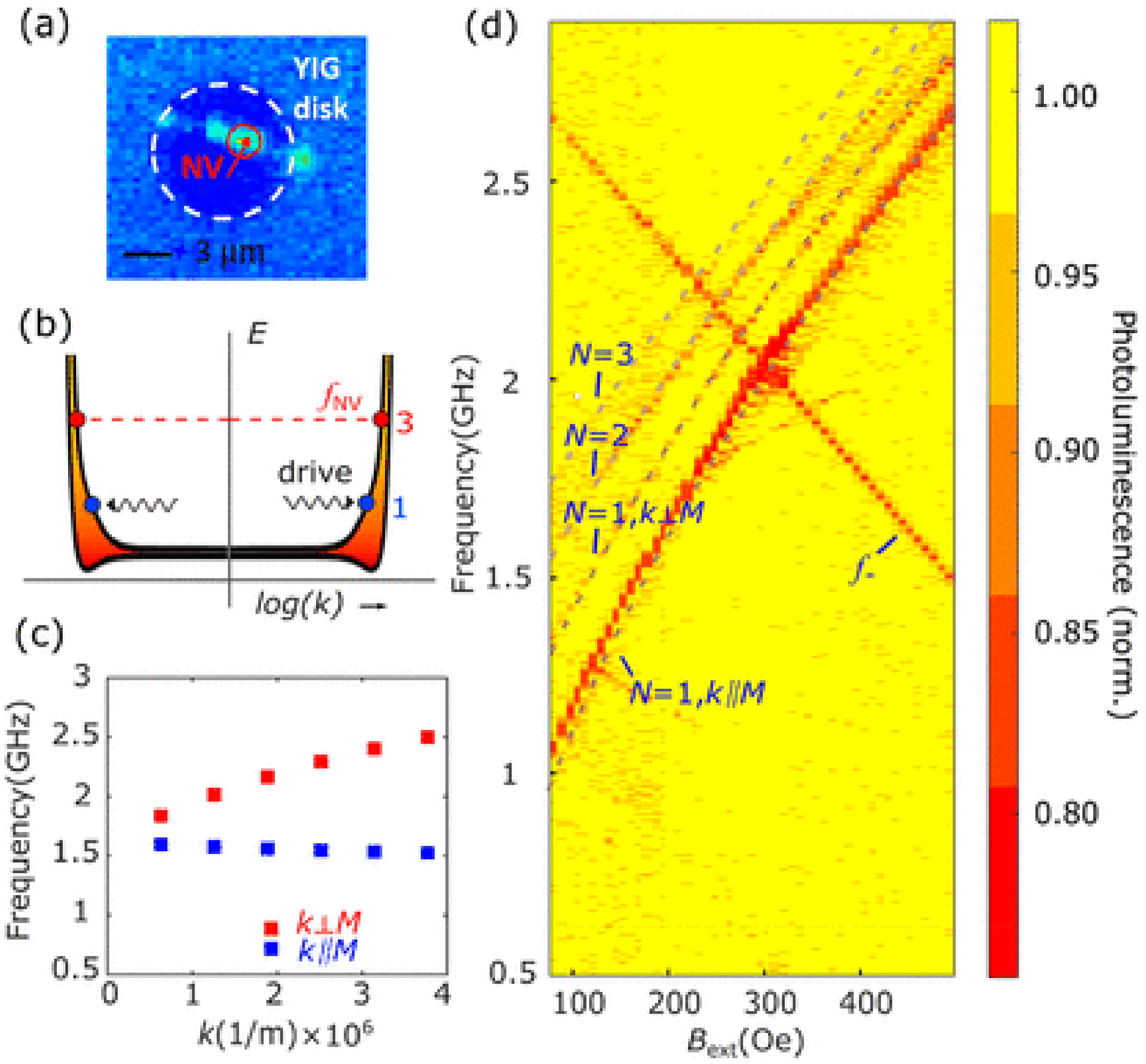

Micromagnetic Simulation

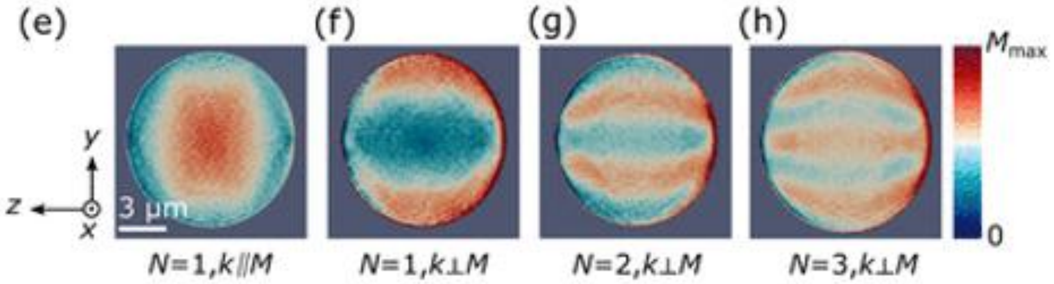

- Confined by the size of the disk, only discrete values of the wavevectors $k = N\pi/R$ are allowed. N is an integer and R is the radius of disk.

E. Lee-Wong *et al.*, *Nano Lett.* **20**, 3284 (2020)

Probing spin fluctuations of AF (FM) using NV relaxation rate measurement

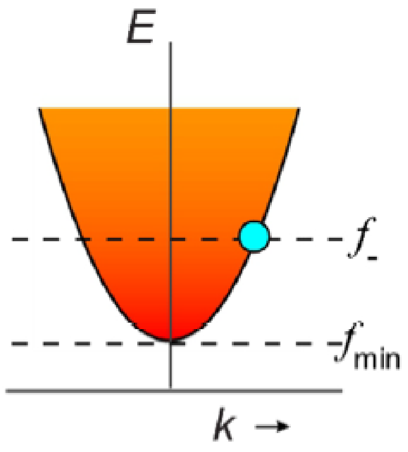

One magnon noise

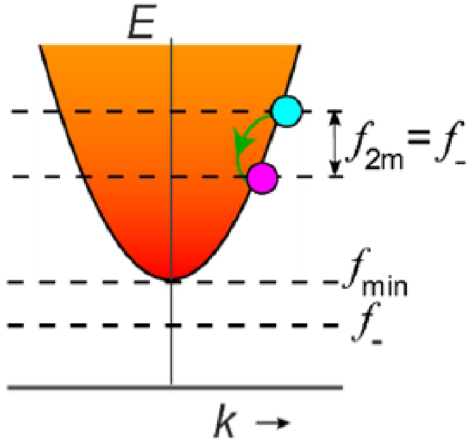

Two-magnon noise

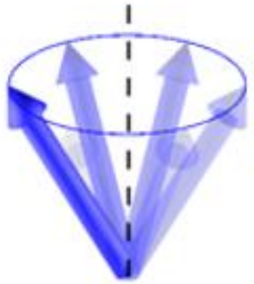

Transverse spin fluctuation

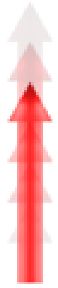

Longitudinal spin fluctuation

Works for most magnets with large exchange energy and the uniaxial magnetic anisotropy, such as CrI_3, $CrPS_4$, MBT, Fe_2O_3 etc…

Longitudinal spin fluctuation induced NV relaxation rate:

Diffusive transport:

$$\partial_t s_\parallel - D\nabla^2 s_\parallel = -\frac{1}{\tau_s} s_\parallel$$

Spin diffusion constant

Fluctuation-dissipation theorem:

magnetic susceptibility

$$\Gamma_\pm(f_\pm) = \frac{(\gamma\tilde{\gamma})^2 k_B T}{2\pi f_\pm}\int f(\mathbf{k},d)\,\chi''(\,D,\chi_0)\,d\mathbf{k}$$

filter function

dynamic spin susceptibility

B. Flebus et al., *Phys. Rev. Lett.* **121**, 187204 (2018)

Yaroslav Tserkovnyak (UCLA)

Shu Zhang (OIST)

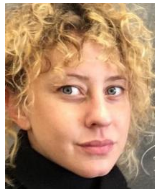

Benedetta Flebus (BC)

We can locally probe:

- Spin transport properties noninvasively
  H. L. Wang, … C. H. Du, *Science Advances* **8**, eabg8562 (2022)
- Magnetic phase transition temperature
  N. McLaughlin…C. H. Du, *Nano Letters* **22**, 5810 (2022)

Noninvasive quantum sensing of spin transport of an antiferromagnetic (AF) insulator

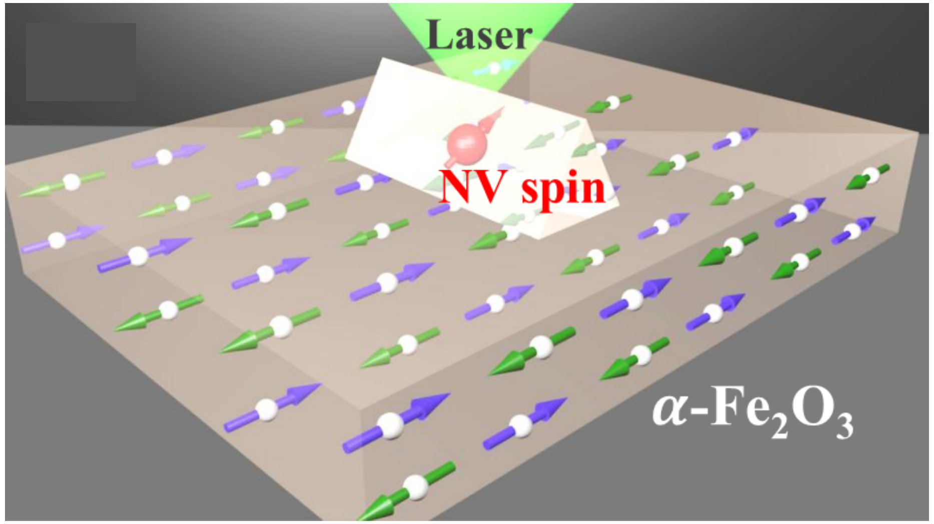

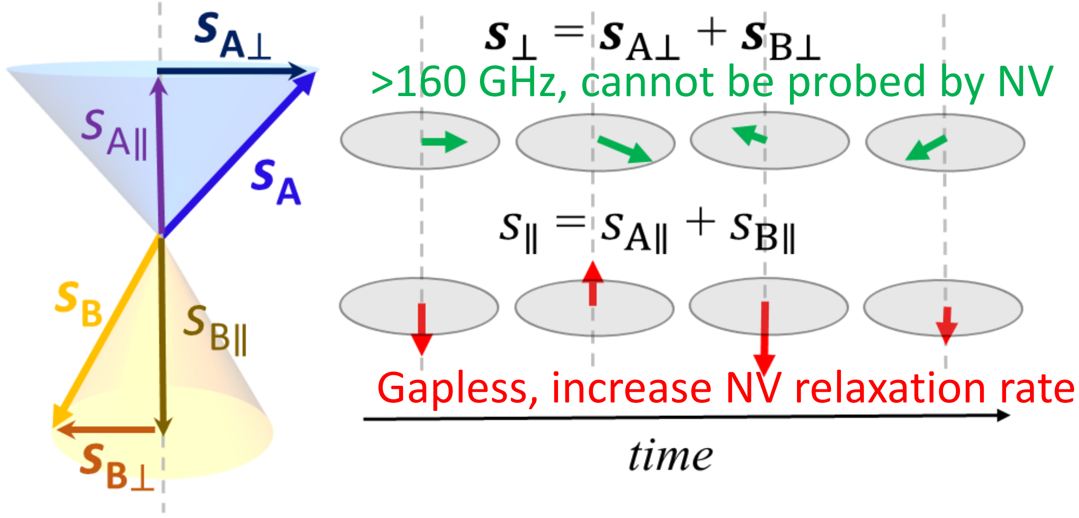

H. L. Wang, … C. H. Du, *Science Advances* **8**, eabg8562 (2022)

Diffusive transport:

$$\partial_t s_\parallel - D\nabla^2 s_\parallel = 0$$

D is spin diffusion constant

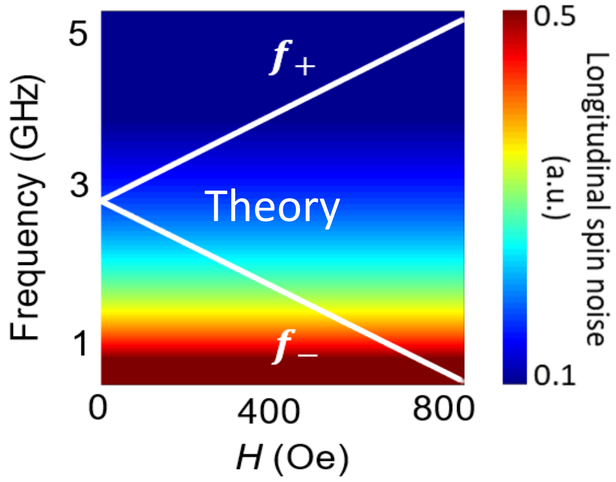

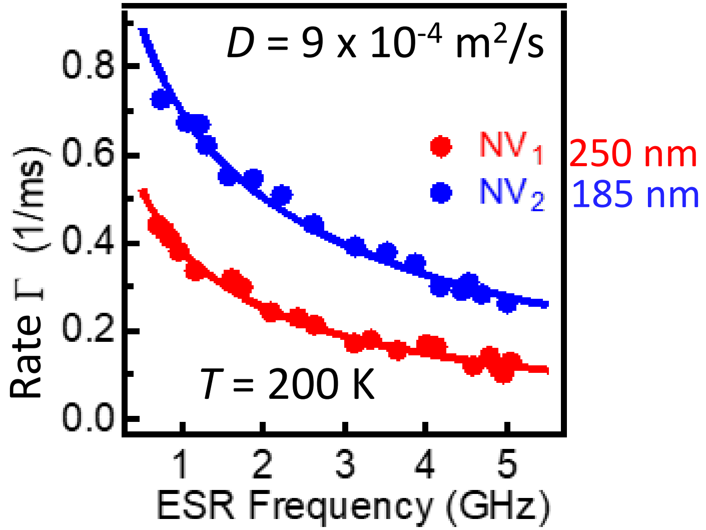

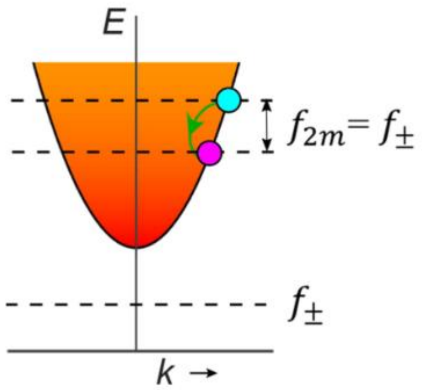

Spin diffusion length $\lambda = \sqrt{D\tau_s} \sim 3\ \mu m$ (for τ_s = 10 ns)

Agree with transport results

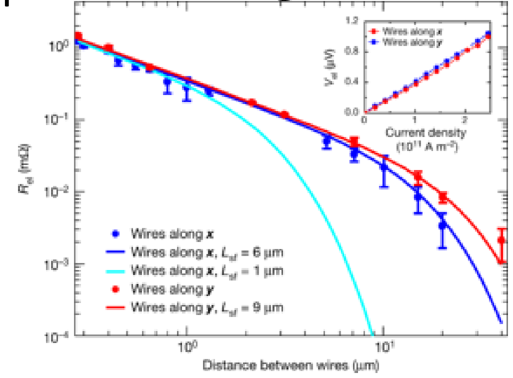

R. Lebrun et al., *Nature* **561**, 222 (2018)

Observation of two very distinct phase transitions within a moiré supercell

Twisted double trilayer (tDT) CrI_3 (Twist angle ~ 0.25 deg)

Liuyan Zhao
(U Michigan)

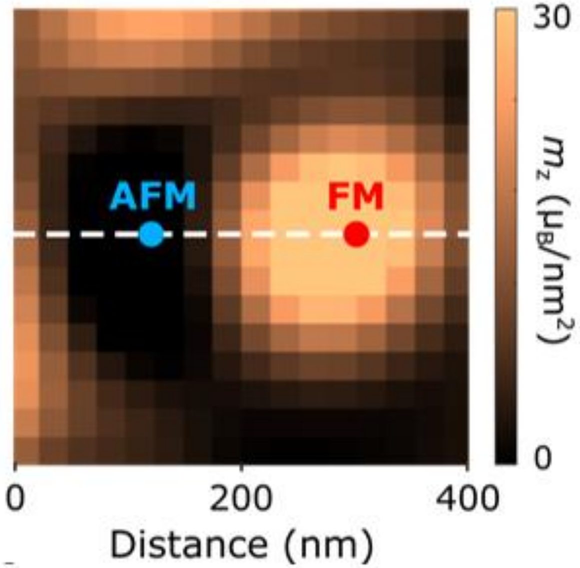

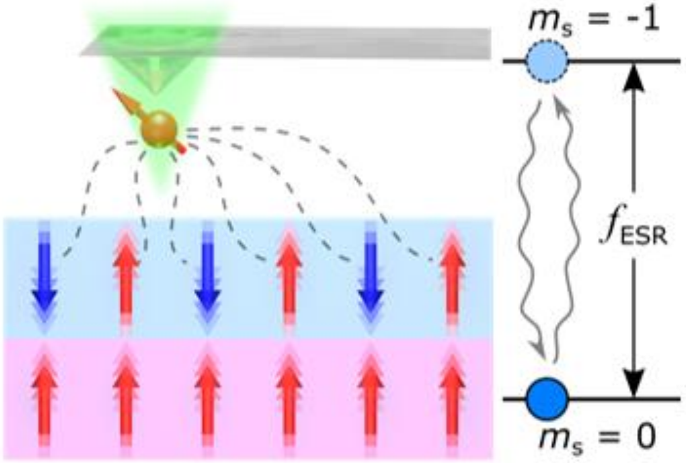

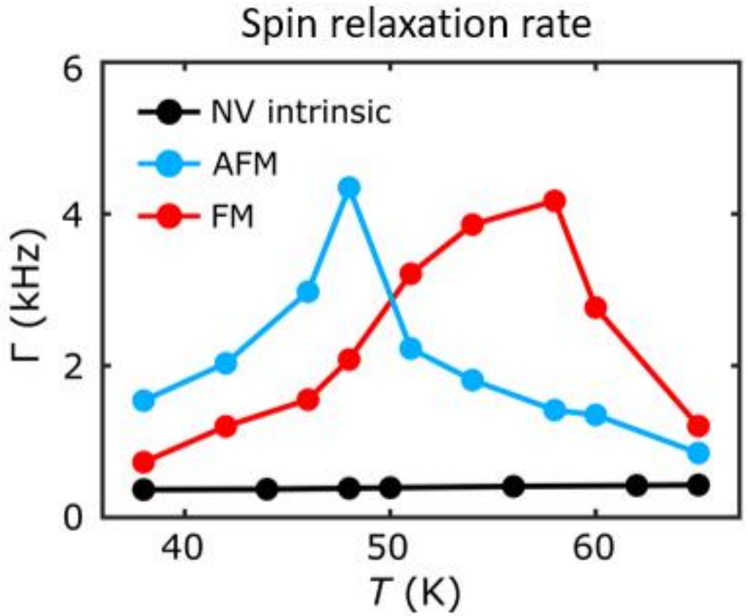

- We measure local spin fluctuations in 0.15° tDT CrI_3 using NV spin relaxometry measurement
- NV relaxation rate reaches a peak value at T_c due to enhanced magnetic susceptibility
- FM region exhibit a much higher T_c up to ~58 K in comparison with that of ~48 K for AFM areas

S. Li et al., *Nature Communications* **15**, 5712 (2024)

Stacking engineered magnetic phase transitions within moiré supercells

Twist angle
~0.15 deg
tDT

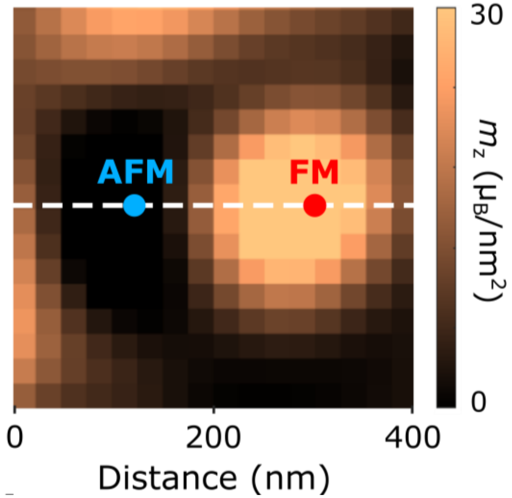

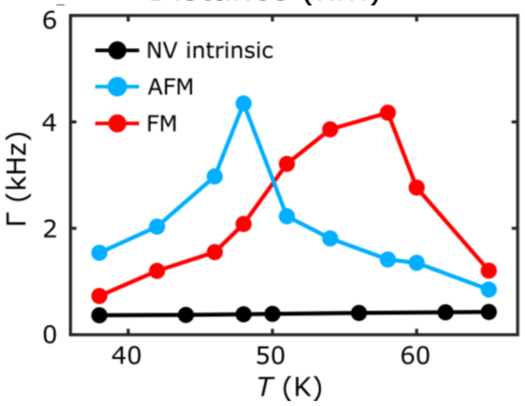

$J_R > J_M$ [*Nano. Lett.* **18**, 7658–7664 (2018)]

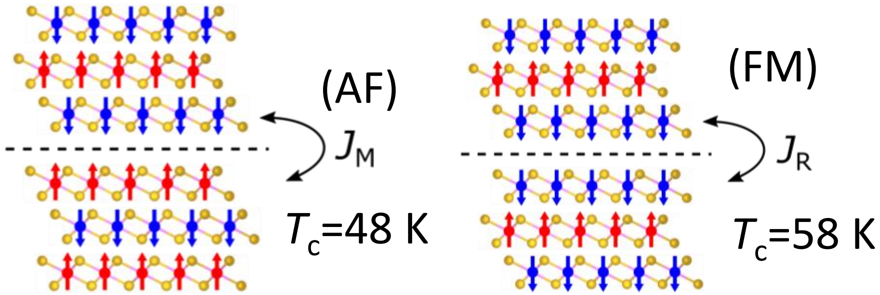

Bulk CrI_3

R stacking (FM)

T_c~ 61 K

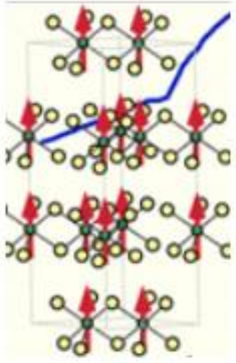

M. A. McGuire et al., *Chem. Mater.* **27**, 612 (2015)

Pristine 3L CrI_3

M stacking (AF)

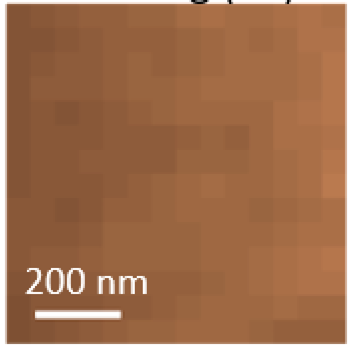

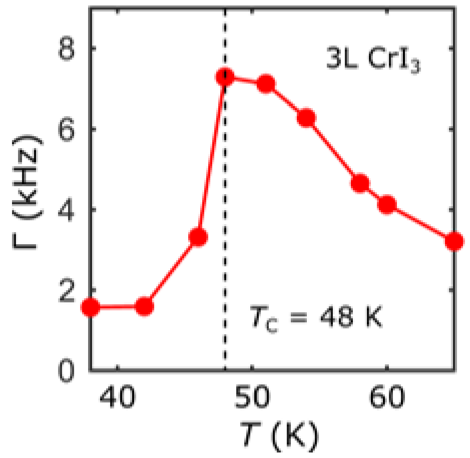

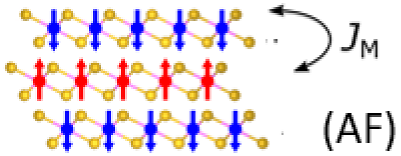

Layer-resolved magnetic phases of small-twist-angle tDT CrI_3 with different stacking orders

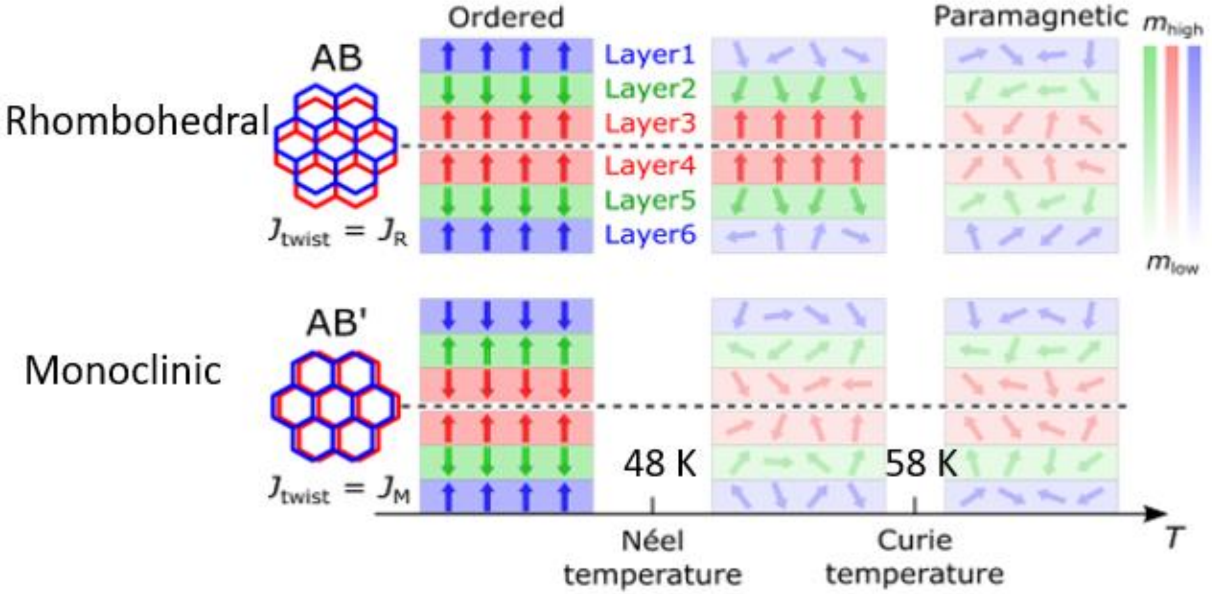

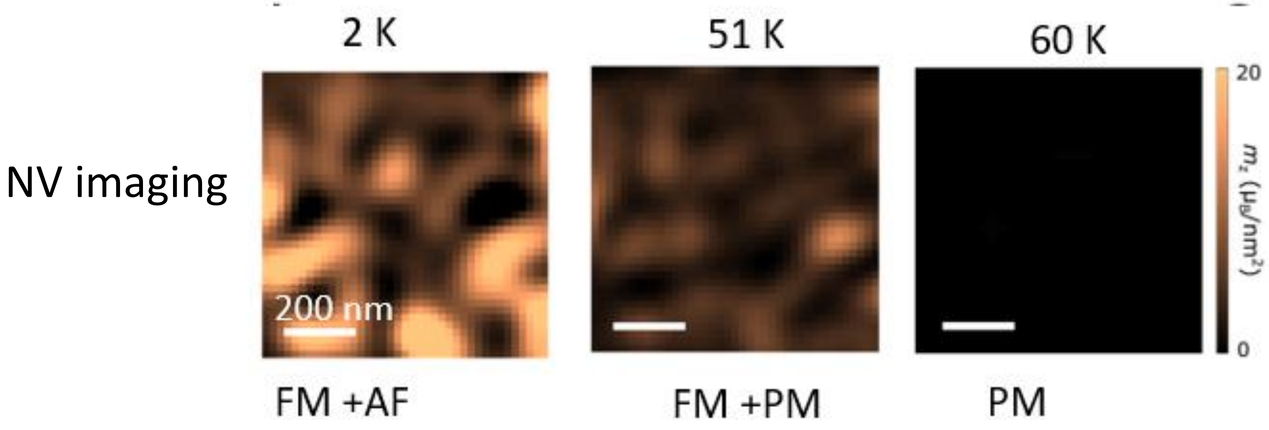

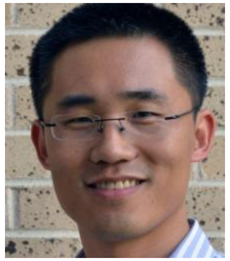

Hua Chen (Colorado state U)

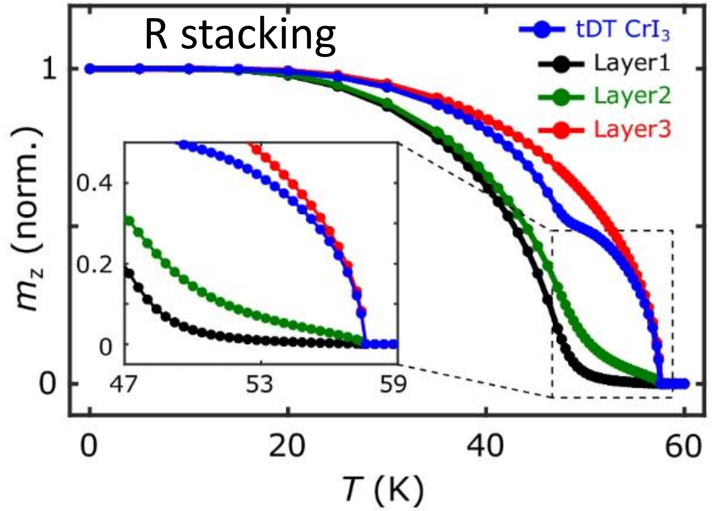

Mean-field theory calculations

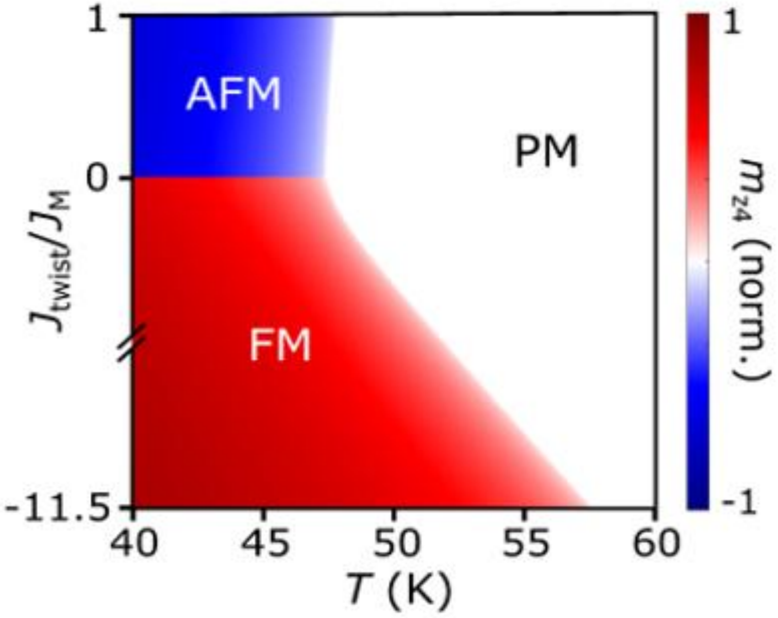

- At R stacking site, middle CrI_3 layer (layer 3) exhibits a higher T_c
- As the magnitude of the FM-like coupling J_{twist} increases, T_c enhances

S. Li et al., *Nature Communications* **15**, 5712 (2024)

Part 3: Emerging quantum sensing platforms and hybrid quantum devices

- ❑ ***Quantum sensing of magnetic noise in metal and superconductor***
- ❑ ***Quantum sensing in 2D hBN***
- ❑ ***Hybrid quantum devices***

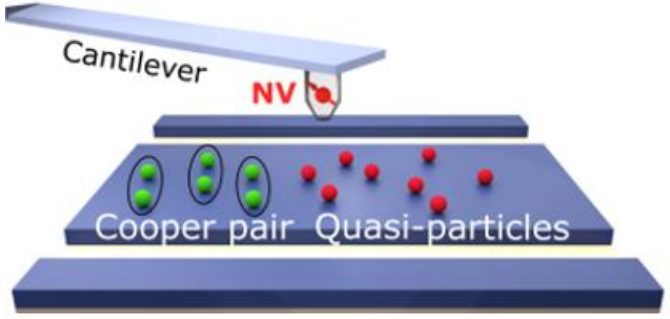

S. Li et al., *Phys. Rev. Lett.* **136**, 076004 (2026)

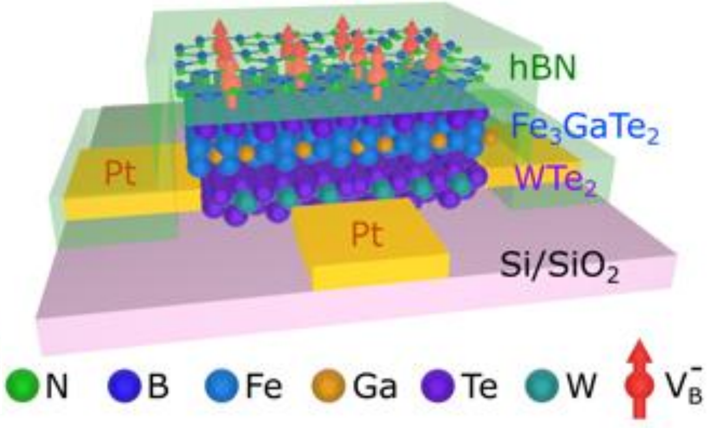

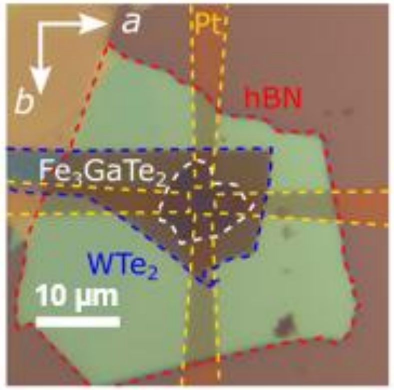

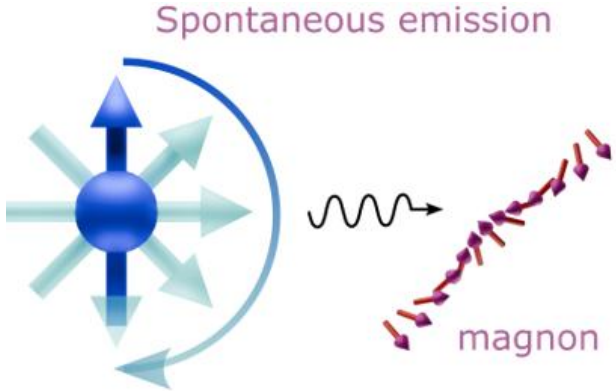

X. Zhang et al., Nature Communications (2026) arXiv:2502.04561

L. Zhou et al., arXiv:2606.20996 (2026)

Quantum sensing of Johnson noise

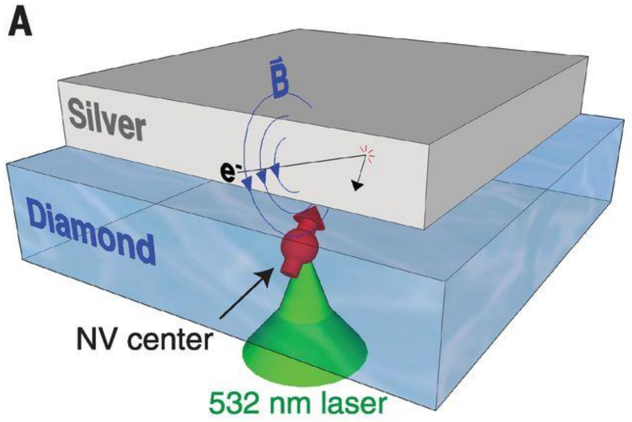

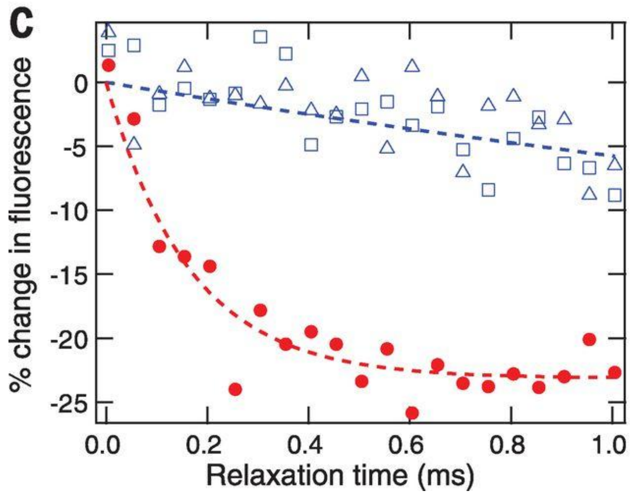

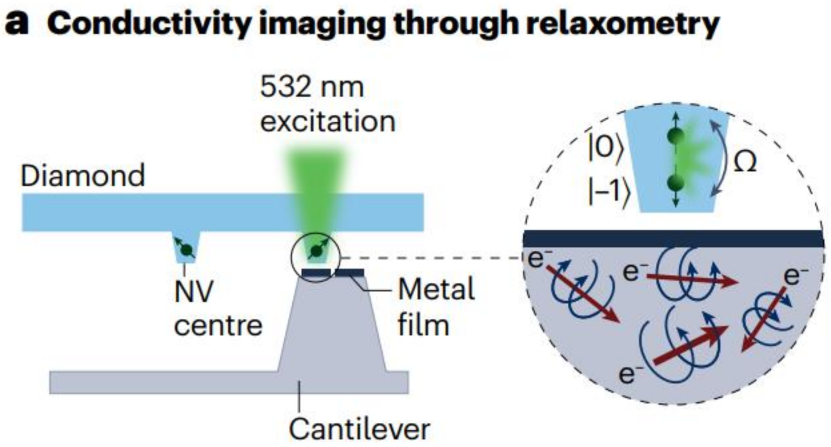

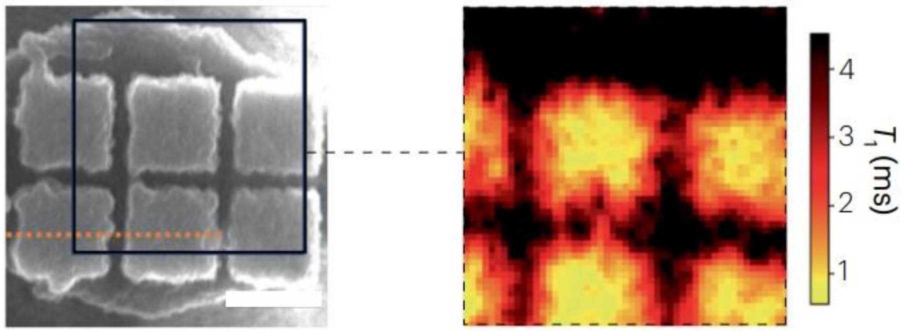

$$\Gamma = \frac{1}{T_1} = \frac{3g^2\mu_B^2}{2\hbar^2} S_B^z \left(1 + \frac{1}{2}\sin^2(\theta)\right) \qquad S_B^z = \frac{\mu_0^2}{16\pi}\frac{k_B T \sigma}{d}$$

Conductivity of the metal

J. Rovny et al., *Nat. Rev. Phys.* **6**, 753 (2024)
S. Kolkowitz et al., *Science* **347**, 1129 (2015)

Quantum sensing of superconducting resonator

- **Superconducting resonators are utilized to readout/couple qubit states and perform quantum sensing experiments**

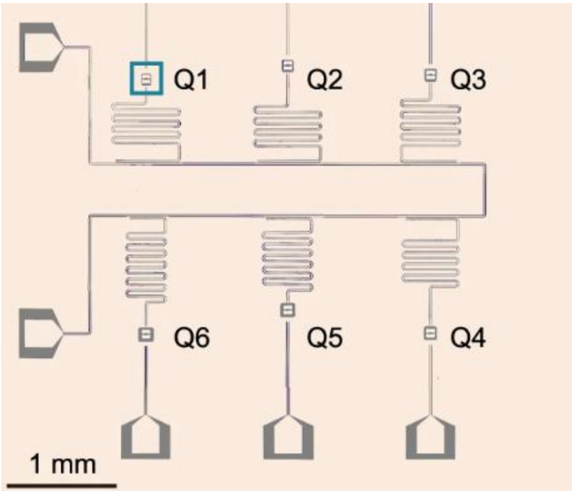

X. Pan *et al. Nat Commun.* **13**, 7196 (2022).

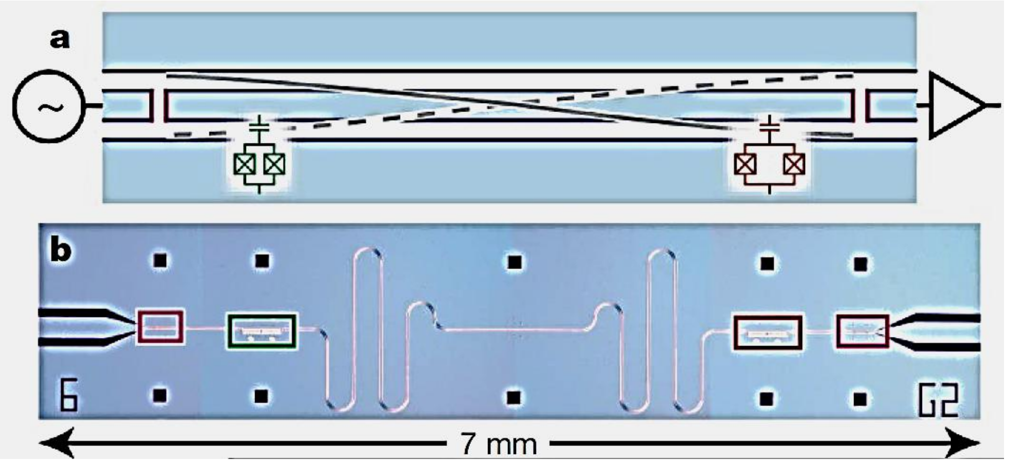

J. Majer *et al.*, *Nature* **449**, 443 (2007)

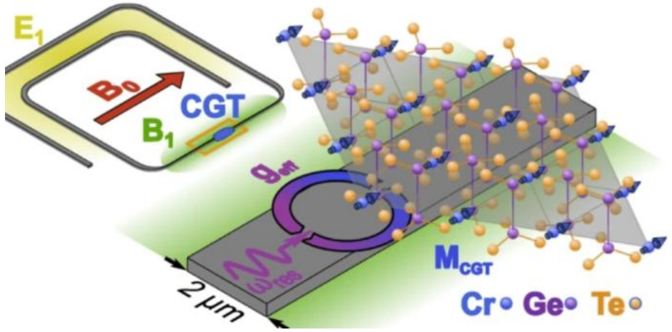

C. W. Zollitsch et al., *Nat Commun.* **14**, 2619 (2023)

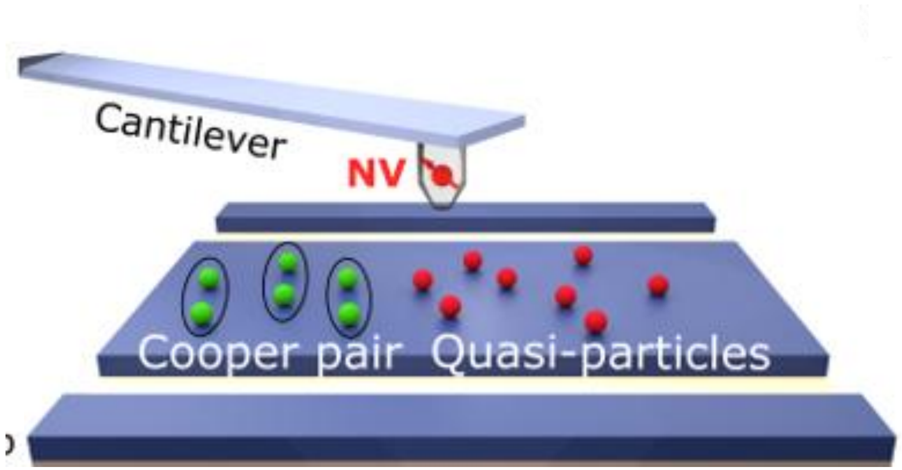

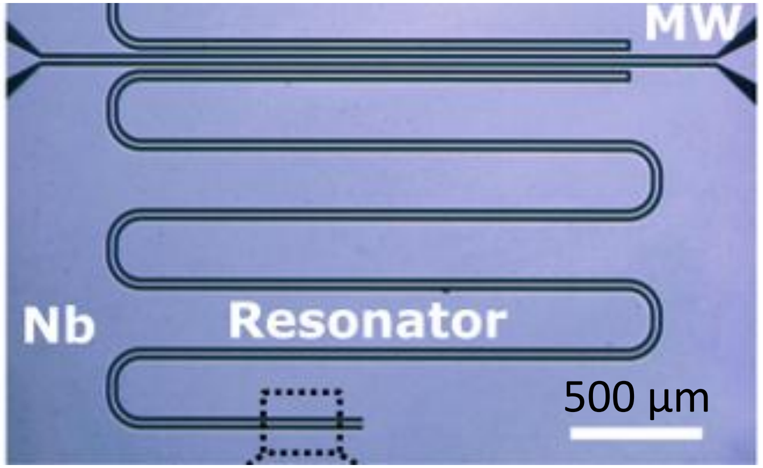

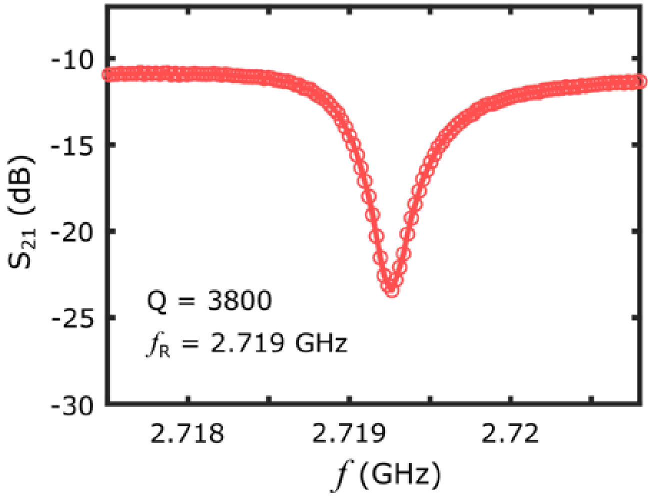

S. Li et al., *Phys. Rev. Lett.* **136**, 076004 (2026)

Quantum sensing of superconducting resonator

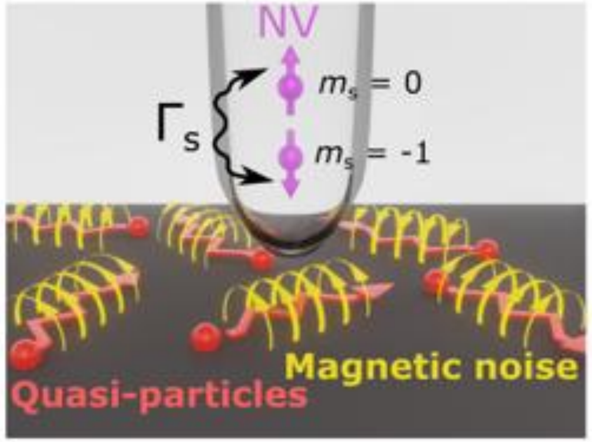

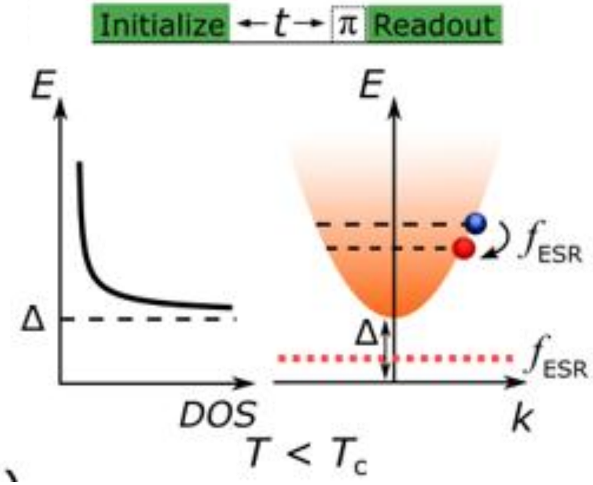

- **Quantum sensing of quasiparticle-generated magnetic noise in Nb resonator in thermal equilibrium condition**

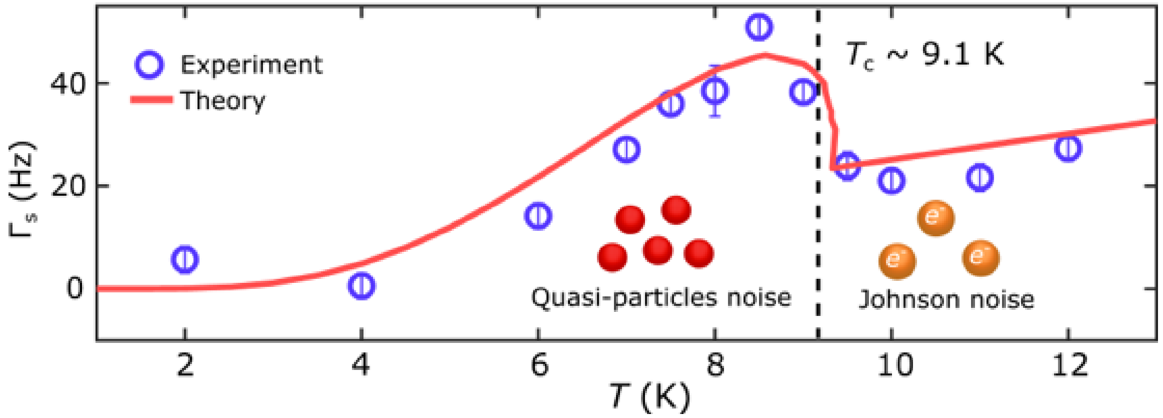


Yaroslav Tserkovnyak


Shane Kelly

- **We observed Hebel-Slichter peak signature by an external sensor outside of a superconductor**.

S. Li et al., *Phys. Rev. Lett.* **136**, 076004 (2026); Theory arXiv.2412.05465 (2024).

Quantum sensing of superconducting materials

s wave Nb

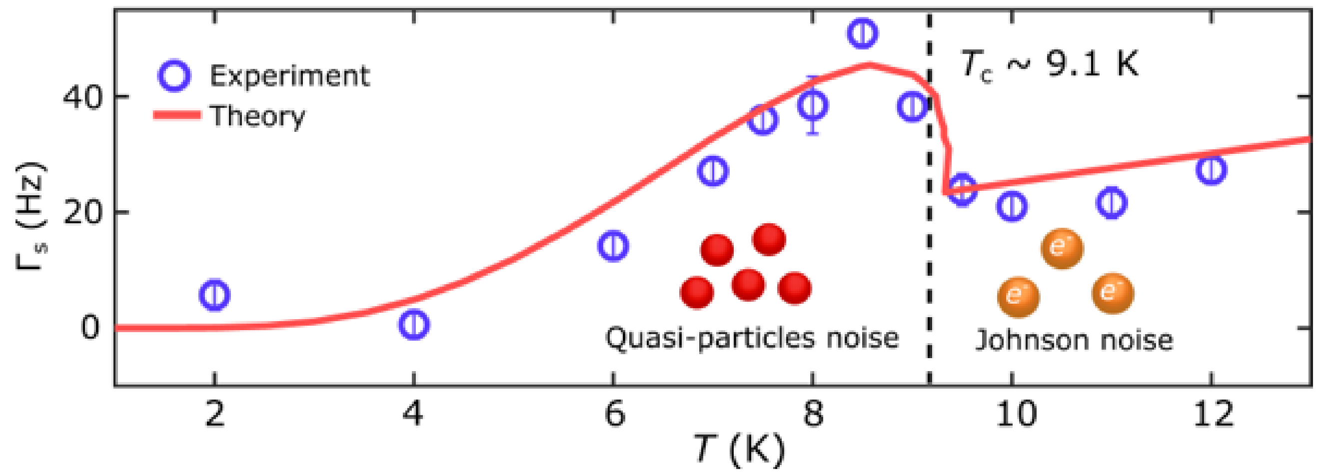

S. Li et al., *Phys. Rev. Lett.* **136**, 076004 (2026); Theory arXiv.2412.05465 (2024).

Probing pairing symmetry:

- For a s-wave (gapped) superconductor, magnetic noise gets suppressed exponentially at low temperature
- For a *d*-wave (nodal) superconductor, quasiparticle induced magnetic noise follows T^2 dependence

Probing Berezinskii-Kosterlitz-Thouless vortex unbinding transition and time reversal symmetry breaking:

J. B. Curtis et al., *Phys. Rev. B* **110**, 144518 (2024); S. De et al., *Phys. Rev. X* **16**, 011001 (2026)

d wave BSCCO

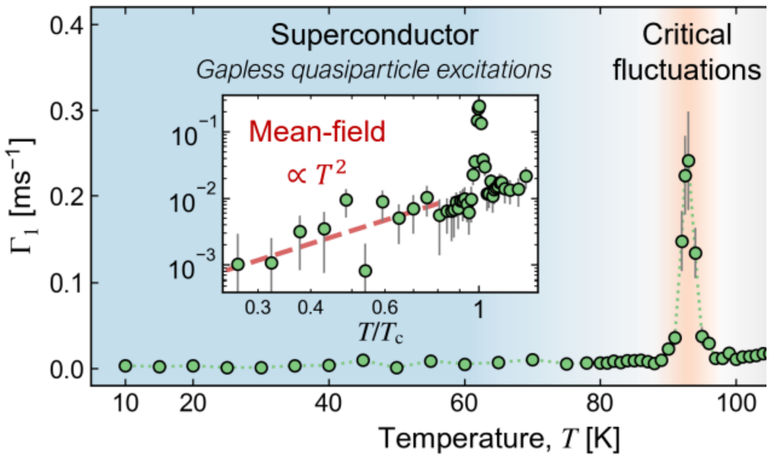

Z. Liu et al., arxiv. 2502.04439 (2025)

Nanoscale observation and control of quasiparticle induced magnetic noise

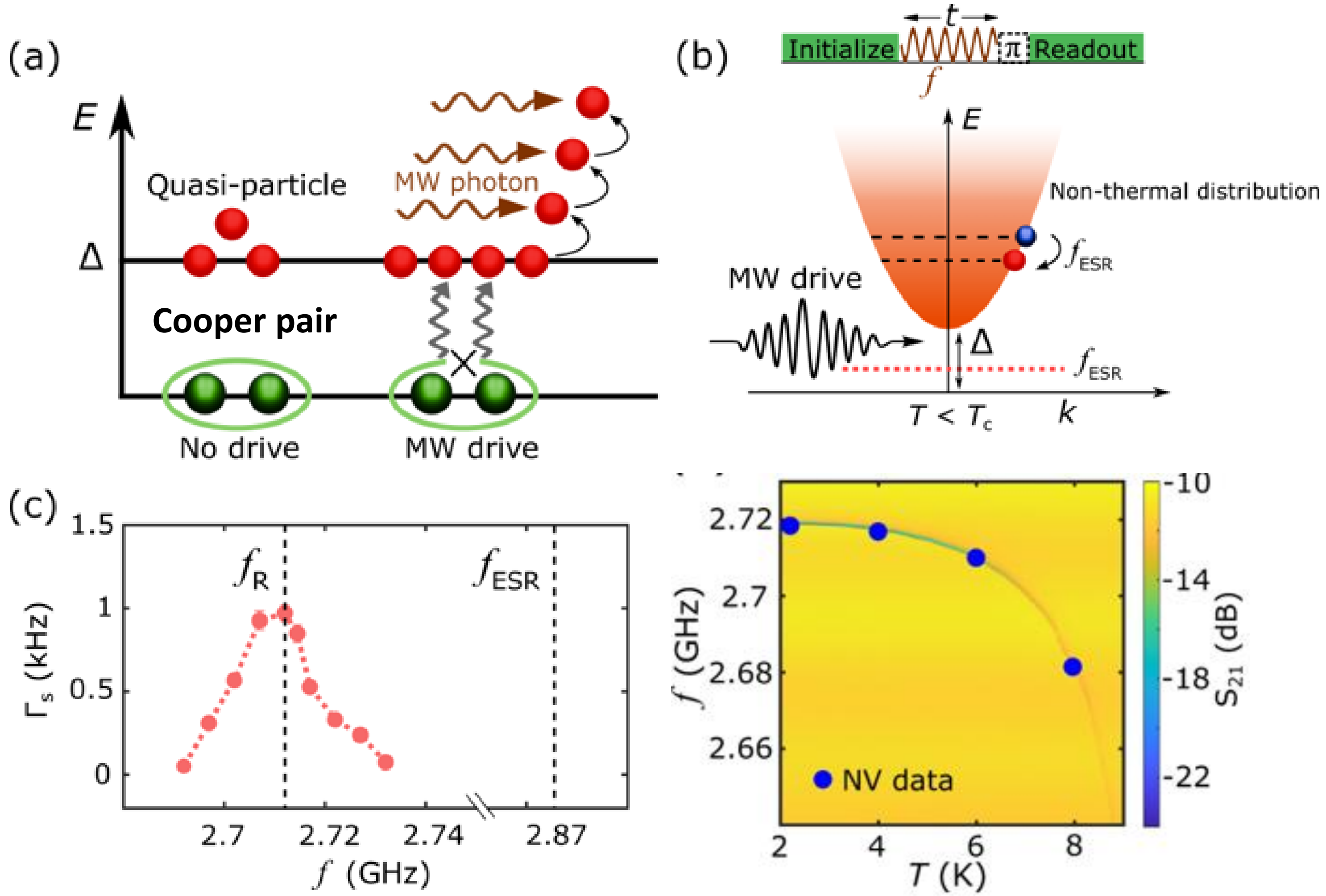

- **External microwave drive at f_R significantly increased the quasiparticle density and magnetic noise.**
- **Allow local detection of resonator mode.**

S. Li et al., *Phys. Rev. Lett.* **136**, 076004 (2026)

Quantum sensors in 2D materials

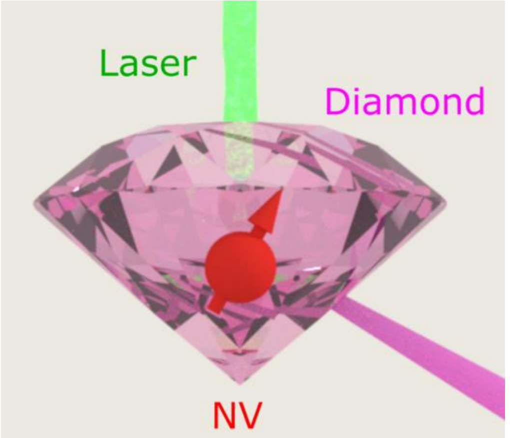

Spin defect in diamond **(3D)**

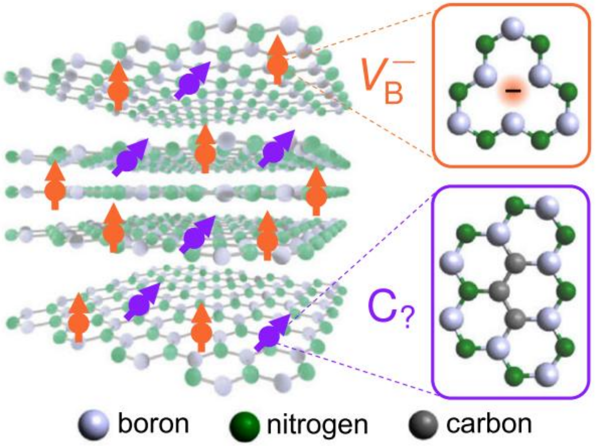

Spin defect in hBN **(2D)**

Gottscholl, A. et al. Nat. Mater. **19**, 540 (2020)
Gao, X. et al. *Nat. Mater.* **21**, 1024 (2022)
H. Stern et al., *Nat. Mater.* **23**, 1379–1385 (2024)

Distance > = 50 nm

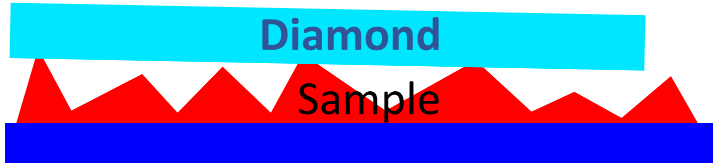

Atomic scale detection sensitivity and imaging resolution?

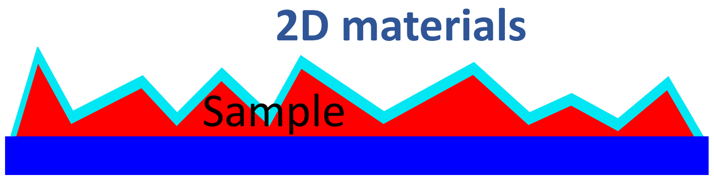

- Advantage of closer sample-sensor distance:
  - ❑ Large signal
  - ❑ Sensitivity to higher *k*

Fluctuation-dissipation theorem:

$$\Gamma_\pm(f_\pm) = \frac{(\gamma\tilde{\gamma})^2 k_B T}{2\pi f_\pm}\int f(\mathbf{k},d)\chi''(D)\mathrm{d}\mathbf{k}$$

filter function — dynamic spin susceptibility

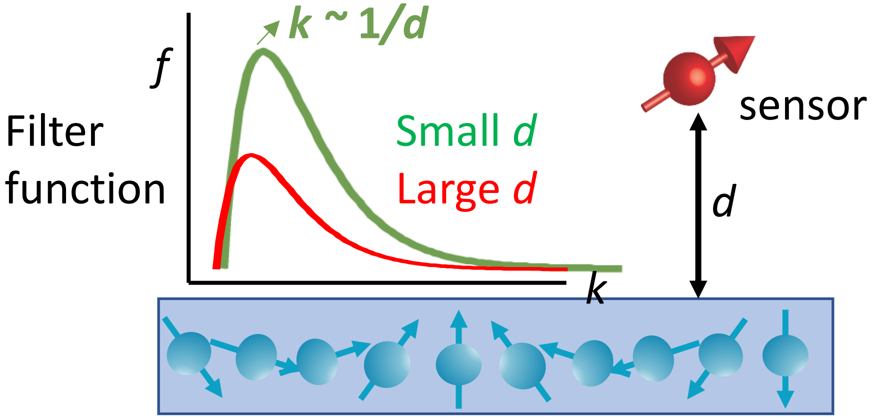

Quantum sensing using spin defect in 3D and 2D materials

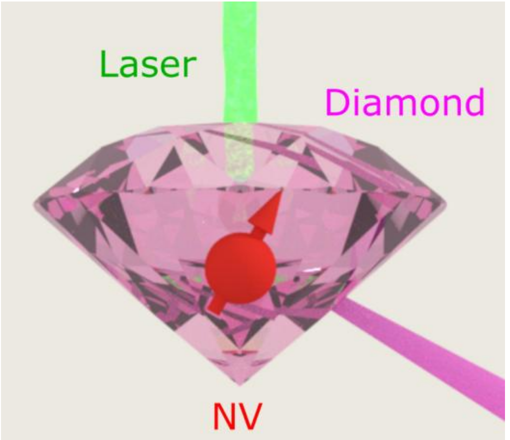

Distance ≥ 50 nm

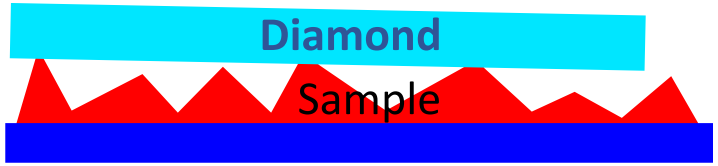

Atomic scale detection sensitivity and imaging resolution?

2D materials

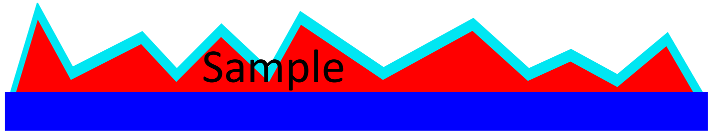

Spin defect in diamond **(3D)**

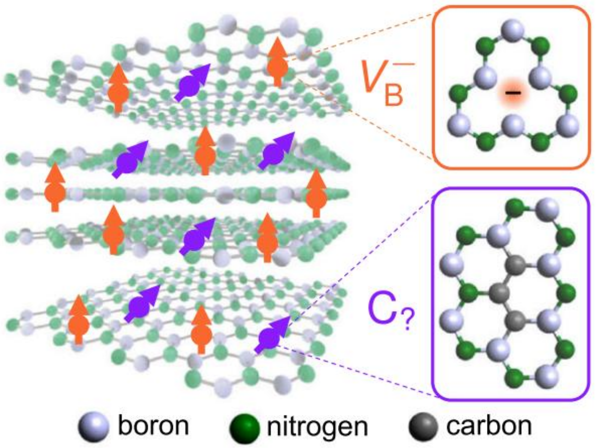

Spin defect in hBN **(2D)**

Gottschol, A. et al. Nat. Mater. **19**, 540 (2020)

Mathur, N. et al. *Nat. Commun.* **13**, 3233 (2022)

Gao, X. et al. *Nat. Mater.* **21**, 1024 (2022)

Clua-Provost, T. et al. *Phys. Rev. Lett.* **131**, 126901 (2023)

Gong, R. et al. *Nat. Commun* **15**, 104 (2024)

H. Stern et al., *Nat. Mater.* **23**, 1379–1385 (2024)

Scholten, S.C. et al. *Nat. Commun.* **15**, 6727 (2024)

ODMR

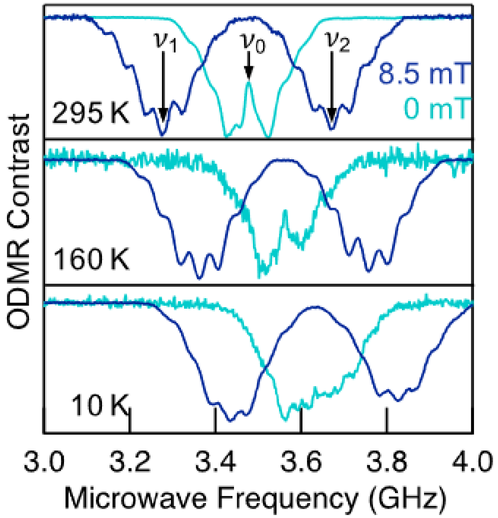

Nat. commun. **12**, 4480 (2021)
Nat. Mater. **19**, 540 (2020)

Rabi oscillation and relaxation

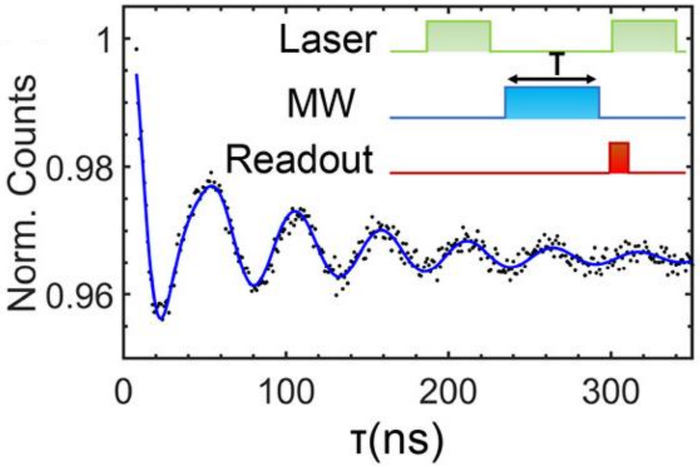

Nano Lett. **21**, 7708 (2021)
Nat. commun. **13**, 5369 (2022)

Quantum sensing based on color centers in 2D and 1D materials

Static stray field

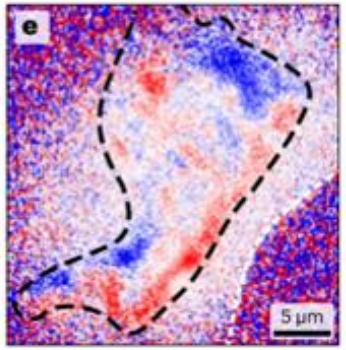

Healey, A.J. et al. *Nat. Phys.* **19**, 87–91 (2023)

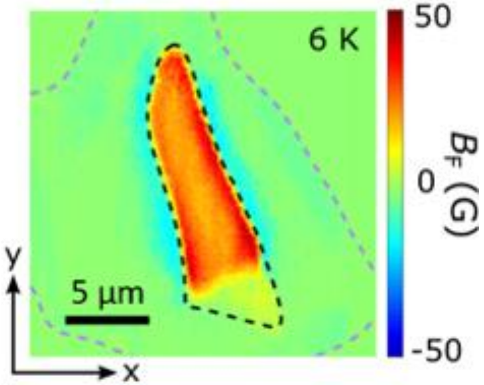

Huang, M. et al. *Nat. Commun.* **13**, 5369 (2022)

Pressure

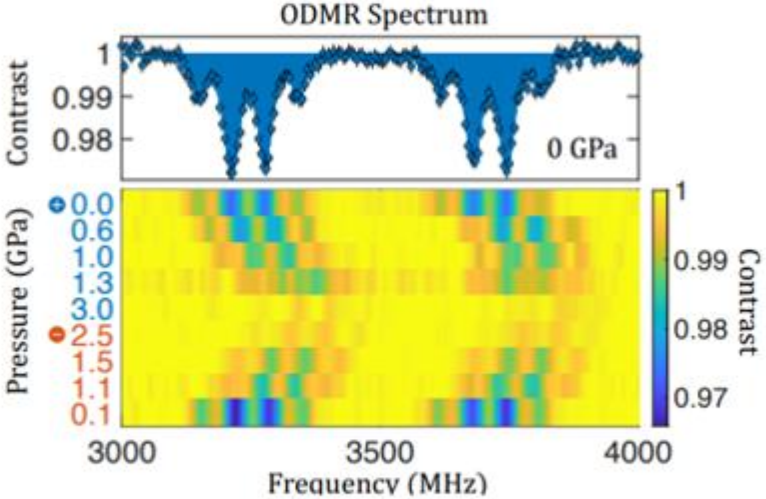

Mu, Z. et al., *Nat. Comm.* **16**, 8574 (2025)
He, G., et al., *Nat. Comm.* 16, 8162 (2025)

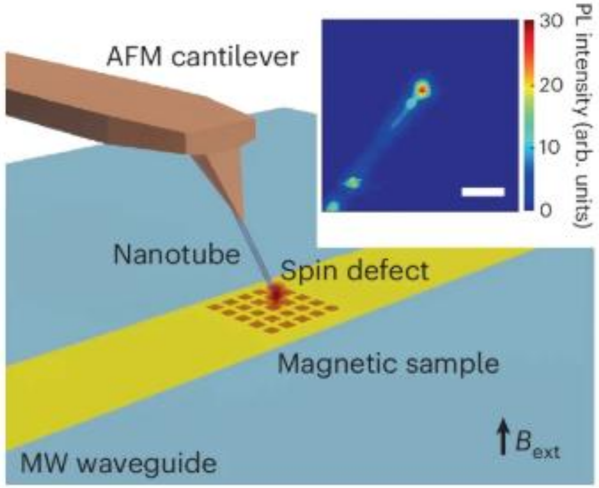

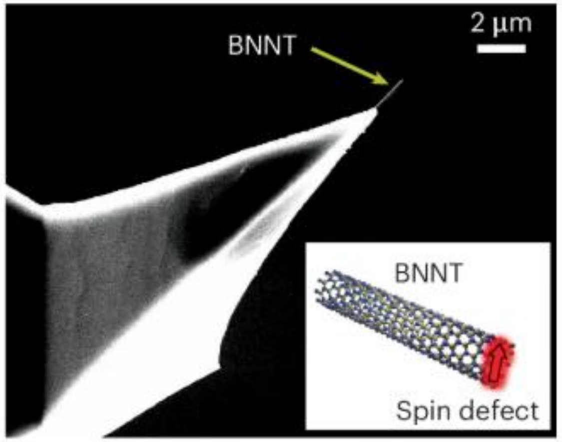

Current

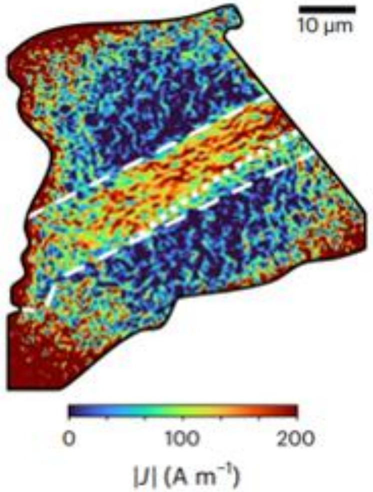

Temperature

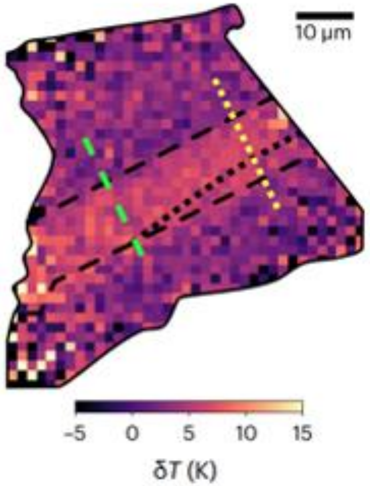

Gao, X. et al. *Nat. Commun.* **15**, 7697 (2024)

Boron vacancy centers in hBN

Carbon defect in BNNT

vdW quantum sensing platform to study spin orbit torque devices

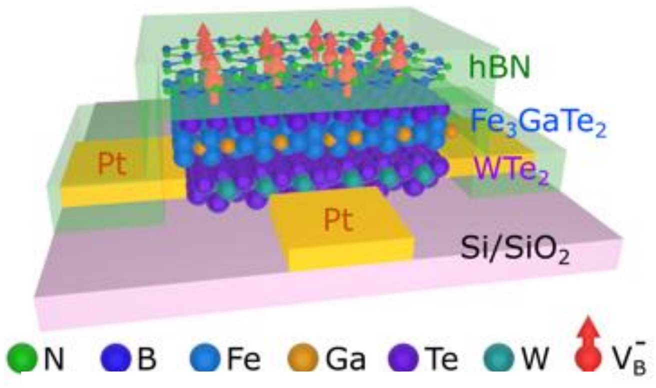

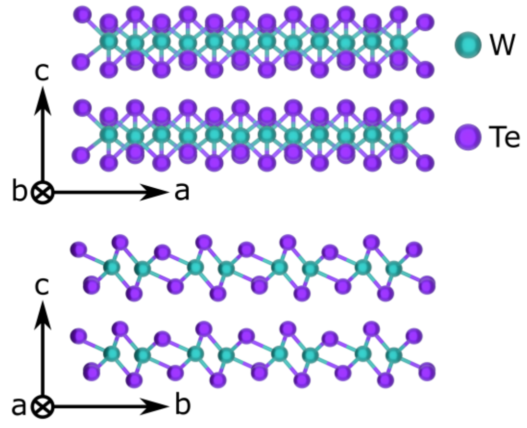

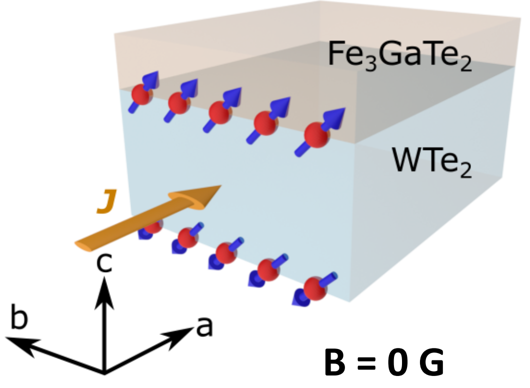

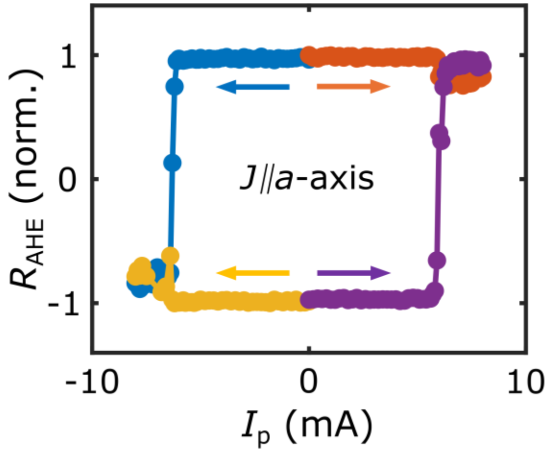

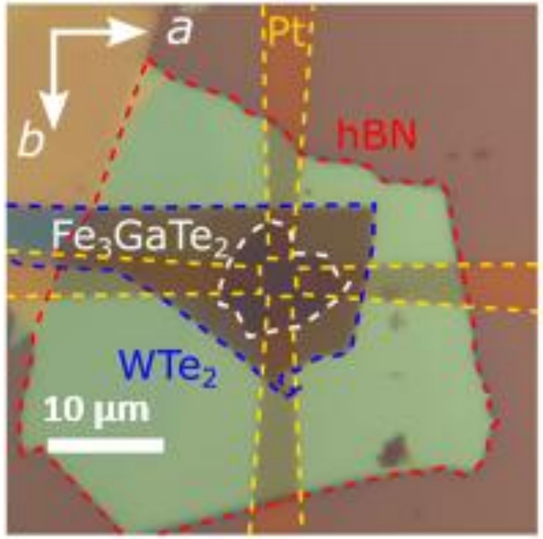

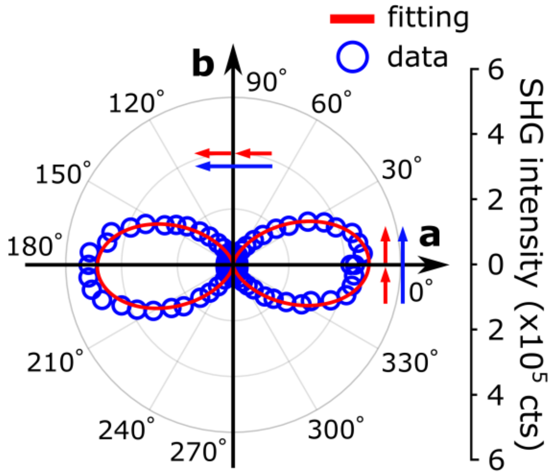

Second Harmonic Generation Measurement

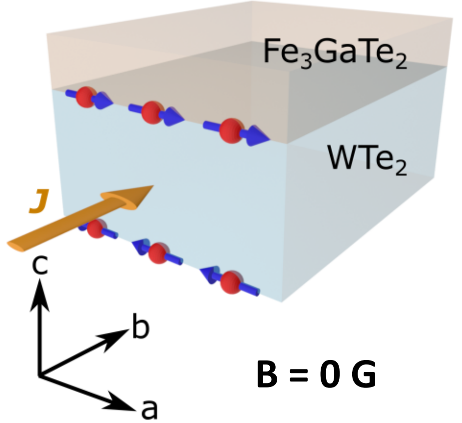

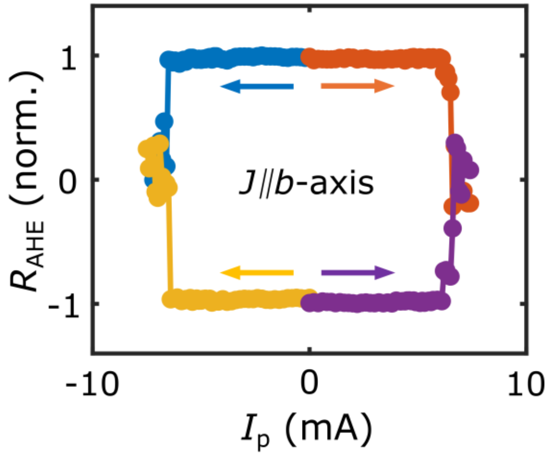

Zhang et al., *arXiv:2502.04561. Nature Communications* (2026)

Nanoscale Imaging of Deterministic Magnetic Switching

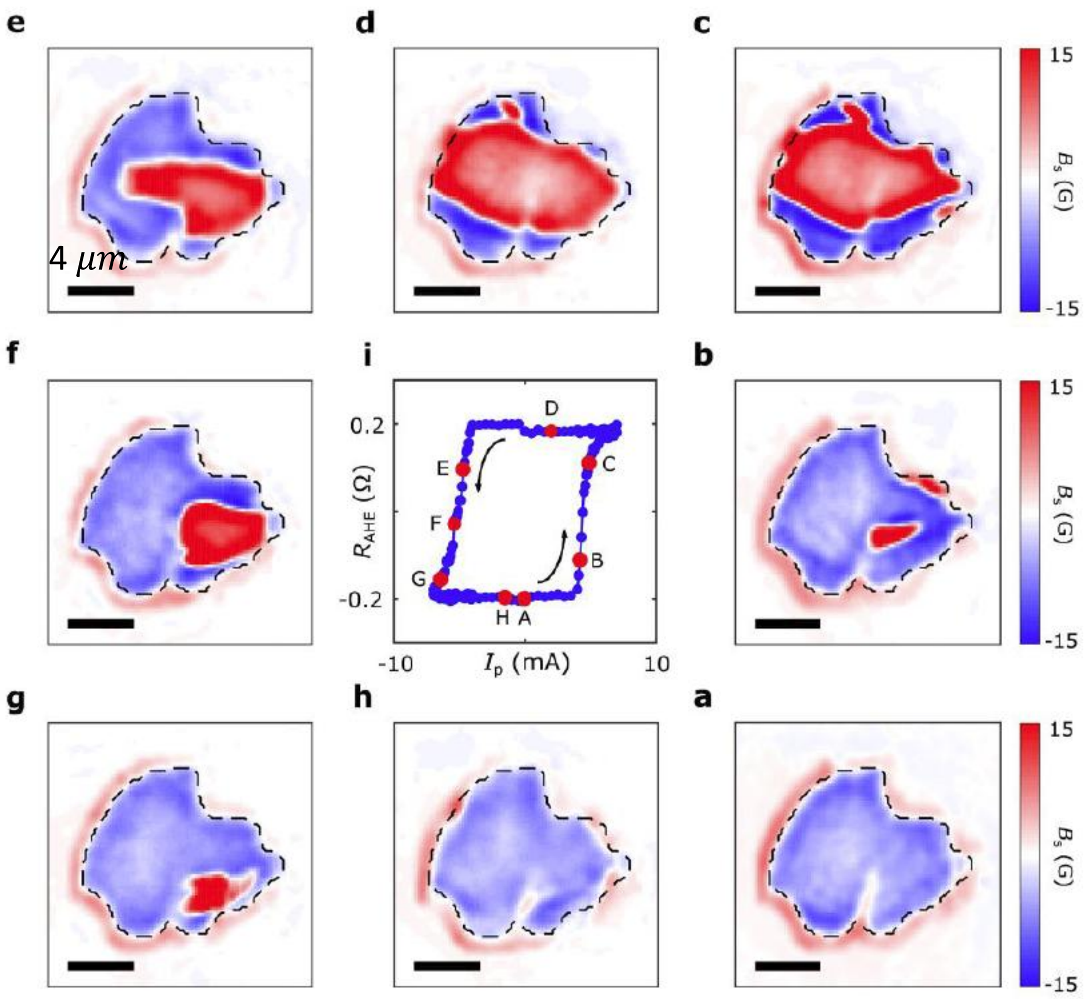

- **Deterministic magnetic switching**

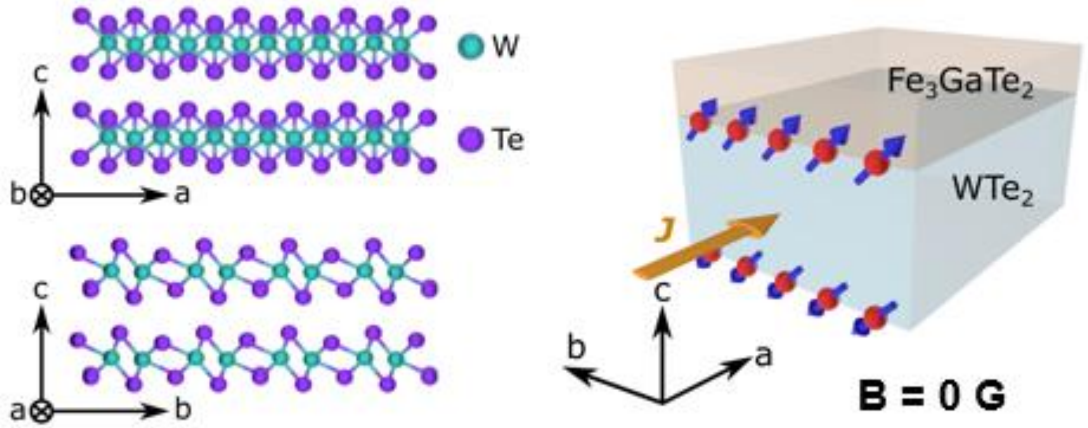

- Magnetization reversal initiates with nucleation of small local domains which are expanded via domain wall propagation.

Zhang et al., *arXiv:2502.04561. Nature Communications* (2026)

Current Control of Field-free Magnetic Switching

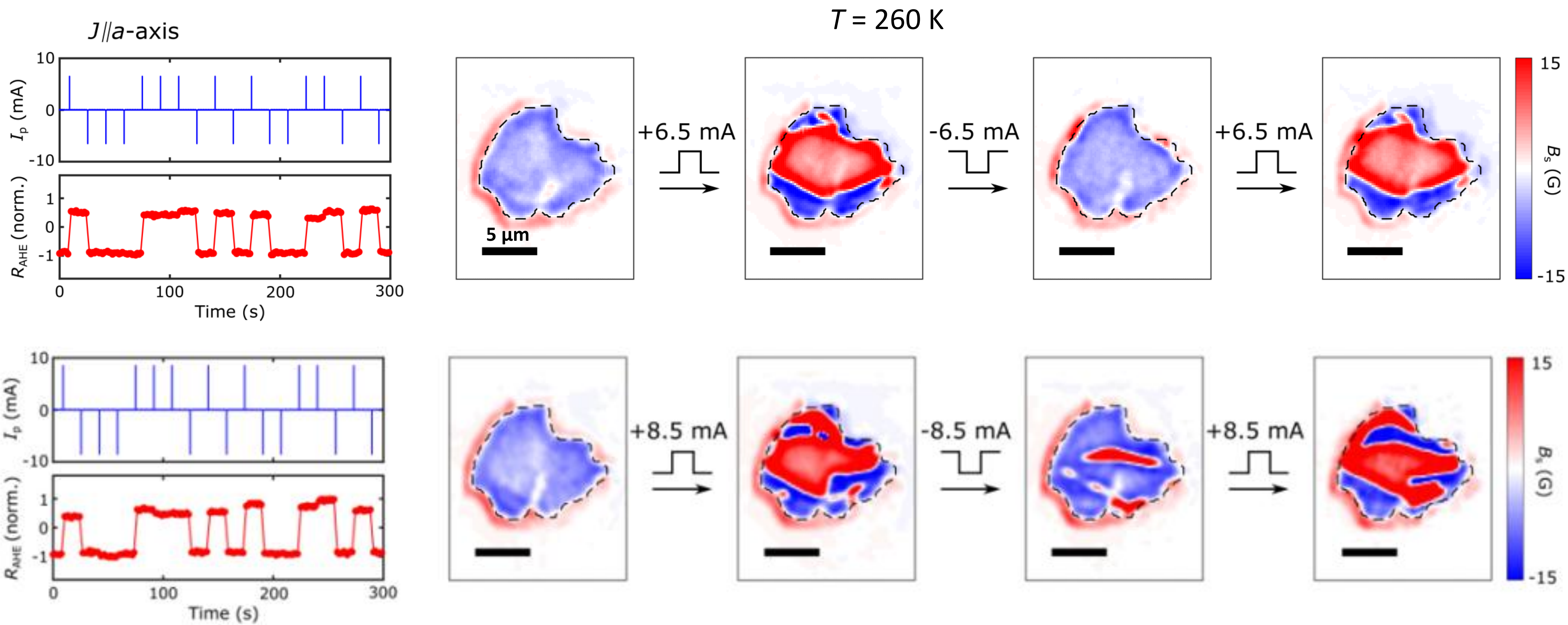

- With a larger current, a small portion of the FGT magnetic domains cannot be switched reproducibly due to local Joule heating

Zhang et al., *arXiv:2502.04561. Nature Communications* (2026)

Current Control of Field-free Magnetic Switching

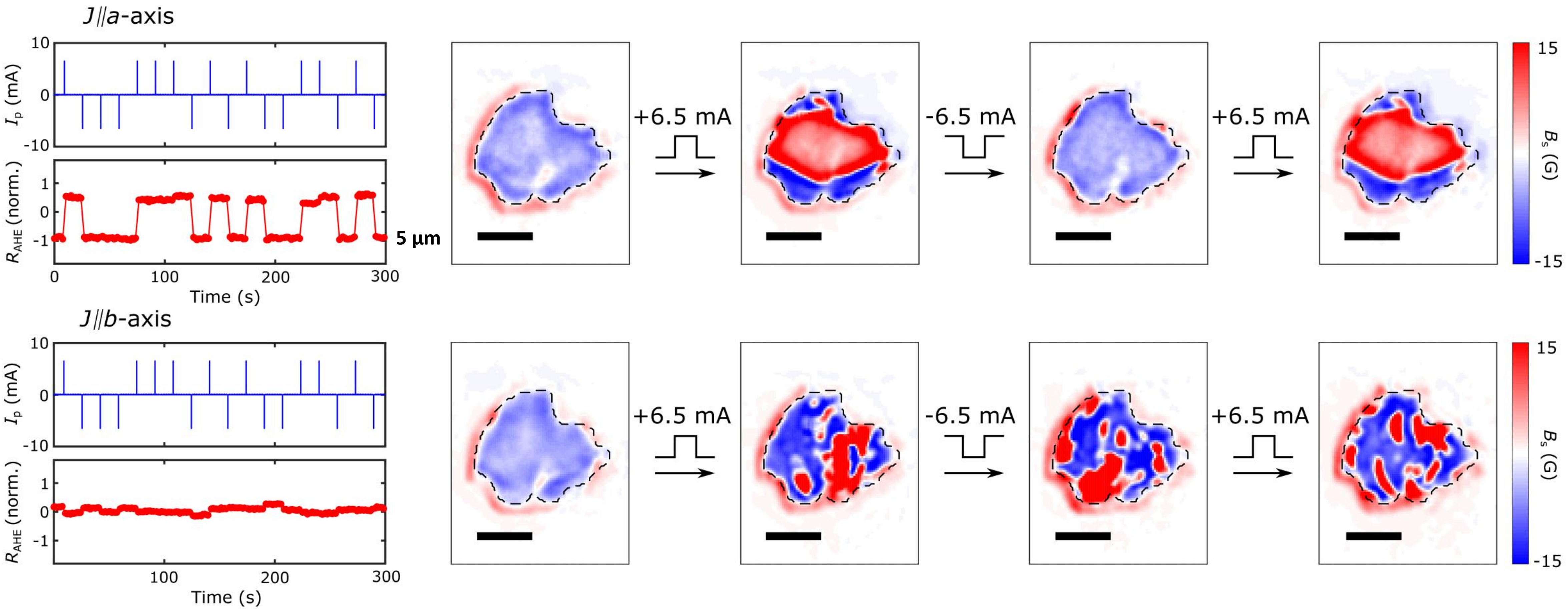

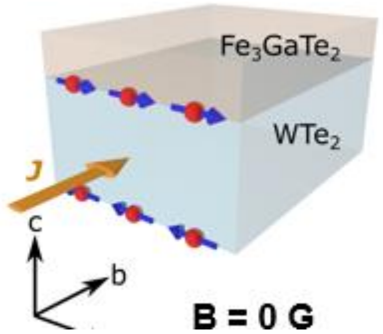

- When current is along *b* (high symmetry) axis, magnetic switching is indeterministic.
- Fully randomly oriented magnetic domains are formed due to the absence of out-of-plane spins

Zhang et al., *arXiv:2502.04561. Nature Communications* (2026)

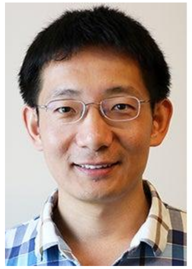

Ran Chen

Kuangyin Deng

Multimodal quantum sensing

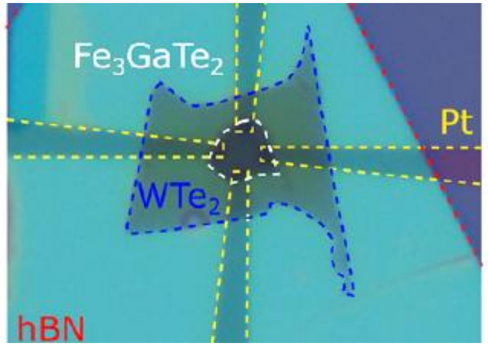

Current

J // a axis

Magnetic switching

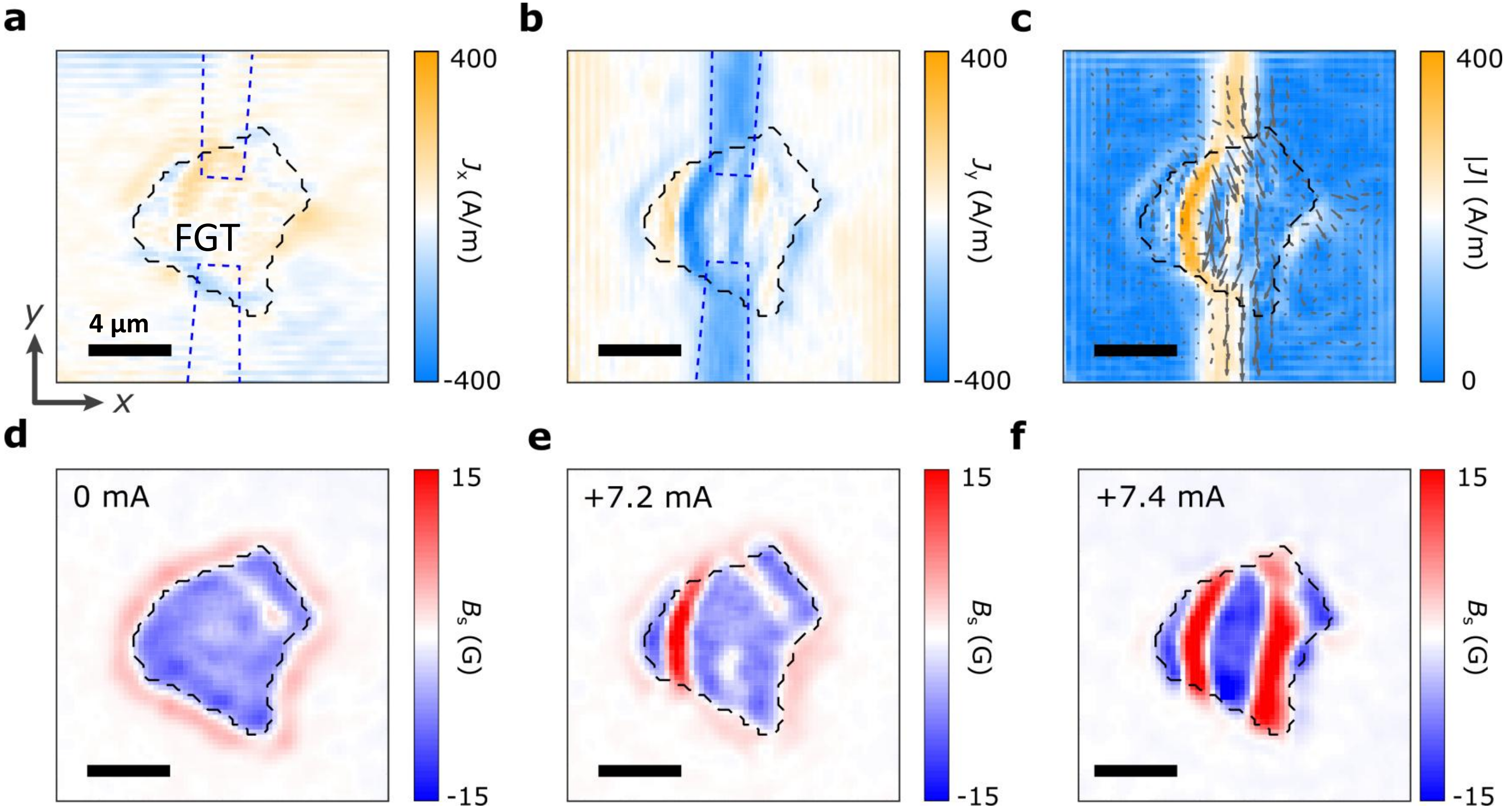

- Microscopic current flow patterns are correlated with the spatially resolved SOT-driven magnetic switching behaviors

Zhang et al., *arXiv:2502.04561. Nature Communications* (2026)

Sensing Spin Wave Excitations by Spin Defects in Few-layer Thick hBN

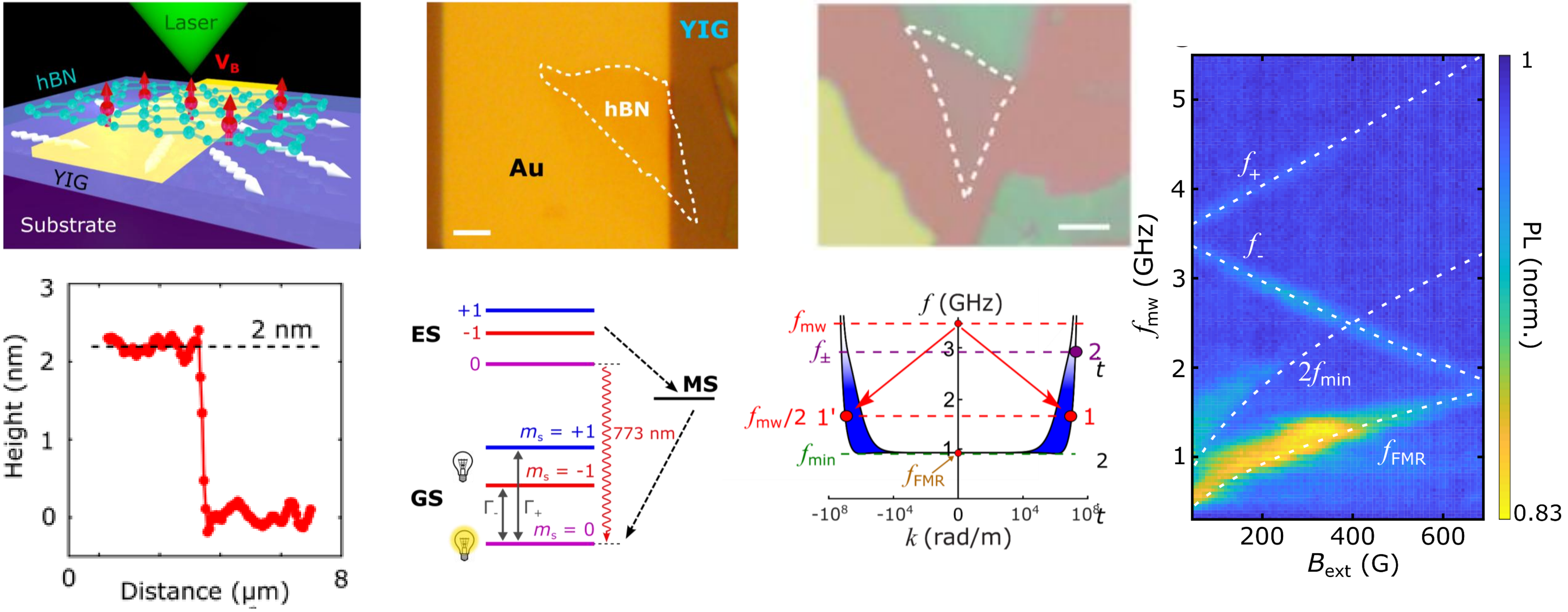

- Quantum sensing platform based on few-layer thick hBN enables detection of spin wave with large wavevectors

J. Zhou et al, *Science Advances* **10**, eadk8495 (2024)

Long range entanglement of NV spins?

- ❑ **Long coherence time and high working temperature make NV a promising qubit**

- ❑ **The application to quantum computing is limited by the scalability of NVs**

- Direct entanglement of NV spins over 30 nm is challenging

Quantum spin transducers

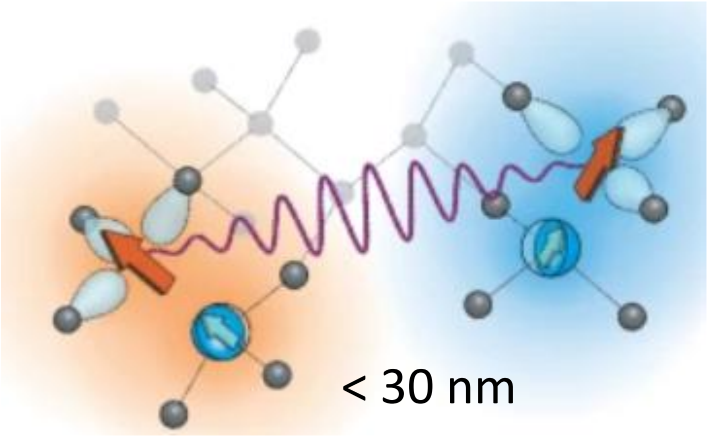

F. Dolde *et al.*, *Nat. Phys.* **9**, 139 (2013)

Spin wave modes

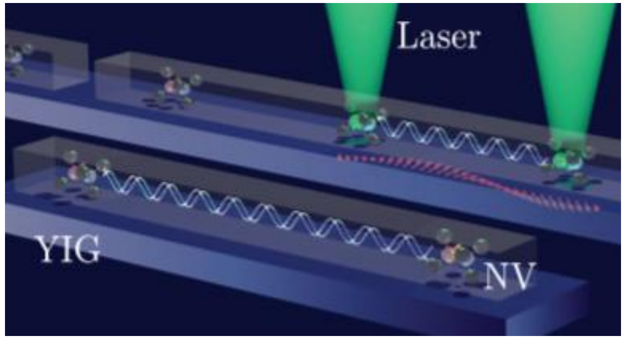

P. Andrich *et al.*, *npj Quantum Inf.* **3**, 28 (2017)

M. Fukami *et al.*, *PRX Quantum* **2**, 040314 (2021)

Magnetic domain wall

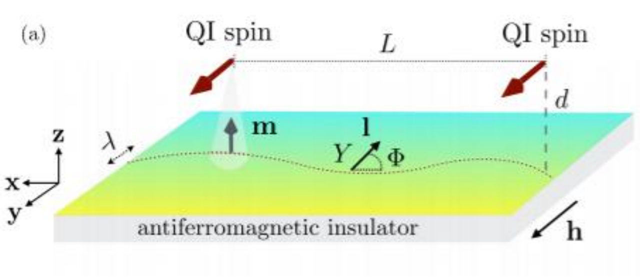

B. Flebus et al.,
Phys. Rev. B **99**, 140403(R) (2019)

Magnon mediated long-distance quantum entanglement between spin qubits?

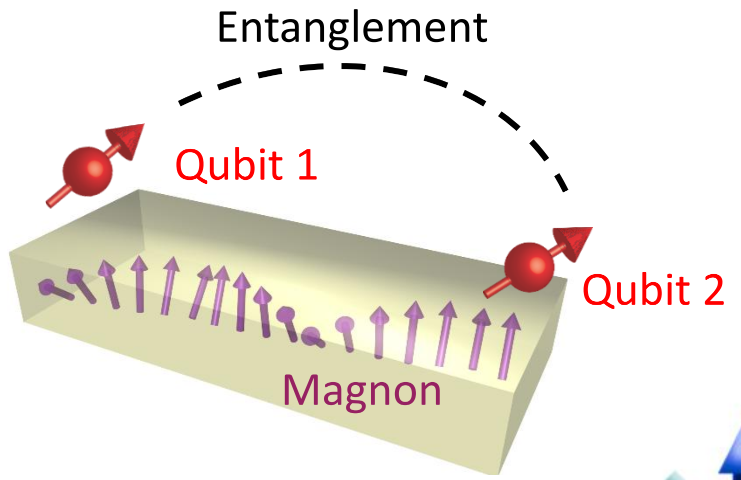

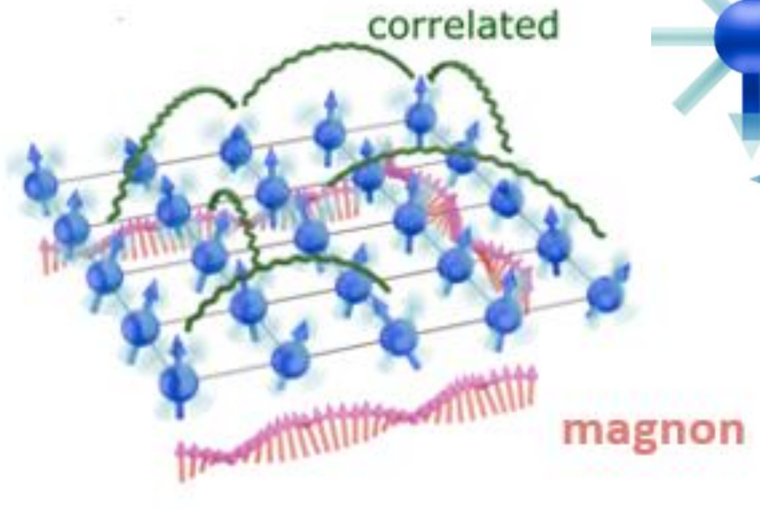

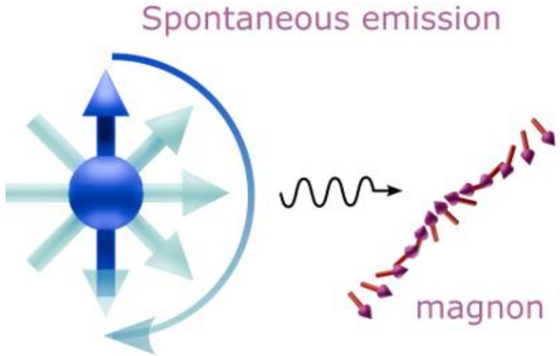

Zero temperature limit

$T \ll 150$ mK

$k_B T > hf_{ESR}$

Spontaneous emission

Thermal magnon

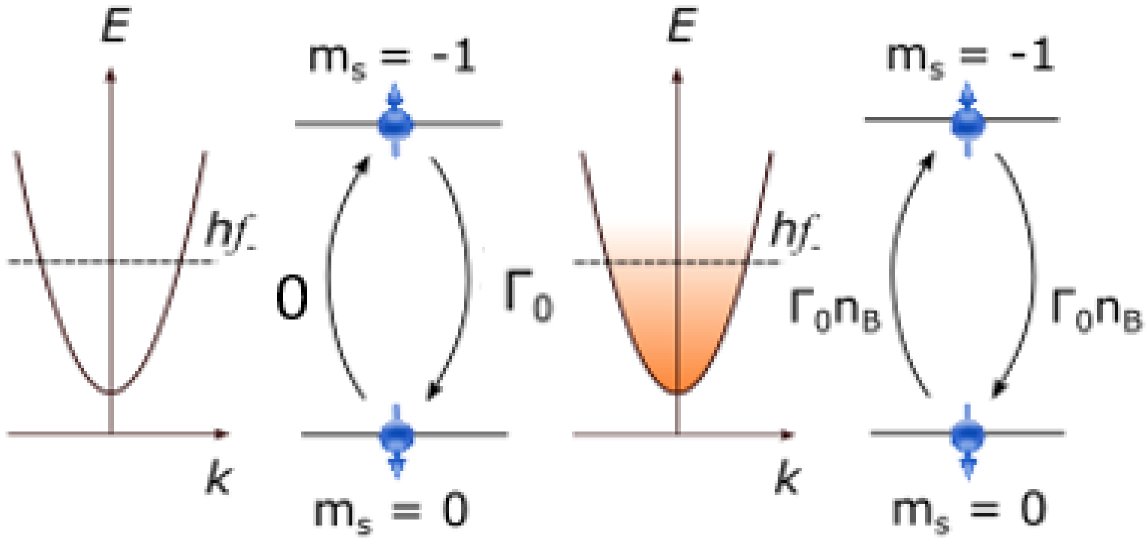

- Freezing out thermal magnon contribution is critical to achieve magnon mediated quantum correlation/entanglement (requires to work at mK temperature regime)

Bose-Einstein Distribution Function:

$$n_B = (e^{hf/k_B T} - 1)^{-1}$$

Intrinsic spin relaxation rate of V_B^- at sub-Kelvin temperatures

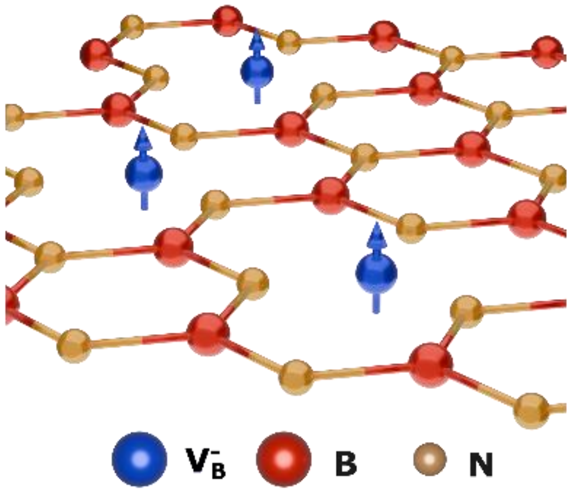

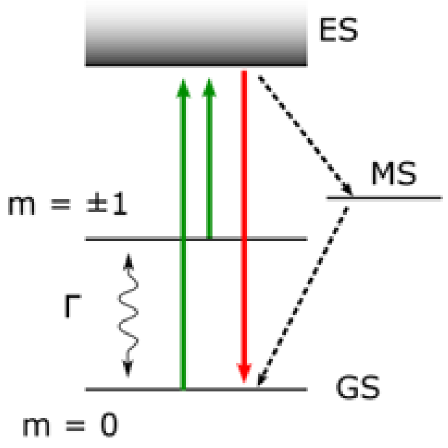

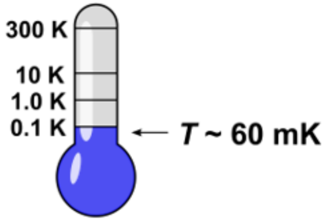

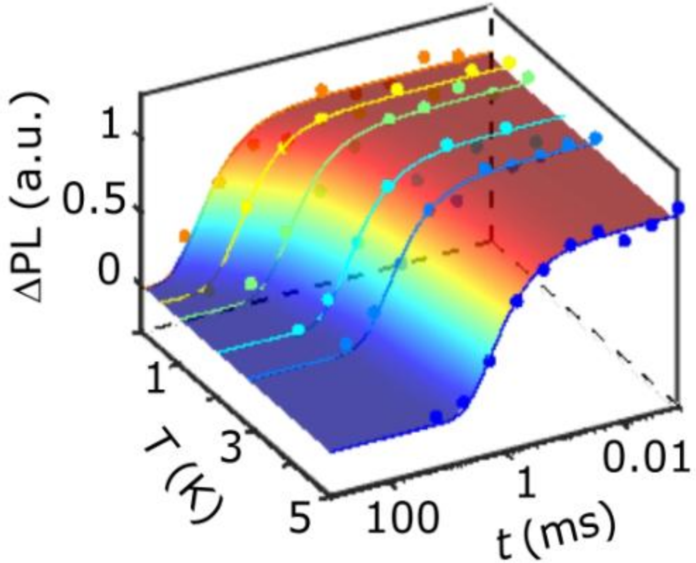

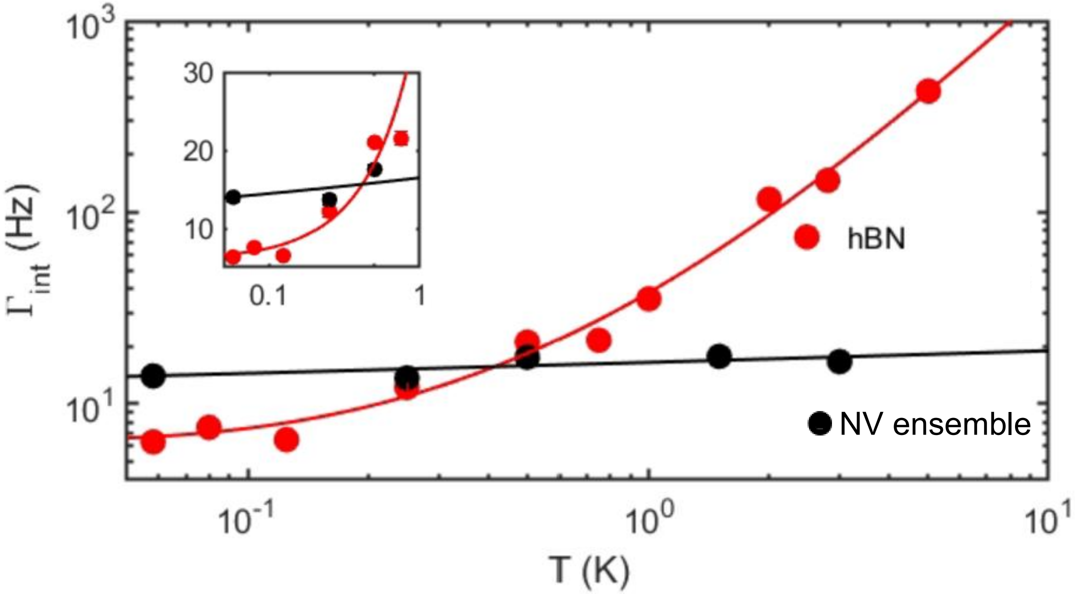

- Γ_{int} for V_B^- shows a dramatic decrease with temperature
- hBN is an ideal quantum sensing platform at mK

L. Zhou et al., arXiv:2606.20996 (2026)

Observation and control of spontaneous magnon emission

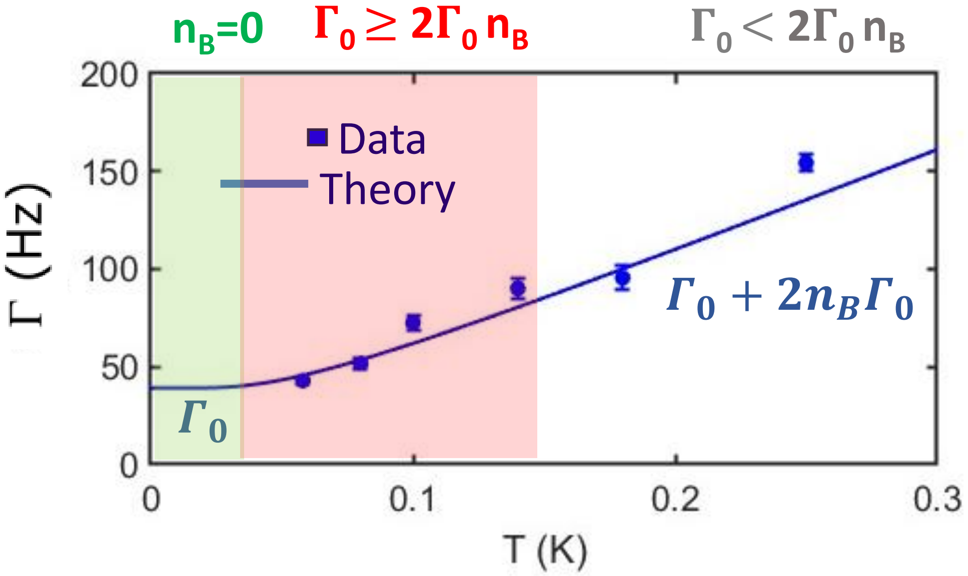

T << 150 mK

$k_B T > hf_{ESR}$

Spontaneous emission

Thermal magnon

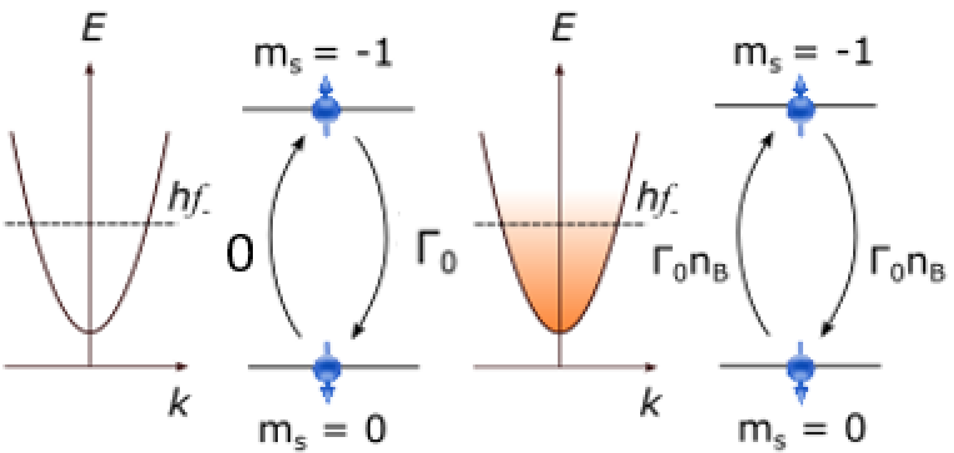

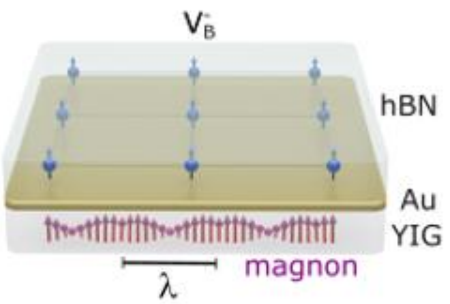

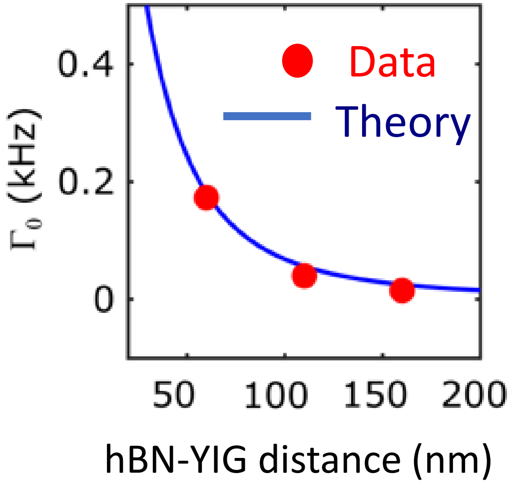

Theory:

$$\Gamma = \Gamma_0(1 + 2n_B) = \Gamma_0\left(1 + \frac{2}{e^{hf_-/k_B T} - 1}\right)$$

$$\Gamma_0 = \frac{1}{t_{hBN}} \iint_{t_{Au}}^{t_{Au}+t_{hBN}} D(f_-, \boldsymbol{k}) F(\boldsymbol{k}, t)\, d\boldsymbol{k}\, dt$$

D is the magnon spectral density, t is the distance between V_B^- centers and the top surface of the YIG film, t_{hBN} and t_{Au} are the thickness of hBN flake and Au stripline, $F(\boldsymbol{k}, t)$ is the transfer function describing magnon-generated magnetic fields at V_B^- center sites.

L. Zhou et al., arXiv:2606.20996 (2026)

Outlook of hybrid spin defect/magnon system

- Hybrid spin defects/magnons system with tailored quantum mechanical properties opens new avenues for developing scalable quantum technology

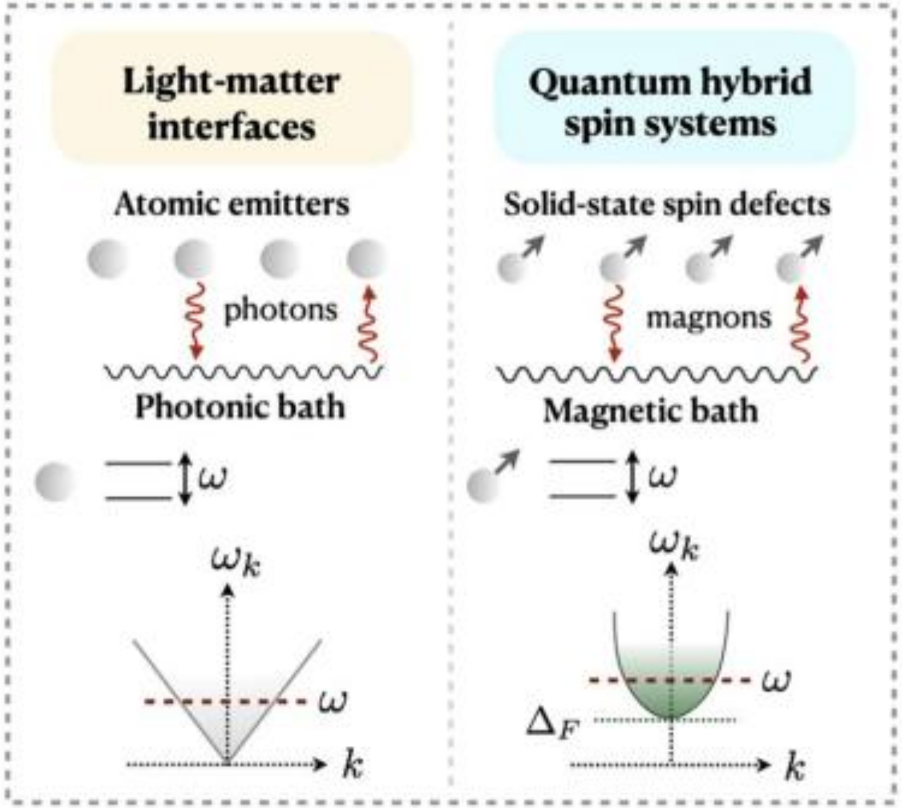

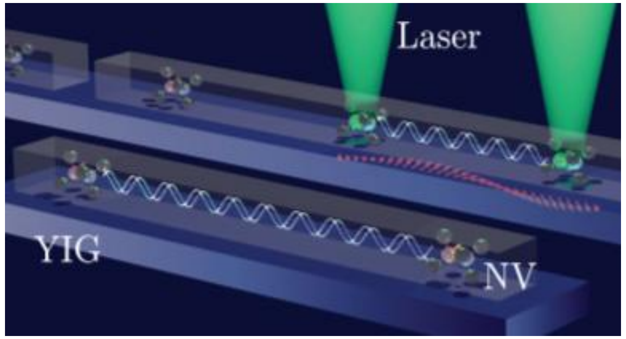

M. Fukami *et al.*, *PRX Quantum* **2**, 040314 (2021)

PHYSICAL REVIEW B **111**, 064424 (2025)

Editors' Suggestion

Solid-state platform for cooperative quantum dynamics driven by correlated emission

Xin Li[1,*] Jamir Marino[2] Darrick E. Chang,[3,4] and Benedetta Flebus[1]

[1]*Department of Physics, Boston College, 140 Commonwealth Avenue, Chestnut Hill, Massachusetts 02467, USA*
[2]*Institut für Physik, Johannes Gutenberg-Universität Mainz, D-55099 Mainz, Germany*
[3]*ICFO-Institut de Ciencies Fotoniques, The Barcelona Institute of Science and Technology, 08860 Castelldefels (Barcelona), Spain*
[4]*ICREA-Institució Catalana de Recerca i Estudis Avançats, 08010 Barcelona, Spain*

Generating Single- and Many-Body Quantum Magnonic States

V. Williams,[1,*] J. M. P. Nair,[1,†] Y. Tserkovnyak,[2,‡] and B. Flebus[1,§]

[1]*Department of Physics, Boston College, 140 Commonwealth Avenue, Chestnut Hill, Massachusetts 02467, USA*
[2]*Department of Physics and Astronomy and Bhaumik Institute for Theoretical Physics, University of California, Los Angeles, California 90095, USA*

(Dated: April 21, 2026)

The growing interest in quantum magnonics is driving the development of advanced techniques for generating, controlling, and detecting non-classical magnonic states. Here, we explore the potential of an ensemble of solid-state spin defects coupled to a shared magnetic bath as a source of such states. We establish a theoretical framework to characterize the quantum correlations among magnons emitted by the ensemble into the bath and investigate how these correlations depend on experimentally tunable parameters. Our findings show that the emitted magnons retain the quantum correlations inherent to the solid-state emitters, paving the way for the deterministic generation of quantum many-body magnonic states.

Summary

cdu71@gatech.edu

NV based quantum sensing

Moiré magnetism

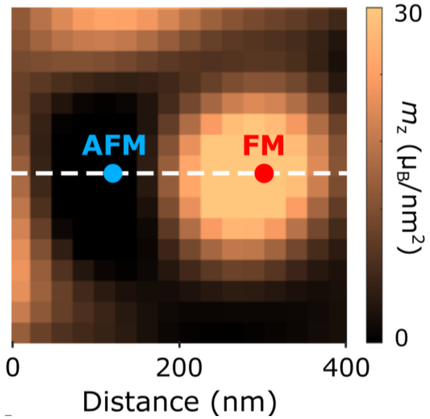

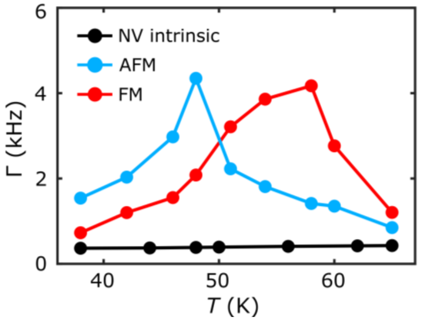

Nat. Commun **15**, 5712 (2024)
Nat. Commun **14**, 5259 (2023)

Surface magnetism in MnTe

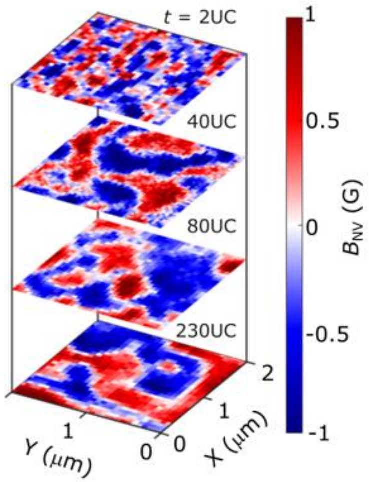

Zhou, et al. arXiv:2605.25241 (2026)

Nb resonator

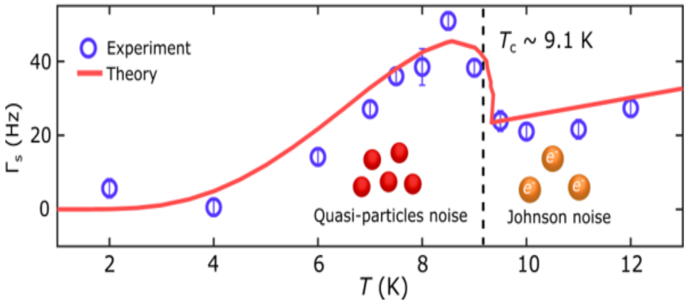

Phys. Rev. Lett. **136**, 076004 (2026)

Quantum sensors in 2D hBN

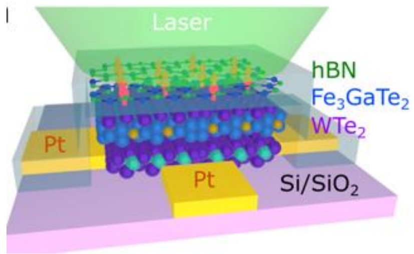

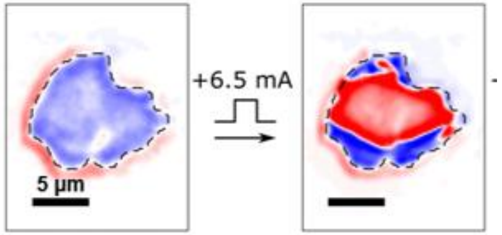

Nat. Commun **13**, 5369 (2022)
Science Advances **10**, eadk8495 (2024)

Hybrid quantum devices

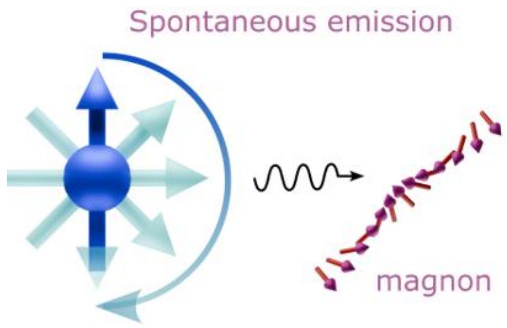

arXiv:2606.20996 (2026)

Outlook:

- ***Multi-modal quantum sensing platform for quantum materials***
  (Unconventional magnetism/superconductivity, ferroelectricity, topology)
- ***Hybrid quantum devices***

Further readings:

S. Li et al., *Nature Materials* (2026)
H. L. Wang et al., *Science Advances* **8**, eabg8562 (2022)
H. L. Wang et al., *Phys. Rev. Lett.* **127**, 117202 (2021)
G. Q. Yan et al., *Advanced Materials*, 2200327 (2022)
N. McLaughlin et al., *Nano Letters* **22**, 5810 (2022)
S. Li et al., *Nano Letters* **23**, 5326 (2023)
N. McLaughlin et al., *Nano Letters* **21**, 7277 (2021)
E. Lee-Wong et al., *Nano Lett.* **20**, 3284 (2020)
X. Wang et al., *npj Quantum Inf.* **6**, 78 (2020)
C. H. R. Du et al., *Science* **357**, 195 (2017)

Acknowledgement

Quantum sensing

Senlei Li
Lingjie Zhou
Jingcheng Zhou
Yiran Zhao
Haoyu Liu
Renzhi Sun
Hanyi Lu
Zelong Xiong
Gerald Yan
Nathan McLaughlin

Quantum sensing and quantum materials

Hailong Wang
(Georgia Tech)

CrI_3 devices and SHG measurement

Liuyan Zhao (UMich)
Zeliang Sun

Mean-field theory for CrI_3

Hua Chen (CSU)
Afsana Sharmin

hBN Crystals

James H Edgar (KSU)
Zhigang Jiang (GT)
Sumedh Rathi

MnTe Films

Cui-Zu Chang (PSU)
Zijie Yan

MnTe Theory

Binghai Yan (PSU)
Chaoxing Liu
Yufei Zhao

Fe_3GaTe_2 Crystal

Jiun-Haw Chu
(U Washington)
Xiaodong Xu
Chaowei Hu

Theory on WTe_2/ Fe_3GaTe_2

Ran Chen (UC Riveside)
Kuangyin Deng

YIG spin chemical potential

Amir Yacoby (Harvard)
Toeno van der Sar (UT Delft)
Tony Zhou

Theory on NV detection of magnetic noise

Yaroslav Tserkovnyak (UCLA)
Shane Kelly
Shu Zhang (OIST)
Benedetta Flebus (BC)
Jayakrishnan M. P. Nair

cdu71@gatech.edu